



US Army Corps
of Engineers

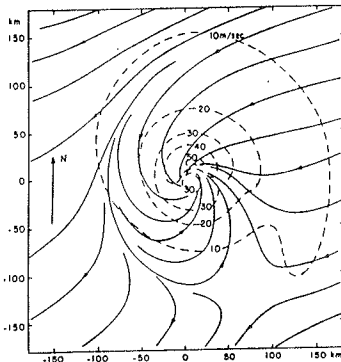
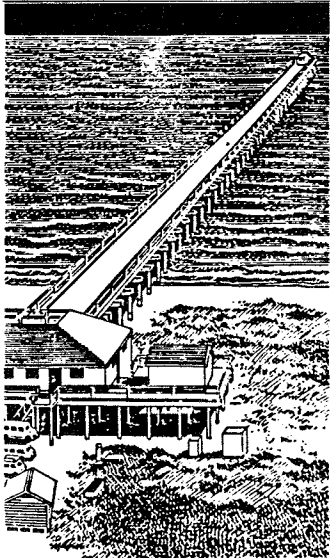
CONTRACT REPORT CERC-92-1

UNIFIED PROGRAM FOR THE SPECIFICATION OF HURRICANE BOUNDARY LAYER WINDS OVER SURFACES OF SPECIFIED ROUGHNESS

by

Vincent J. Cardone, Catherine V. Greenwood
J. Arthur Greenwood

Oceanweather, Inc.
5 River Road, Cos Cob, Connecticut 06807



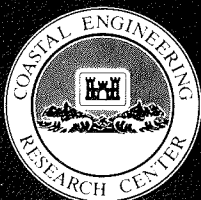
September 1992
Final Report

Approved For Public Release; Distribution Is Unlimited

Prepared for DEPARTMENT OF THE ARMY
US Army Corps of Engineers
Washington, DC 20314-1000

Under Work Units 12114 and 32683
Contract No. DACW39-78-C-0100

Monitored by Coastal Engineering Research Center
US Army Engineer Waterways Experiment Station
3909 Halls Ferry Road, Vicksburg, Mississippi 39180-6199



**Destroy this report when no longer needed. Do not return it
to the originator.**

**The findings in this report are not to be construed as an
official Department of the Army position unless so
designated by other authorized documents.**

**The contents of this report are not to be used for
advertising, publication, or promotional purposes.
Citation of trade names does not constitute an
official endorsement or approval of the use
of such commercial products.**

REPORT DOCUMENTATION PAGE			Form Approved OMB No. 0704-0188	
Public reporting burden for this collection of information is estimated to average 1 hour per response, including the time for reviewing instructions, searching existing data sources, gathering and maintaining the data needed, and completing and reviewing the collection of information. Send comments regarding this burden estimate or any other aspect of this collection of information, including suggestions for reducing this burden, to Washington Headquarters Services, Directorate for Information Operations and Reports, 1215 Jefferson Davis Highway, Suite 1204, Arlington, VA 22202-4302, and to the Office of Management and Budget, Paperwork Reduction Project (0704-0188), Washington, DC 20503.				
1. AGENCY USE ONLY (Leave blank)	2. REPORT DATE September 1992	3. REPORT TYPE AND DATES COVERED Final report		
4. TITLE AND SUBTITLE Unified Program for the Specification of Hurricane Boundary Layer Winds Over Surfaces of Specified Roughness			5. FUNDING NUMBERS	
6. AUTHOR(S) Vincent J. Cardone, Catherine V. Greenwood, J. Arthur Greenwood				
7. PERFORMING ORGANIZATION NAME(S) AND ADDRESS(ES) Oceanweather, Inc. 5 River Road, Cos Cob, CT 06807			8. PERFORMING ORGANIZATION REPORT NUMBER Contract Report CERC-92-1	
9. SPONSORING / MONITORING AGENCY NAME(S) AND ADDRESS(ES) USAE Waterways Experiment Station, Coastal Engineering Research Center, 3909 Halls Ferry Road, Vicksburg, MS 39180-6199; US Army Corps of Engineers, Washington, DC 20314-1000			10. SPONSORING / MONITORING AGENCY REPORT NUMBER	
11. SUPPLEMENTARY NOTES Available from National Technical Information Service, 5285 Port Royal Road, Springfield, VA 22161.				
12a. DISTRIBUTION / AVAILABILITY STATEMENT Approved for public release; distribution is unlimited.			12b. DISTRIBUTION CODE	
13. ABSTRACT (Maximum 200 words) A method is developed to specify the surface stress and the wind speed and direction in the planetary boundary layer of a tropical cyclone from meteorological storm parameters available for historical hurricanes. The method is based upon a numerical primitive-equation model of the planetary boundary layer in a moving tropical cyclone. The complete time history of the evolution of the surface wind field is described from a series of characteristic wind field states calculated at discrete times in a storm's history by the steady-state model. A surface drag formulation, based upon a contemporary similarity model (Arya 1977), coupled with a roughness parameter specification for a water surface consistent with Cardone's (1969) law, is incorporated into the numerical model and found to produce a consistent description of the integrated planetary boundary layer wind, the surface stress and its direction, and the wind speed and direction at anemometer level. The surface winds calculated in several recent hurricanes are found to be in excellent agreement with available, representative surface wind measurements made from offshore platforms and data buoys.				
14. SUBJECT TERMS Hurricanes Tropical storms Wind fields Numerical modeling Winds			(Continued) 15. NUMBER OF PAGES 201	
			16. PRICE CODE	
17. SECURITY CLASSIFICATION OF REPORT UNCLASSIFIED	18. SECURITY CLASSIFICATION OF THIS PAGE UNCLASSIFIED	19. SECURITY CLASSIFICATION OF ABSTRACT	20. LIMITATION OF ABSTRACT	

13. (Concluded).

Transformations based upon an equilibrium planetary-boundary-layer similarity model are developed to specify the surface wind over terrain of specified roughness, including lake surfaces, from the over-water wind-field solution. Calculated over-land and over-lake winds are compared to the limited measurements available for several recent storms. Agreement is generally good.

The method is incorporated in a computer program, which provides surface winds on a variable-resolution rectangular grid. This report includes program documentation and sample grid results for a test simulation performed on Hurricane Betsy (1965).

PREFACE

This report describes the methods incorporated in a computer program developed to provide hurricane surface wind fields. The wind fields can be used in wave and surge modeling activities. The report also serves to document the computer program delivered as part of the study.

The work described in this report was originally performed under Work Unit No. 12114, "Wave Information Studies," Coastal Field Data Collection Program. Publication of the report is funded by Work Unit No. 32683, "Wind Estimation for Coastal Modeling," Coastal Research Program. Both programs are sponsored by Headquarters, US Army Corps of Engineers (HQUSACE). Messrs. John H. Lockhart, Jr., and John G. Housley were the HQUSACE Technical Monitors. Ms. Carolyn M. Holmes of the Coastal Engineering Research Center (CERC), US Army Engineer Waterways Experiment Station (WES), was Program Manager. Drs. Jon M. Hubertz and Edward F. Thompson were the Principal Investigators of Work Unit Nos. 12114 and 32683, respectively.

This study was conducted under Contract No. DACW39-78-C-0100 by Oceanweather, Inc., Cos Cob, Connecticut, and provided to CERC on October 31, 1979. This report is the original contract report provided to CERC. It is being published as a CERC Contract Report at this time because CERC has used and continues to use the study results extensively to estimate wave growth in hurricanes. This report provides an important historical basis for present CERC practice. The hurricane wind model described in this report has recently been modified under Work Unit No. 32683 and included in CERC's Coastal Modeling System (Instruction Report CERC-91-1). Both work units are under the direct supervision of Dr. Martin C. Miller, Chief, Coastal Oceanography Branch, and Mr. H. Lee Butler, Chief, Research Division, and under the general supervision of Mr. Charles C. Calhoun, Jr., Assistant Director, CERC, and Dr. James R. Houston, Director, CERC.

The authors express their appreciation to the technical contract monitor at the time the work was performed, Dr. Robert W. Whalin, and to the late Dr. Charles E. Abel, both of WES, for their support, assistance and patience throughout the course of the work. The authors also acknowledge the role of the late Dr. John Wanstrath, who recognized the critical need for improved wind field models in hurricane surge modelling, and whose intense interest

stimulated the initiation of this research study.

At the time of publication of this report, Director of WES was Dr. Robert W. Whalin. Commander and Deputy Director was COL Leonard G. Hassell, EN.

CONTENTS

	<u>Page</u>
PREFACE	1
CONVERSION FACTORS, NON-SI TO SI (METRIC) UNITS OF MEASUREMENT	4
PART I: INTRODUCTION	5
Statement of Problem	5
Review of Prior Methods	7
Relevant Recent Research	9
PART II: THE HURRICANE PBL MODEL	12
Review of Chow's (1971) Vortex Model	12
A Consistent Surface Stress Parameterization	17
Numerical Experiments over Mixed Terrain	25
Equilibrium Theory Terrain Transformations	29
Results for Test Storms	35
PART III: THE COMPUTER PROGRAM	43
Program Description	43
Remarks	54
Printed Output	79
PART IV: CONCLUSIONS AND RECOMMENDATIONS	81
LITERATURE CITED	83
FIGURES 1-31	
APPENDIX A: NAMELIST	A1
APPENDIX B: PROGRAM LISTING	B1
APPENDIX C: PROGRAM HIST LISTING OF TEST STORM (BETSY) INPUT AND SAMPLE ANNOTATED OUTPUT	C1

CONVERSION FACTORS, NON-SI TO SI (METRIC)
UNITS OF MEASUREMENT

Non-SI units of measurement can be converted to SI (metric) units as follows:

<u>Multiply</u>	<u>By</u>	<u>To Obtain</u>
degrees (angle)	0.01745329	radians
feet	0.3048	metres
knots (international)	0.5144444	metres per second
miles (US nautical)	1.852	kilometres

A UNIFIED PROGRAM FOR THE SPECIFICATION OF HURRICANE BOUNDARY
LAYER WINDS OVER SURFACES OF SPECIFIED ROUGHNESS

PART I: INTRODUCTION

Statement of Problem

1. Specification of the wind velocity and vector wind stress near the sea surface in tropical cyclones is required for the description of ocean surface phenomena (such as ocean currents, the storm surge, and surface gravity waves) related to such cyclones. Dynamical-numerical computer-based models to describe such phenomena continue to be developed: for example, the work of Jelesnianski (1970) and Wanstrath et al. (1976) on the open coast surge, Forristall (1974) on currents, Cardone et al. (1976) on waves, and Wanstrath (1978) on the surge, including coastal flooding.

2. In most studies very simple descriptions of the hurricane wind field have been used to drive very complicated ocean response models. This disparity has hindered further refinement and validation of ocean response models and has limited the defensibility of climatological series, design criteria, and like results based upon the application of such models. The lack of near-surface wind measurements in hurricanes serves as an excuse for applying simple wind models: in fact, the most widely applied empirical model, discussed below, of surface marine wind distribution in hurricanes is calibrated against wind measurements made in a lake during the passage of a single storm.

3. In recent years, however, great progress has been made in our understanding of the basic physical and dynamical characteristics of tropical cyclones, including the part of such storms relevant to this discussion: the planetary boundary layer (PBL). Further, a series of measurement programs, both public and private, employing offshore oil and gas production platforms, automated data buoys, and low-flying aircraft, have made available a wealth of data on wind structure in the PBL in

tropical cyclones.

4. Cardone et al. (1976), exploiting this recent progress, developed a method for specifying the surface wind field in hurricanes over the ocean by applying a dynamical-numerical model of the PBL in hurricanes. The method, requiring as input only a description of the surface pressure field and specification of storm motion and latitude, has been used to model the surface wind field in nearly every major hurricane to affect the Gulf of Mexico or the East coast of the United States in the past decade (Camille, 1969; Delia, 1973; Eloise, 1975; Belle, 1976). At least one representative series of wind measurements over water was available in each of those storms to validate the method for the intended environment (open water) and the intended parameter (time-averaged winds at a specific height). Those studies confirm that the model is able to give a convincing numerical representation of how friction, latitude, storm motion, and the shape and intensity of the sea-level pressure pattern in a severe storm interact to produce an asymmetrical vertically integrated flow in the PBL. The model, however, includes an empirically based scaling law to relate the integrated boundary layer wind to the effective 19.5 meter level wind. Further, the surface stress distribution in the numerical solution has not been validated.

5. The purpose of the study reported here is to generalize the method so that it can be applied to specify surface wind and wind stress in hurricanes in a self-consistent way not only over the open sea but over waters typical of the near-shore environment, over inland bodies of water (lakes), and over terrain of varying roughness in general (e.g. open marshland, dense forest, cities). Such a capability is required for the application of surge models which treat the open-coast storm tide and inland flooding of coastal areas (e.g. the Mississippi delta and Lake Pontchartrain area) or those applied to surge studies of large inland bodies of water (e.g. Lake Okeechobee).

6. The goal of this study was the development of an efficient algorithm, implemented as a computer program free from proprietary constraints, that can be used to specify hurricane-generated surface winds and wind stresses, in historical storms or hypothetical storms, from the

kind of meteorological information available for historical storms.

Review of Prior Methods

7. Considered theoretically, the problem of surface wind specification in tropical cyclones is to solve the basic equations of hurricane-scale circulation, subject to appropriate initial and boundary conditions. As a part of the system of equations, consider the primitive equations of motion in cylindrical coordinates r , λ , z , with origin at the center of the cyclone, for u and v , the (horizontal) tangential and radial components of the wind:

$$\begin{aligned} \rho \left\{ \frac{\partial u}{\partial t} + u \frac{\partial u}{\partial r} + \frac{v}{r} \frac{\partial u}{\partial \lambda} + w \frac{\partial u}{\partial z} - fv - \frac{v^2}{r} \right\} \\ = \frac{\partial \rho}{\partial r} + \frac{\partial \tau_{zr}}{\partial z} + \left\{ \frac{\partial \tau_{rr}}{\partial r} + \frac{1}{r} \frac{\partial \tau_{\lambda r}}{\partial \lambda} + \frac{\tau_{rr} - \tau_{r\lambda}}{r} \right\} \end{aligned} \quad (1a)$$

$$\begin{aligned} \rho \left\{ \frac{\partial v}{\partial t} + u \frac{\partial v}{\partial r} + \frac{v}{r} \frac{\partial v}{\partial \lambda} + w \frac{\partial v}{\partial z} + fu + \frac{uv}{r} \right\} \\ = \frac{1}{r} \frac{\partial \rho}{\partial \lambda} + \frac{\partial \tau_{z\lambda}}{\partial z} + \left\{ \frac{\partial \tau_{r\lambda}}{\partial r} + \frac{1}{r} \frac{\partial \tau_{\lambda\lambda}}{\partial \lambda} + \frac{2\tau_{r\lambda}}{r} \right\} \end{aligned} \quad (1b)$$

where w is the vertical component of the wind and the τ 's are the radial, tangential, and vertical eddy stresses of the tangential and radial velocity components.

8. Lack of knowledge how to solve equations (1), in particular lack of knowledge how to specify the eddy stresses, has until rather recently prevented a straightforward application of the primitive equations to the study of tropical cyclones. Practical demands, however, dictated the development of surface wind models as early as the late 1940's and the early 1950's. Even today the most widely applied method for wind specification derives from a procedure first published in a se-

ries of reports of the U.S. Weather Bureau, Hydrometeorological Section, during the 1950's. This method, hereafter referred to as the HP (Hydro-meteorological-Parametric) method, may be considered a three-parameter method: it requires knowledge of only three quantities related to a storm's structure, to specify the entire areal distribution of surface wind.

9. The basic steps involved in the HP method are the following:

- a. Assume that the sea-level pressure distribution in a tropical cyclone is symmetric; specify pressure as a function of radius r ,

$$p(r) = p_0 + \Delta p e^{-R/r},$$

where p_0 is the central pressure (at the eye), Δp is a storm pressure anomaly, and R is a scale radius related to the radius of maximum wind.

- b. Compute the profile of gradient wind as a function of radius: this step basically solves the u equation of motion for the steady-state, frictionless, locally horizontally homogenous solution:

$$u_{gr} + \frac{u^2}{fr} = \frac{1}{\rho f} \frac{\partial p}{\partial r}.$$

- c. Attempt to compensate for neglect of *all* other terms by reducing the gradient wind to the equivalent wind over water at 10 meters, using a reduction of the form

$$u_{10}/u_{gr} = F(r/R)$$

where F varies from .865 at the radius of maximum wind to about .60 at the periphery of the storm.

- d. Add asymmetry to the storm by vectorially adding 50% of the storm's forward motion V_f to the right side of the storm and subtracting 50% from the left side.
- e. Partition the reduced winds into tangential and radial components by specifying an inflow angle that is a function of r/R alone; in effect, this step attempts to compensate for the neglect of all physical effects contained in the v equation of motion.

10. The function F was derived from pressure and wind measurements made in and around Lake Okeechobee, Florida, during the passage of two hurricanes in 1949 and 1950; in fact, the constant .865 was chosen

from measurements in that single storm deemed more representative.

11. An attempt to solve by graphical means a less simplified version of equations (1), proposed by Myers and Malkin (1961), was applied to the determination of the wind field in hurricane Helene, 1958, by Schauss (1962). The study of Myers and Malkin (1961) was the first to demonstrate the dynamical inconsistencies in the HP method, especially the fallacy that superposition of storm motion on a circularly symmetric wind field can produce the right/left asymmetry observed in hurricanes. Schauss (1962) represented the eddy stresses in terms of friction coefficients which in turn were estimated indirectly from sea-level pressure analyses and ships' wind observations in hurricane Helene. An important element of Schauss' study was the realization that the pressure field about tropical cyclones is not axisymmetric. Schauss varied Δp and R by quadrant; he found that he could reliably estimate the quadrantal variation from conventional coastal measurements and marine pressure data, even though Helene remained offshore, east of the East coast of the United States.

12. The method of Myers and Malkin and Schauss is not, to our knowledge, in use today; the HP method, however, is in widespread use in design studies, climatological studies, and real-time forecast systems. Variants of the HP method are described by Patterson (1972) and Bretschneider (1976); the latest version is documented in Memorandum HUR7-120, Hydrometeorology Branch, Office of Hydrology, NOAA.

Relevant Recent Research

13. Much of our current basic knowledge of the structure, dynamics, and energetics of tropical cyclones has been generated only within the past 10 or 15 years. This progress is a result of two factors: first, an extensive data base has been created as a result of the program of reconnaissance by NOAA research aircraft begun in the late 1950's; second, models of the tropical cyclone, based upon numerical integration of the primitive equations, have provided new insight into the basic dynamical and thermodynamic processes operative in tropical cyclones.

14. As a result of analysis of the reconnaissance data, the general distribution of pressure, wind, and temperature throughout the free atmosphere above the friction layer in the inner core of hurricanes has been revealed. Shea and Gray (1973), for example, composited all aircraft data obtained between 1957 and 1969, and derived the distribution of the mean tangential and radial components of actual winds at various levels including the 900 mb level, the level closest to the boundary layer. Their analysis suggested that at that level, the asymmetry in the tangential component exceeds the forward motion of the storm, and that the radial (inflow) component is not symmetrically distributed about the storm axis, as is assumed in the HP model.

15. In the area of numerical modelling, at least a dozen distinct prognostic models have been developed since 1964. Anthes (1974) summarized numerical models down to about 1972, several of which continue to be further developed today. Changes have been mainly in the use of increased horizontal and vertical resolution and in parametrizing the effects of cumulus convection.

16. Models of the prognostic type are designed to study the dynamics and energetics of tropical cyclones, to expose the mechanisms of hurricane formation from incipient tropical disturbances, to study the sensitivity of the tropical cyclone to boundary conditions at the lower boundary (in particular sea surface temperature), and to assess the prospective influence of various proposed schemes for artificially modifying such cyclones (e.g. cloud seeding near the eye wall). Such models typically can not be used directly to specify the distribution of surface wind or wind stress in hurricanes, because the models suffer from relatively low horizontal resolution, crude parametrization of the boundary layer, and time-dependent integration schemes: in fact, the models were designed not as diagnostic tools, but rather to describe the evolution of the circulation from an arbitrary set of initial conditions.

17. Recently there has been greater emphasis on the boundary layer of tropical cyclones in hurricane research: this is because the boundary layer is an important dynamical component of the total circulation in cyclones; additionally, much of the new knowledge gained within

the past decade about the structure of the surface and planetary boundary layers of the atmosphere over the sea can be profitably applied to the boundary layer in hurricanes. Elsberry et al. (1974) obtained realistic solutions for the temperature and moisture distribution within the boundary layer of an axisymmetric storm by applying the marine PBL model of Cardone (1969), originally developed for application to the extratropical atmosphere. More recently, Moss and Rosenthal (1975) estimated the vertical exchange rates of momentum, heat, and cloud mass in the boundary layer of hurricanes by combining the boundary layer model of Deardoff (1975) with the roughness parameter formulation of Cardone (1969). Anthes and Chang (1978) used a new parameterization of the planetary boundary layer in an axisymmetric numerical hurricane model to study the response of a hurricane boundary layer to changes of sea surface temperature.

18. In this study, a diagnostic model of the hurricane PBL, developed originally by Chow (1971) and applied later by Cardone et al. (1976), is modified to produce a consistent description of the vertically integrated wind in the PBL, the surface drag and the wind speed and direction at anemometer height in a moving hurricane with asymmetric horizontal wind distribution over water. Equilibrium PBL theory is used to extend the surface wind description to terrain of specified roughness. The wind model is incorporated in a computer program to provide a gridded temporal and spatial history of the surface wind for use in surge models.

PART II: THE HURRICANE PBL MODEL

Review of Chow's (1971) Vortex Model

19. As time dependent numerical hurricane models have been extended to three dimensions, it has become necessary to find efficient numerical schemes of solving the primitive equations on the high resolution grids required and to give more emphasis to the asymmetry of planetary boundary layer flow. The latter is important because frictionally induced convergence in the boundary layer (Ekman pumping) is an important mechanism in organizing moist convection and triggering the instability responsible for the development of tropical cyclones. Those requirements served as the principal motivation for Chow's study.

20. Chow's model concerned the planetary boundary layer (PBL) only and sought the solution for the wind field and horizontal convergence in the PBL of a moving tropical cyclone from the equations of motion. The pressure field in the boundary layer was prescribed and fixed, so that there would be no gravity waves excited in the numerical solution. This facilitated the use of a nested grid system, which allowed grid spacings as small as 5 km near the hurricane inner region without sacrifice of overall computational efficiency.

21. The model is based upon the equation of horizontal motion, vertically averaged through the depth of the PBL, written in coordinates fixed to the earth as

$$\frac{d\hat{V}}{dt} + f|\mathbf{k} \times \hat{V} = -\frac{1}{\rho} \nabla p + \nabla \cdot (K_H \nabla \hat{V}) - \frac{C_D}{h} |\hat{V}| \hat{V} \quad (2)$$

where

$$\frac{d}{dt} = \frac{\partial}{\partial t} + \hat{V} \cdot \nabla;$$

$\frac{\partial}{\partial t}$ is the time change local to the fixed coordinates; ∇ the two-dimensional del operator; \hat{V} the vertically averaged horizontal velocity; f the Coriolis parameter; $|\mathbf{k}$ the unit vector in the vertical direction; ρ the mean air density; p the pressure; K_H the horizontal eddy viscosity coefficient; C_D the drag coefficient; h the

depth of the planetary boundary layer. It is assumed that the vertical advection of momentum is small compared to the horizontal advection and can be neglected and that the shearing stress vanishes at the top of the PBL.

22. The pressure is prescribed as the sum of p_c and \bar{p} ;

$$p = p_c + \bar{p}$$

where p_c , not necessarily axisymmetric, is the pressure field representing the tropical cyclone and assumed to translate with the storm at a specified speed \vec{V}_c ; and \bar{p} is a large scale pressure field which may be specified by the corresponding constant geostrophic flow, \vec{V}_g , as

$$f|K \times \hat{V}_g = -\frac{1}{\rho} \nabla \bar{p} \quad (3)$$

With this pressure specification, equation (2) may be written:

$$\frac{d\hat{V}}{dt} + f|K \times (\hat{V} - \hat{V}_g) = -\frac{1}{\rho} \nabla p_c + \nabla \cdot (K_H \nabla \hat{V}) - \frac{C_D}{h} |\hat{V}| \hat{V} \quad (4)$$

With respect to a moving Cartesian coordinate system (x, y) whose origin is located at the moving low center of p_c , equation (4) is transformed into

$$\frac{d\vec{V}}{dt} + f|K \times (\vec{V} - \vec{V}_g) = -\frac{1}{\rho} \nabla p_c + \nabla \cdot (K_H \nabla \cdot \vec{V}) - \frac{C_D}{h} |\vec{V} + \vec{V}_c| (\vec{V} + \vec{V}_c)$$

where

$$\frac{d}{dt} = \left(\frac{\partial}{\partial t}\right)_c + \vec{V}_c \cdot \nabla$$

$$\left(\frac{\partial}{\partial t}\right)_c = \frac{\partial}{\partial t} + \vec{V}_c \cdot \nabla$$

$$\vec{V} = \hat{V} - \vec{V}_c$$

$$\vec{V}_g = \hat{V}_g - \vec{V}_c$$

\vec{V} is now the horizontal wind relative to the low center; \vec{v}_g the effective geostrophic flow relative to the low center; and $(\frac{\partial}{\partial t})_c$ the time change local to the moving coordinates.

23. Chow solves equation (5) in component form

$$\frac{\partial u}{\partial t} = fv - Au - Pu + Hu - Fu \quad (5a)$$

$$\frac{\partial v}{\partial t} = -fu - Av - Pv + Hv - Fv \quad (5b)$$

where

$$Au = u \frac{\partial u}{\partial x} + v \frac{\partial u}{\partial y}$$

$$Av = u \frac{\partial v}{\partial x} + v \frac{\partial v}{\partial y}$$

$$Pu = fv_g + \frac{1}{\rho} \frac{\partial P_c}{\partial x}$$

$$Pv = -fu_g + \frac{1}{\rho} \frac{\partial P_c}{\partial y}$$

$$Hu = \frac{\partial}{\partial x} (K_H \frac{\partial u}{\partial x}) + \frac{\partial}{\partial y} (K_H \frac{\partial u}{\partial y})$$

$$Hv = \frac{\partial}{\partial x} (K_H \frac{\partial v}{\partial x}) + \frac{\partial}{\partial y} (K_H \frac{\partial v}{\partial y})$$

$$Fu = \frac{C_D}{h} [(u + u_c)^2 + (v + v_c)^2]^{\frac{1}{2}} (u + u_c) \quad (6a)$$

$$Fv = \frac{C_D}{h} [(u + u_c)^2 + (v + v_c)^2]^{\frac{1}{2}} (v + v_c) \quad (6b)$$

24. The general formulation is completed with the specification of the form of C_D , K_H and the boundary condition at the outermost boundary of the grid. Following Smagorinsky (1963)

$$K_H = 2\kappa^2 \left(\frac{\Delta}{2}\right)^2 |\text{Def}|$$

where $|\text{Def}|$ is the total deformation, Δ is the mesh size and κ is a non-dimensional constant ($\kappa = .4$ is assumed). The drag coefficient was assumed to increase linearly with wind speed

$$C_D = (0.5 + 0.6 |\vec{V}|) \times 10^{-3} \quad (\vec{V} \text{ in m/sec}) \quad (7)$$

At the outermost boundary of the grid, the acceleration and the horizontal diffusion of momentum are neglected, implying a balance between Coriolis force, pressure gradient force and the surface frictional force

$$f|K \times (\vec{V} - \vec{V}_g) = -\frac{1}{\rho} \nabla p_c - \frac{C_D}{h} |\vec{V} + \vec{V}_c| (\vec{V} + \vec{V}_c)$$

25. The computational grid is a rectangular nested grid system consisting of five nests, within each of which the mesh is constant. Figure 1 shows the inner three nests in one quadrant of the grid system; if the mesh size of the innermost nest is say 5 km, the second through fifth mesh sizes are 10, 20, 40, and 80 km respectively, and the entire grid covers an area of $(1600 \text{ km})^2$.

26. The details of the finite difference formulation and of the computational scheme are given by Chow (1971) and will not be repeated in detail here. Basically, a combination of diagonal and ordinary upstream differencing is used for spatial derivatives in order to reduce computational errors in the calculation of the advection terms and at the intermesh boundaries. The computation starts with an initial guess field consisting of the gradient wind components (computed from p_c). At each grid point, the equations (5) are integrated forward in time until the acceleration $(\partial \vec{V} / \partial t)_c$ is tolerably small. For an innermost grid mesh of size 5 km, the time step is 60 sec. Chow found that 800

iterations (equivalent to 13 hours 20 min) were sufficient to achieve a steady state solution.

27. Chow studied the accuracy of the numerical scheme by obtaining numerical solutions for a frictionless ($K_H, C_D = 0$) stationary ($\vec{V}_c = 0$) vortex in gradient balance. The pressure field was axisymmetric and defined by the well known exponential pressure law

$$p_c = p_o + \Delta p e^{-R_p/r} \quad (8)$$

where p_o is storm central pressure, Δp is the storm pressure anomaly, R_p is the scale radius and r is the radial distance from the eye.

For the test storm ($\Delta p = 50$ mb, $R = 40$ km), the truncation error decreased with the spacing of the inner nest mesh size. For a spacing of 5 km, the numerical solution for the radial and tangential components is compared to the analytical gradient-wind solution, which of course contains only a tangential component, in Figure 2. It is seen that the truncation error appears only in the radial component and serves to introduce a small inward-directed radial component.

28. Figure 3 shows the integrated boundary layer wind solution found by Chow for the same test storm but with friction, storm motion (10 m/sec) and a steering gradient of 10 m/sec aligned with the motion. The pattern is remarkably realistic, at least qualitatively, and displays considerable asymmetry in both speed and direction. In several sensitivity experiments Chow deduced that, at least for the test storm, friction and storm motion effects combine non-linearly to produce a strongly asymmetric inflow pattern. Storm motion is primarily responsible for front-back asymmetry in wind speed, while the asymmetric pressure field in the steering-flow case is mainly responsible for the left-right asymmetry in wind speed. These characteristics of the hurricane PBL wind field were proposed much earlier by Myers and Malkin (1961) on the basis of graphical integration of a vector equation of motion similar to equation (2), without lateral friction, but including both tangential and normal vertical friction forces.

A Consistent Surface Stress Parameterization

The model of Cardone et al. (1976)

29. Cardone et al. (1976) adapted Chow's model in order to specify hurricane surface winds in historical storms. While Chow's model provided a good qualitative description of the PBL wind field, Cardone et al. found it necessary to modify the model in several ways in order to attain good quantitative agreement between the modelled winds in real hurricanes and the limited amount of measured wind data available.

30. The model calibration rested mostly on the wind record measured on an oil rig directly in the path of Camille, 1969; at the time, this wind trace was believed to be the only existing accurate wind record representative of the surface boundary layer over open sea in a well-documented extreme hurricane.

31. The first modification made was to generalize the storm input parameter specification scheme adopted by Chow. The 3-parameter scheme, requiring only ΔP , R , and \vec{V}_c , was retained; as was the 4-parameter scheme, which adds an ambient geostrophic (\vec{V}_g) pressure gradient directed normal to the storm track, a so-called steering flow. A 5-parameter scheme allowed the angle between the storm track and the ambient gradient to be varied. Finally the option to specify Δp and R in equation 8 by storm quadrant was added, providing up to an 11-parameter scheme. The motion and pressure parameters, along with storm latitude, completely defined the integrated boundary-layer wind solution for a given storm.

32. The calibration against Camille data, and to a lesser extent Carla wind direction information, involved two major modifications to the model. First, it was necessary to modify the boundary layer depth formulation. Chow had assumed a constant depth of 1 km. In the modified version, the depth was allowed to increase toward the storm center from a minimum depth of 1 km at the storm periphery to nearly 2 km in the vicinity of the eye wall of intense storms. This modification primarily affected the directional properties of the integrated boundary-layer wind solution.

33. Second, since the model was needed to drive a wave prediction model which required wind data at 20 meter elevation, the wind speed calibration incorporated a scaling law to reduce the integrated boundary-layer wind to 20 meters. The law was found to be dependent on wind speed, with low winds reduced only slightly and winds of 50 m/sec reduced by about 60%.

34. The modified vortex model has been applied to the specification of the time history of surface winds in many historical storms (Ward et al., 1979) and in many recent storms which have affected the U.S. coast (Cardone and Ross, 1977; Ross and Cardone, 1977; Cardone and Ross, 1978). Since most hurricanes are not strictly in steady state (though the calibration storm Camille was remarkably so), a wind time history in a given storm is interpolated from several characteristic states computed from the vortex model, on the implicit assumption that there is a rapid mutual adjustment between the wind field and pressure field in hurricanes. The simulated storms all included some direct PBL wind data measured from offshore platforms, data buoys or aircraft. The model appears to provide a good surface wind description for a fairly wide range of storm types.

Shortcomings

35. Recent theoretical and field studies of the structure of the PBL in hurricanes have revealed several shortcomings in the modified model described above. First, with regard to the depth of the PBL, the evidence now suggests a much lower height than 1-2 km as assumed above. Moss (1978) studied the PBL turbulence structure from aircraft measurements for a peripheral portion of Eloise, 1975; the data support a PBL height of about 650 meters.

36. Moss and Rosenthal (1978) estimated PBL variables in two intense storms by applying Deardoff's (1972) PBL parameterization scheme to bulk data to compute the surface exchange coefficients. Cardone's (1969) relation for the roughness length was used and found to provide drag coefficients in reasonable agreement with previous estimates. The calculation included the estimation of the PBL depth under the assumption that the top of the PBL coincides with the cloud base, which was

taken as the lifting condensation level of surface air. Figure 4 shows the PBL depth calculated for the storms studied. A depth of 600-700 meters characterized both storms except near the eye wall where the depth lowers to about 500 meters. Finally, Chang (1977) added a PBL parametrization of contemporary formulation to a time dependent multilevel primitive equation model and derived the radial distribution of the PBL height in both steady and unsteady cyclones. Figure 5 shows that in the steady-state hurricane the depth varies between 380 and 450 m with the PBL height lifted slightly near the eye wall. The PBL height was not found to exceed these heights significantly in the several unsteady cases studied.

37. Another inconsistency in the model results from the retention of the drag law, equation (7), used by Chow. That law is actually intended for use with marine wind data at standard height (10 m). Since the drag coefficient decreases with increasing height in the PBL, the use of (7) with vertically integrated winds implies overestimation of the surface drag. In addition, new evidence (Figure 6) for the behavior of the 10 m drag coefficient; C_{10} , at sea reported by Garratt (1977) supports a Charnock-type roughness law

$$z_o = a \frac{u_*^2}{g} \quad (9)$$

where z_o is the roughness parameter, u_* is friction velocity and g is the gravitational constant. The Charnock constant a proposed was .0144 though the value is sensitive to the value assumed for the Kármán constant in the PBL model applied.

38. The scaling law adopted by Cardone et al. (1976) apparently compensates for the shortcomings noted above, at least insofar as the specification of the 20 meter wind speed is concerned. However, the computed surface wind is not consistent with the surface drag, which itself is likely to be incorrect. The integrated boundary-layer wind therefore is also likely to be in error in a given storm and is not suitable for the extension of the model solution to surfaces of arbitrarily specified roughness as required in this study.

39. In the next section, a revised PBL parameterization is adopted and shown to provide an accurate and consistent PBL wind and stress representation within the vortex model.

The revised PBL parameterization.

40. A new framework for parameterization of the fluxes of momentum, heat and moisture in the PBL has been developed within the past decade, beginning mainly with the work of Blackadar and Tennekes (1968) and Zilitinkevich (1969). The parametric relations result from the matching of mean profiles of wind, temperature, and moisture predicted by surface and outer-layer similarity theories for a PBL in which the flow is assumed to be horizontally homogeneous and quasi-stationary.

41. A particularly convenient form of the parameterization, first proposed by Deardoff (1972), expresses the PBL fluxes in terms of layer-averaged mean PBL properties. Deardoff's parameterization, combined with Cardone's roughness parameterization, was found by Moss and Rosenthal (1977) to provide reasonable results for hurricanes. The parameterization adapted here is taken from Arya's (1977) update of Deardoff's scheme.

42. The general form of the parametric relations may be written

$$\frac{ku}{u_*} = - (\ln \hat{z}_0 + A_m) \quad (10a)$$

$$\frac{kv}{u_*} = - B_m \text{ sign } f \quad (10b)$$

$$k(\theta_v - \theta_0)/\theta_* = - (\ln \hat{z}_0 + C_m) \quad (10c)$$

$$k(q - q_0)/q_* = - (\ln \hat{z}_0 + D_m) \quad (10d)$$

where u and v are the vertically integrated (as in equation 5) horizontal wind components (in the direction of the surface shear and perpendicular to it, respectively), θ_v and q are the mean layer virtual potential temperature and specific humidity, respectively, \hat{z}_0 is the roughness parameter normalized by the PBL height (z_0/h), k is von Kármán's constant, θ_* is a potential temperature scale expressed in

terms of the heat flux H , q_* is a specific humidity scale involving the moisture flux, and A_m , B_m , C_m , D_m are universal functions of dimensionless similarity parameters.

43. The Monin-Obukov length L may be expressed in terms of θ_* and u_* since

$$L = \frac{-U_*^3 \theta_v \rho c_p}{kgH} = \frac{-U_*^2 \theta_v}{g\theta_*} \quad (11)$$

44. There exist two competing theories for the form of universal functions. In one theory, known as Rossby-number similarity theory, the boundary layer height is uniquely determined by u_*/f and L . For the near neutral hurricane PBL, that theory predicts the PBL to increase as the ratio u_*/f increases toward the center of storms, in apparent contradiction to observation.

45. In the generalized theory, the depth of the PBL, h , is specified as an independent variable. Arya (1977) presents updated expressions for the similarity functions in terms of this generalized theory as follows:

$$\begin{aligned} A_m &= \ln\left(-\frac{h}{L}\right) + \ln\frac{fh}{u_*} + 1.5 \\ B_m &= 1.8 \frac{fh}{u_*} e^{-.2h/L} \\ C_m &= \ln(-h/L) + 3.7 \end{aligned} \quad \begin{aligned} & \frac{h}{L} \leq -2 \quad (12) \\ & \text{(unstable)} \end{aligned}$$

$$\begin{aligned} A_m &= -.96(h/L) + 2.5 \\ B_m &= .80(h/L) + 1.1 \\ C_m &= -2.0(h/L) + 4.7 \end{aligned} \quad \begin{aligned} & \frac{h}{L} \geq +2 \quad (13) \\ & \text{(stable)} \end{aligned}$$

For near-neutral conditions, $-2 < h/L < 2$, A_m , B_m , C_m are assumed to be given by linear interpolation between the above computed values at $h/L = \pm 2$.

46. In terms of the similarity relations (10), the drag coeffi-

cient with respect to the integrated PBL wind is

$$C_d = \frac{k^2}{[(\ln \hat{z}_o + A_m)^2 + B_m^2]} \quad (14)$$

while the angle β , between the surface wind and the integrated PBL wind is

$$\beta = \tan^{-1}(v/u) \quad (15)$$

47. To incorporate the similarity theory in the hurricane model, two cases were considered:

- a. Land. In a PBL over land, the following parameters are prescribed: f , z_o , h , $\theta_v - \theta_o$. The parametric relations then define the following functions

$$C_d = F_1(|\vec{V}|)_{f, z_o, h, \theta_v - \theta_o} \quad (16)$$

$$\beta = F_2(|\vec{V}|)_{f, z_o, h, \theta_v - \theta_o} \quad (17)$$

- b. Water. Over water, the roughness parameter is not known but can be expressed in terms of u_* through a Charnock-type relation (equation 9) or the form proposed by Cardone (1969). The parametric relations can then be solved for

$$C_d = F_3(|\vec{V}|)_{f, h, \theta_v - \theta_o} \quad (18)$$

$$\beta = F_4(|\vec{V}|)_{f, h, \theta_v - \theta_o} \quad (19)$$

48. Arya (1977) gives solutions graphically only for the condition $fh/u_* = 1$, in which case C_d and β can be expressed, for a given latitude, in terms of z_o and a bulk Richardson number. In this form, the theory is an updated version of Deardoff's scheme, which did not include dependence of A_m , B_m , C_m , D_m on fh/u_* . In general, however, fh/u_* or z_o are not known a priori; equations (10-15) are solved by iteration starting from an initial guess on u_* .

49. In order to avoid the prohibitive computational expense of solving equations 10-15 iteratively at each grid point within the numerical vortex model, the assumptions are made that over water the air-sea

temperature difference and boundary layer height can be considered to be invariant over the domain of the storm. In view of the preceding discussion on h , this appears to be a reasonable approximation. Except for hurricanes crossing major ocean-current boundaries, the assumption of horizontal homogeneity of $\theta_v - \theta_o$ also seems reasonable, especially for Gulf of Mexico and lower U.S. East Coast hurricanes. Little is known about the characteristics of the PBL in hurricanes over land. However, given the high level of turbulent mixing there in hurricanes, it is reasonable to assume that an adiabatic lapse rate is established and that at least in the near-coastal zone, the boundary layer depth is close to that assumed for the over-water case.

50. Given the above conditions, the parametric relations F_1 , F_2 , F_3 , F_4 can be found once for a given storm by iteration, and expressed in terms of tables. In practice, the upwind and crosswind drag coefficients, the ratio $u_x/|\vec{V}|$ and the angle, β , between the surface wind and the integrated wind are computed for $|\vec{V}| = 0.8(.8)80$ m/s and tabled. Values for intermediate wind speeds are found by linear interpolation.

Test results for the general parameterization

51. The behavior of the over water drag coefficient for typical hurricane conditions ($\theta_v - \theta_o = -2^\circ\text{C}$, $h = 650$ m, $f = 10^{-4}$) according to the general parameterization is shown in Figure 7. The over water cases are computed for two separate values of the Charnock constant: .0144 and .035. The former value was recommended by Garratt (1977). However, in this model, $k = .35$, to be consistent with the Arya formulation, and $a = .035$ provides a better fit to the 10 meter drag coefficient measurements analyzed by Garratt. The drag coefficient for the land case is for a roughness parameter of .08 m, a boundary layer depth of 650 m and neutral stability. For comparison, Figure 7 also includes the form adopted by Chow.

52. While it is reasonable to expect the new theory to yield drag coefficients lower than equation (7), the magnitude of the decrease and the form of the wind dependence seen was surprising. The revised parameterization was tested in the numerical vortex model with the Camille

inputs used in the study of Cardone et al. (1976). The revised solution was referred to 20 meters by solving

$$V_{20} = \frac{u_*}{k} \ln \left(\frac{20}{z_0} \right)$$

where u_* and z_0 are determined by the numerical model, since for typical hurricane conditions, stability effects can be neglected in the surface layer.

53. Figure 8 compares the new solution and that derived by Cardone et al. Clearly, the general parameterization is underestimating the surface stress and therefore the surface wind. The difficulty with the general Arya formulation was traced to the dominating influence of the scale-height ratio fh/u_* on the similarity variables. This parameter was added by Arya mainly to describe the relative influence of the Coriolis force in an Ekman-type layer over a wide range of latitudes. In a hurricane, however, the parameter varies over two orders of magnitude because of the variation of u_* over an extreme range (typically 0-200 cm/sec) over a short distance. Considering the highly curved nature and spatial inhomogeneity of the flow in the hurricane PBL, that parameter is apparently irrelevant. Its influence was controlled therefore by restricting the solution to $fh/u_* = 1$.

54. The results of restricting the scale-height ratio to unity were dramatic. The revised dependence of drag coefficient on wind speed is shown in Figure 7 and the revised 20-meter wind profiles in Camille, for two boundary layer heights ($h = 650, 325$ m) are shown in Figure 8. The comparisons of modelled and measured wind speeds at Rig 50 in Camille for three PBL heights are shown in Figure 9. In the range of $h = 325-650$ m, the new theoretical calculation fits the measurements as well as the calibrated solution of Cardone et al. (1976).

Properties of the over-water solution

55. The final PBL parameterization chosen for the over-water case consists of the Arya (1977) parameterization, with the scale height ratio restricted ($fh/u_* = 1$) and with the crosswind drag term retained both in the calculation of the surface stress in the numerical solu-

tion and in the derivation of surface-layer wind direction from the integrated boundary-layer wind direction. The Charnock constant, a , is assignable as is the value of k . However, since a value of k of .35 is consistent with Arya's model, an a of .035 provides a better fit to Garratt's (Figure 6) drag coefficient data than the value suggested by Garratt.

56. The properties of the new over-water hurricane wind model solution are most directly seen in the relatively simple case of a stationary, symmetric vortex. The solution may then be compared more readily to the gradient wind. This is done in Figure 10 for a stationary symmetric vortex with the scale radius ($R_p = 12$ n.mi)* and pressure anomaly ($\Delta p = 105$ mb) of Camille. Note that the comparisons are only made at and outside the radius of maximum wind, since inside that radius, truncation errors remain fairly large for a small storm such as Camille.

57. The vortex model predicts integrated PBL winds which are supergradient within a radius of about $3 \times R_p$. The 20-meter winds, however, vary from 75 to 85% of the gradient wind. The surface inflow reaches a maximum of 25° at a radius of about $5 \times R_p$ and decreases sharply at the eye wall. These features are entirely consistent with those deduced by Shea and Gray (1973) from composited low level aircraft data in hurricanes. Comparisons of modelled and measured winds over water in several recent storms will be presented in a later section.

Numerical Experiments over Mixed Terrain

58. The similarity PBL theory as modified above may be easily applied to the specification of C_D and β in the hurricane PBL over land. For a neutral PBL, the revised theory predicts that C_D and β are functions only of z_0 . For h of 500 m, some typical values of C_D (β) are 1.78×10^{-3} (13.6°) for $z_0 = .04$ m and 2.54×10^{-3} (16.3°) for $z_0 = .16$ m.

59. The revised theory was tested in two ways. First, the numerical model was solved for the steady state wind field in a stationary

* A table of factors for converting non-SI units of measurement to SI (metric) units is presented on page 4.

symmetric intense hurricane situated entirely over homogeneous terrain. While this case is unrealistic, it was intended to provide an indication of the sensitivity of the numerical solution to a greatly increased drag. Second, the solution was sought for the more realistic case of an intense hurricane situated at the coast with terrain of homogeneous roughness under the northern half of the storm and open sea beneath the southern half. The storm was stationary since only in such a case is the numerical model, formed in a moving coordinate system, rigorous.

60. Solutions typical of both cases are shown in Table 1 where they are compared to the open-sea solution discussed above. The cases were run with symmetric stationary Camille inputs. The all-land case returned a symmetric solution as expected. The case shown is for $z_0 = .08$ m, which is typical of open, level, countryside with low vegetation. Within about 200 km of the eye, the integrated PBL wind is found to be larger than the open-sea case, though surface winds are slightly lower. The inflow angle is about 50% greater than the open-sea solution. In effect, the increased surface drag results in a more intense vortex for a given pressure field, reflecting the well known dual role of friction in tropical cyclones. In nature, decreased evaporation is largely responsible for hurricane decay over land, and rapid decrease in PBL winds.

61. Two typical examples of the mixed land/sea solution are shown in Table 1. The solutions in these cases were quite asymmetrical. In general, the solution over-land matched quite closely the solutions found in strictly over land cases for comparable z_0 . However, over-water, the solution departed significantly from the reference over-water case. In particular, for all values of land roughness attempted, the PBL winds over water downwind of land increased to values above the all-water case, thus causing the formation of a distinct wind maximum in the left rear quadrant (with respect to north) of the storm.

62. In Table 1, the vertically integrated winds over sea in the mixed land/sea solution are taken along a radial extending south from the storm center. For a land z_0 of .04 m the maximum wind over water

Table 1

Comparison of over water, over land, and mixed terrain radial wind speed profiles in vortex model numerical solutions for a stationary, symmetric storm with pressure profile parameters $\Delta p = 105$ mb, $R_p = 12$ n.mi., and modified ($f_h/U_* = 1$) Arya (1977) similarity PBL parameterization.

R	Vg	Over water		Over land $z_0 = .08m$		Half land/sea $z_0 = .04m$		Half land/sea $z_0 = .32m$	
		\vec{V}	V ₂₀	\vec{V}	V ₂₀	\vec{V} sea	\vec{V} land	\vec{V} sea	\vec{V} land
800	6.9	7.2	7.2	7.3	5.1	7.3	7.3	7.1	7.3
400	20.6	20.2	19.7	18.6	13.0	20.3	19.0	20.3	17.5
200	42.3	41.2	34.9	37.9	26.5	41.5	38.7	41.8	35.5
100	66.5	67.0	53.5	64.5	45.1	69.0	64.7	70.4	61.0
50	90.7	94.2	72.7	97.2	67.9	100.2	91.7	104.9	88.6
40	97.6	102.4	78.3	108.1	75.5	110.0	99.3	116.9	95.1
30	105.2	108.4	82.4	116.9	81.7	116.7	104.6	129.4	98.9
20	111.2	112.5	85.2	117.0	81.8	116.9	109.6	133.9	103.5

Explanation of table:

- R radial distance from hurricane center (km)
- Vg magnitude of the gradient wind
- \vec{V} integrated boundary layer wind speed
- V₂₀ 20 meter wind speed
- \vec{V} |sea in mixed terrain solution, the over-sea values are taken from radial over sea extending out from eye (at coast) normal to coastline.
- \vec{V} |land as above except radial extended over land

All wind speeds are expressed in knots.

is increased about 5% over the all-water case, and about 15% for a land z_0 of .32 m. Even greater increases were found in the left rear quadrant. A similar experiment for actual Camille inputs (not shown) led to comparable results, showing an unrealistic speed maximum in the left rear quadrant, whereas the nominal over-water Camille solution displayed a maximum in the right hand quadrant.

63. It is difficult to explain the precise cause of the anomalous model behavior in the mixed-terrain case. Test cases were run with modified over-land drag laws derived from Rossby-number similarity theory but no change in the basic structure of the solution was noted. The solution was verified to be steady-state in trial integrations carried out for 1600 rather than 800 iterations of the vortex model. Indeed, the behavior might be attributed to the basic model formulation, which forces a steady state solution unrealistically. However, in an experiment with a three-level, three-dimensional nested-grid numerical model, reported by Moss and Jones (1978), behavior similar to that found here has been seen in a simulation of an intense hurricane approaching the coastline. In their integration, it was noted that as the hurricane approached the coastline, even though the sea-level pressure in the storm began to rise, a transient wind-speed maximum greater than found in the all-water control case was established over water on the landward side of the vortex and extending to the left side of the circulation (looking down the track toward land).

64. Moss and Jones attribute the anomalous behavior of the wind field near landfall to changes in the pressure field induced by greatly increased inflow in the part of the wind field over land. In our simulation, however, the anomalous behavior is present even though the pressure field is fixed. More likely, the behavior is caused by the simplified treatment of the PBL vertical structure and the neglect of boundary-layer-adjustment processes which occur on vertical scales of the order of the depth of the PBL and on horizontal scales of the order of the grid spacing.

65. Basic knowledge of the behavior of the PBL flow across discontinuities in roughness is in a remarkably inchoate state.

The theories fall into two classes: (1) those which treat surface boundary layers only (e.g. Elliott, 1958); (2) those which treat the Ekman layer as a whole. Nearly all the available field data are restricted to the former case: there is considerable evidence that upon crossing a change in surface roughness, the wind profile is modified from below as a new (internal) boundary layer grows in thickness at a rate which depends upon stability and roughness. As a crude rule, the new boundary layer is established to a height given by one tenth the distance to the upwind change in roughness. If we were to extend this rule to the hurricane PBL, whose height is typically 500 m, we would expect the flow to adjust within 5 km. However, the more general Ekman-layer adjustment theories (e.g. Taylor, 1969) suggest a more complicated process, in which the wind-speed profile near the surface adjusts rapidly as in the surface-layer theories, but in which the surface stress, the turbulence structure and the wind direction take much longer (by nearly an order of magnitude) to attain equilibrium with the new surface. The theory and scant available data (Jensen, 1978) suggest also that the process is not symmetrical with respect to roughness transitions with the adjustment from rough to smooth conditions taking place at a slower rate than from smooth to rough. It appears therefore that the basic process of PBL adjustment in hurricanes needs to be better understood before the simulation of PBL flow across discontinuities within numerical hurricane models can be improved.

Equilibrium Theory Terrain Transformations

Empirical Evidence

66. The numerical experiments described above indicated that the numerical model could not of itself provide reliable wind fields over terrain of arbitrary roughness. This raised three questions:

- (a) are fetch effects near roughness discontinuities important enough to be accounted for empirically in the specification of surface winds in hurricanes?
- (b) can over-land PBL winds be prescribed from the over water numerical solution?

- (c) are winds over lakes such as Pontchartrain and Okeechobee different from winds over open water, apart from fetch effects, other factors being equal?

67. Extensive empirical studies of the effect of fetch on winds over water downwind of the coastline have been reported by Richards et al. (1966) and Phillips and Irbe (1976), who processed large data sets obtained around and in the Great Lakes. Both studies employed the same analytical method. Extensive series of simultaneous surface wind measurements from coastal land stations and downwind ships and buoys were paired and stratified by wind speed, fetch, and stability. Both studies employed the same fetch and stability classes. The stability was parametrized by the temperature difference (land air minus lake water).

68. The problem of concern here is the adjustment of the surface wind over a shallow inland lake of the dimensions of lakes Pontchartrain and Okeechobee (fetch < 40 n.mi) in hurricane conditions. The latter are characterized by winds > 8 m/sec and near-neutral stability. The data of Phillips and Irbe, and Richards et al., in those wind-speed and stability categories are plotted in Figure 11. Clearly, up to a fetch of at least 40 n. mi., no significant trend with fetch is evident in the wind-speed ratio (over-land ÷ over-water). The ratio tends to be slightly larger for the more recent study, because the over-water winds in the recent study were measured at 3 meter height while in the study of Richards et al. the anemometer height was 10 meters. Since the first fetch class covered the range 0-5 n.mi., the implication is that the wind speed over the lake in the indicated classes and at heights up to 10 m attained equilibrium with the lake surface within the first few miles of the coast. This behavior is consistent with the height-to-fetch ratio of 1:10 noted above for surface layer adjustment.

69. It should be noted that, in both of the studies cited, a dependence of the wind ratio on fetch is proposed. The dependence however appears mainly in data from low wind speed (< 8 m/sec) classes and very stable or unstable stability classes. The fetch dependence therefore probably is caused by an adjustment of the turbulence in the PBL due to changes in stability rather than in surface roughness and is therefore

not likely to be important in the hurricane environment.

70. An interesting corroborative piece of evidence has been provided recently by remote sensing data. The Seasat mission has proved that the marine surface wind speed as might be measured at 10 m height from say a data buoy, can be measured by a radar scatterometer to an accuracy of 1 m/s or better. The radar backscatter cross-section of the sea surface (σ_0) therefore appears to be mainly dependent on surface stress and wind speed (Jones et al. 1978). Ross and Jones (1978) reported several aircraft experiments in which a scatterometer was flown directly downwind off the U.S. East Coast in moderately strong offshore wind conditions. The σ_0 measurements were plotted versus fetch (Figure 12), beginning within 1 km of the shoreline. There was found to be no fetch dependence at least to 40 km offshore, which suggests that the surface stress, the friction velocity, and the surface wind speed adjusted quickly to the surface roughness.

71. The above studies all suggest strongly that the adjustment scale for near-surface wind speed in strong-wind, near-neutral conditions is a few kilometers at most, which is a small distance compared to the dimensions of lakes Okeechobee and Pontchartrain. A dependence of wind speed on fetch may therefore be omitted. The situation with regard to wind direction is not as clear. There are no comparable field data for the adjustment of PBL wind direction across a roughness discontinuity. The available theories suggest a much longer adjustment scale. In the adopted scheme, no fetch-dependent adjustment for wind direction is incorporated; however, the case is allowed whereby the wind speed adjusts to the lake roughness immediately while throughout the lake, the wind direction is computed in accordance with the roughness of the terrain surrounding the lake (subroutine BREEZE/SPECIAL). This is correct if the adjustment scale for wind direction in the PBL is larger than the lake dimension. Field measurements are required to test this hypothesis.

72. Apart from fetch considerations, the surface winds over a large lake in hurricanes might be different from equivalent over-ocean winds because of differences in the surface roughness between a lake and

open sea. That is, the drag coefficient over a lake might be different from the drag coefficient over open sea, particularly for uniformly shallow lakes in which the surface wave structure can be expected to differ significantly for a given wind from deep-water surface waves. Unfortunately, the correct drag formulation for a shallow lake is much less certain than for the sea. Whitaker, Reid and Vastano (1973) have inferred a drag law for Lake Okeechobee which is quite different from the form proposed by Garratt. The scheme adopted below therefore includes the allowance for the specification of over-lake winds relative to an altered lake specification of surface roughness.

The Transformation Model

73. In this section a simple model is proposed to derive the surface wind and stress over terrain of arbitrary roughness from the numerical wind-field solution computed exclusively from the revised over-water drag formulation. The approach is to employ equilibrium PBL theory to relate the over-water integrated PBL wind to the flow at the top of the PBL and then to employ a consistent equilibrium model to compute the surface wind stress from the wind at the top of the PBL for terrain (including lakes) of arbitrarily specified roughness. The model proposed assumes that the PBL over land or inland lakes in a hurricane is neutrally stratified.

74. The transformations are derived quite simply from consideration of the alternate forms of the similarity PBL theory adapted in this study. To parameterize the surface drag in the numerical vortex model we applied equations 10a and 10b which relate the stress to the integrated PBL wind. Alternatively (Arya, 1977), the surface drag may be referenced to the wind at the top of the PBL u_h, v_h :

$$\frac{ku_h}{u_*} = - (\ln \hat{z}_0 + A) \quad (20a)$$

$$\frac{kv_h}{u_*} = - B \text{ sign } f \quad (20b)$$

or to the surface geostrophic wind components

$$\frac{ku_g}{u_*} = - (\ln \hat{z}_0 + A_0)$$

$$\frac{kv_g}{u_*} = - B_0 \text{ sign } f$$

As noted by Arya, A_0 and B_0 may be expected to differ from A and B due to the presence of baroclinicity and also in very low latitudes where winds are strongly geostrophic. In hurricanes, baroclinicity in the PBL may be ignored, but the flow at the top of the PBL is more nearly in gradient balance. The effects of curvature on A , B have not been studied, but the success achieved with the similarity PBL theory in the over water case suggests that such effects are not large. In this model, differences between A , B and A_0 , B_0 are ignored.

75. The relationship between A_0 , B_0 and A_m , B_m is given by Arya (1977) as derived from the equations of mean motion for a barotropic atmosphere in which the momentum flux is assumed to vanish at $z = h$:

$$A_m = A_0 \quad (21a)$$

$$B_m = B_0 - k (fh/u_*)^{-1} \quad (21b)$$

For the restricted case of $fh/u_* = 1$, which we have adopted only for the purposes of attaining a workable parameterization, it can be shown simply from equations 10, 20 and 21 that the flow at the top of the PBL, $z = h$, is related to the vertically integrated flow through

$$u_h = u \quad (22a)$$

$$v_h = v - u_* \quad (22b)$$

In the coordinate system adopted (see Figure 13), v_m is negative, u_* is always positive so the wind speed at the top of the PBL is always larger than and turned clockwise (in the Northern Hemisphere) with respect to the mean layer wind \vec{V} .

76. Given the wind at the level h , the consistent similarity theory defined by equations 20a and 20b may be solved for the surface stress and surface layer wind in a neutral PBL over terrain of specified roughness z_0 . For a neutrally stratified PBL, A_0 and B_0 are reduced simply to constants (1.39, $1.95 + k$, respectively). If z_0 is a constant, as say over a homogeneous land surface, u_{*} may be obtained directly from equations 20a and 20b. However since over a lake, the roughness probably depends on u_{*} , z_0 may in general be prescribed in terms of u_{*} using the general form proposed by Cardone (1969).

$$z_0 = C_1 u_{*}^{-1} + C_2 u_{*}^2 + C_3 \quad (23)$$

where C_1 , C_2 , C_3 are constants to be chosen to impose a desired drag law. (For example, for a Charnock law, $C_1 = C_3 = 0$, $C_2 = a/g$; for land, $C_1 = C_2 = 0$, C_3 is the roughness parameter for the terrain type).

77. The implementation of the above model in the specification of hurricane surface wind fields over terrain of arbitrary roughness or lakes is coded as subroutine UPDOWN, which allows for the calculation of transformations for up to six terrain categories, for each of which roughness constants C_1 , C_2 , C_3 have been specified. The procedure followed is:

- a. Given the integrated boundary layer wind u , v and the conditions of a given hurricane over water (h , $\theta_a - \theta_0$, f , k , a) compute u_{*} from the revised over water similarity parameterization.
- b. From equations 22a, 22b, compute the wind speed and direction at level h , the top of the PBL.
- c. For each terrain roughness, specified in terms of equation 23, use the neutral similarity model (20a, 20b) to compute the friction velocity appropriate to the terrain roughness, u_{*t} , the ratio $u_{*t}/|\vec{V}|$, and the angle between the surface stress and the integrated wind. The ratio and the turning angle are computed for $|\vec{V}| = 0.8(.8)80.0$ m/sec, for each roughness category and stored for use in the specification of surface winds in a given simulation over a grid covering different terrain types.

78. The overall behavior of the transformations is exemplified in Figure 14, which shows the ratio of surface wind speeds at 20 meters (over-land ÷ over-sea) and the difference between the over-land and over-sea inflow angle for two terrain roughnesses: .04m, .32m. For comparison, Figure 14 shows the results for the wind-speed ratio derived from numerical mixed-terrain and over-water solutions for a symmetric stationary vortex (radius and pressure drop as in Camille). To arrive at the indicated quantities, the surface wind speed and direction along a radial extending north of the eye over land in the mixed terrain case was referenced to the (symmetrical) solution along the radial for open ocean. It should be recalled that in the mixed-terrain solution, the wind field over land looked quite reasonable. Apparently, that solution can be retrieved quite simply from the over-water solution using the equilibrium model described above. It is also interesting to note that the form of the dependence shown in Figure 14 conforms quite closely to the empirical wind-speed ratio derived from measurements in hurricanes in and around Lake Okeechobee (U.S. Weather Bureau, Hydrometeorological Section, 1954).

Results for Test Storms

79. In this section, the results of calculations of the entire history of the surface wind field in selected hurricanes are checked at measurement locations at which representative surface wind measurements are available. Indeed, the storms were chosen because over-water wind measurements and, in some cases, representative over-land wind measurements were available, and because extensive analyses of storm pressure and track characteristics had been performed in previous studies. Results are presented for hurricanes Camille, 1969; Betsy, 1965; Delia, 1973; Belle, 1976; Anita, 1977; and the Lake Okeechobee (LO) storm of 1949. Comparisons against over water winds are made in Camille, Delia, Belle, and Anita. A limited evaluation of over-land and over-lake winds in Camille and the LO storm is made. Finally, sample results for Betsy are presented without comparison against measurements, as no represen-

tative measured winds over land or lake are available in that storm.

Camille

80. Hurricane Camille played a crucial role in the calibration of the method developed by Cardone et al. (1976), because at that time, the wind trace in Camille from Rig 50 was deemed to be the only extant representative over-water wind trace in an intense hurricane. Indeed, the empirical law developed by Cardone et al. to scale integrated boundary layer winds to standard anemometer height was based largely on that wind trace. In the present scheme, the assignable model parameters are physical quantities related to fundamental properties of the planetary boundary layer model (PBL height, stability, roughness parameter formulation). Also, the method provides the wind speed as might be measured at any height in the constant-stress surface boundary layer, which in hurricanes may extend to a height of at least 50 meters.

81. The comparison of measured and modelled wind speed at Rig 50 at measurement height in Camille is shown in Figure 15. The agreement is at least as good as that achieved by Cardone et al. (1976). Results for two boundary-layer heights are shown. The numerical solutions differ little, except near the eye, where the lower height ($h = 500$ m) matches the peak measured wind better. This may reflect the fact that near the eye of intense hurricanes, the PBL height lowers slightly. Since the solutions differ little outside the eye, it is perhaps prudent to use a PBL height of 500 m in simulations of strong storms in the Gulf of Mexico.

82. To generate modelled surface-wind time histories at land sites requires knowledge of the roughness parameter representative of the terrain. Typical z_0 values for various terrain types have been given by several workers (e.g. Figure 16 after ESDU 72026, 1972). The roughness parameter is very sensitive to the terrain type within a few kilometers of a given measurement site, and therefore often varies significantly with wind direction at a site. For the sites at which winds have been measured in the selected hurricanes, the roughness parameter has not been determined experimentally. We therefore depict modelled time histories covering a reasonable range of roughness parameters at

land sites. Also, with the exception of the lakefront comparison in Camille, comparisons are restricted to only those measurement sites at which the anemometer was recorded on strip chart, from which 30-minute average wind speed and direction could be extracted.

83. Figure 17 compares measured and modelled winds at Keesler Air Force Base, Biloxi, Mississippi. The anemometer at Keesler is mounted 16 feet above the runway surrounded by fairly level terrain but with the coast less than a block away to the southeast. The anemometer measured winds up to the time of eye landfall at 0000 CDT. Measured wind directions support an over land trajectory up to about 2300 CDT and an over water trajectory thereafter. The modelled wind history for z_0 of .16 m, compares favorably with the measurements up to 2300 CDT; after which the measurements agree better with an equivalent over-water history (also shown in Figure 17). Modelled wind direction is generally within 20° of that measured.

84. The anemometer at Burwood CGS, Southwest Pass, is in a complex environment, with at least some influence of land to be expected, especially for wind directions between northwest and northeast. The wind comparisons in Figures 18 and 19 show better agreement in wind direction for an assumed over-water exposure. For wind speed, however, over-land histories agree better, but the effect of a shift in wind direction to an off-water direction (1800-2000 CDT) can clearly be seen in the measured wind speed.

85. Since fetch effects are not built into the present model, the Burwood and Keesler comparisons present worst-case examples of limitations of the present scheme. Nevertheless, the results appear accurate enough for specification of over-land winds in the coastal zone.

86. An important function of the present model is to specify winds over Lake Pontchartrain in hurricanes. The scheme adopted includes the provision for the specification of winds over the lake different from winds over open water in two ways. First, surface wind speeds may be computed relative to a z_0 specified for lakes which differs from the Charnock law assumed over water. Second, the program accomodates the condition, discussed earlier, whereby the surface layer

wind speed and stress are assumed to adjust to the lake roughness on length scales small compared to the lake width, but the PBL wind direction is governed by the roughness of that terrain upwind of the lake.

87. There is virtually no data on the roughness properties of Lake Pontchartrain. Whitaker, Reid and Vastano (1973) have deduced a drag law for Lake Okeechobee which differs substantially in level and wind dependence from equation 9. Their form was fit to equation 23, and was used to provide test wind histories at measurement sites around and in the lakes in the test simulations. (The form of equation 23 does not provide a particularly accurate fit to the odd form proposed by Whitaker et al., but is within about 20% over the range 10-50 m/s.)

88. The model was used to specify surface wind speed at the location and measurement height of Lakefront Airport, New Orleans, in Camille, for both water and lake roughness laws (Figure 20). The wind direction was computed for the water z_0 and for the special case described above, assuming an upwind terrain roughness of 1 m. Observed 1-minute hourly surface winds from the airport station are also plotted. Quantitative comparison of wind speeds is not warranted because the measurement is poorly averaged and the measurement site may not be representative of over-lake conditions. The reported wind directions should be more representative; the comparisons there suggest that there may indeed be a larger inflow angle for winds over Lake Pontchartrain in hurricanes than returned by the nominal over-water or over-lake transformation. Higher quality measurements in the lake in storm conditions are required to verify this possibility.

89. Figure 20 also shows the wind speed over downtown New Orleans, at 85 feet, calculated with a z_0 of 1 m. Time-averaged measured winds are not available for comparison.

Delia

90. Forristall et al. (1977), using the method of Cardone et al. (1976), ran a simulation of hurricane Delia in order to produce a wind field as accurate as possible, permitting the simulation of the surface wind and current at Buccaneer tower, offshore of Galveston, Texas. Thus

the storm parameters and track were adjusted, within their range of uncertainty, to produce best agreement between measured and modelled winds at the tower. Those storm parameters and track were used, without alteration, as input data to the present scheme and the wind field was computed. The boundary layer height was specified as 500 m.

91. The comparison of measured and modelled wind speed and direction in this storm is shown in Figures 21 and 22. The agreement in wind speed and direction is generally excellent, except for about an 10-20° excess of inflow in the modelled wind directions. Slight alteration of the input parameters and track of this poorly organized highly erratic storm would probably have provided even better agreement.

Belle

92. The wind and wave fields in hurricane Belle have been modelled by Cardone and Ross (1979), using both the methods of Cardone et al. and simpler parametric schemes. Belle moved rapidly up along the east coast. As it did so, the central pressure rose sharply and the eye diameter increased. This storm, therefore, provides a critical test of the present method, which simulates such time changes in terms of a series of steady-state numerical solutions.

93. The center of Belle passed directly over two NOAA data buoys, one EB15 located offshore South Carolina; the other, EB41, located east of New Jersey. As for the Delia simulation, the storm input parameters and storm track determined by Cardone and Ross (1979) was used without alteration to drive the present model. Four steady-state solutions were utilized to attempt to accommodate the rapid changes in storm intensity, shape and speed.

94. The modelled and measured time histories are compared at sensor height at EB15 and EB41, in Figures 23, and 24. Agreement is generally excellent. The departure between modelled and measured wind direction early in the EB41 history is related to the presence of a frontal trough of low pressure which was located off the New Jersey coast and which distorted the pattern of isobars in the forward quadrants of the storm.

Lake Okeechobee Storm of 1949

95. The Lake Okeechobee storm of 1949 has been the subject of much past study. It is particularly important because winds were measured over the lake with calibrated anemometers mounted at 10 meters height. The wind data had been reduced to 10-minute averages by the Hydrometeorological Section, U.S. Weather Bureau. For the comparisons shown in this study, the data were reduced further to 30-minute averages, to be more consistent with the implied averaging interval of modelled winds.

96. Storm input parameters were specified as objectively as possible from the data published on this storm. While there is considerable storm data from the lake stations, there remains some uncertainty in the precise storm track; particularly east of the Florida coast and as the storm recurved northwest of the lake. There is also some uncertainty in the filling rate. In our simulation, no filling is applied until just after the eye of the hurricane has crossed the lake. Storm pressure input parameters ($p_0 = 954$ mb, $R = 22$ n.mi.) prior to the filling stage were taken directly from Graham and Hudson (1960), while the steering flow was estimated from historical Northern Hemisphere Surface Analyses. The four-parameter (Δp_c , R , V_c , V_g) pressure initialization scheme was adopted since the storm appeared to translate in the direction of the steering flow. There did not appear to be sufficient data in this storm to estimate Δp and R by quadrant. Storm track was taken from published track charts, though it is not clear whether the track relates to the pressure center or the center of surface wind circulation.

97. Surface winds were measured reliably at two locations within the lake, stations 14 and 16, shown in Figure 25. The same figure shows the path of the storm schematically. Surface winds were computed for two roughness categories: (1) the over-water Charnock law; (2) the roughness specification, equation 23, with constants consistent with the Lake Okeechobee drag law of Whitaker et al. (1973).

98. Measured and modelled winds at the lake stations are shown in Figures 27 and 28. The histories cover the period from about 8 hours before the occurrence of maximum wind on the lake, at which time the

storm center was between Nassau, Bahamas and West Palm Beach, Florida, and the 8-10 hour period after the occurrence of maximum winds, when the storm was filling rapidly and recurving northward over central Florida.

99. The wind speed comparisons show that in general the lake roughness histories compare better with the measurements than the over-water specification. There is one serious discrepancy between modelled and measured wind speeds: this occurs over a two-hour period just after the occurrence of maximum winds, when the modelled winds show a significant drop before rejoining the measurement history. The measurements also show a drop but to a much lesser degree. The double maximum suggests that the stations "entered" the eye briefly on the western side of the hurricane and that this effect was accentuated in the simulation perhaps because the offset between the wind circulation center and the pressure center was larger in the numerical model than actually occurred. Another possibility is that the pressure field in this storm was simply more complex than could be described by three parameters.

100. The modelled wind directions agree well with measurements at Station 14 in the forward quadrant of the storm and at Station 16 in the rear quadrant of the storm; otherwise systematic departures of 20-40° are evident. The sense of the discrepancy is that there is less inflow than modelled in the forward quadrants and more inflow than modelled in the rear quadrants, over the lake. Frictional effects associated with the presence of roughness boundaries are not as likely to be the cause of systematic effects of this nature as are differences between the actual large scale pressure field in this storm and the one simply modelled.

Betsy

101. Hurricane Betsy served to test the complete history program, including the specification of surface wind fields over a rectangular high resolution grid, each hour, throughout a 24-hour history run. Input data and sample output fields are included in Appendix C.

102. As a part of the test, surface wind histories were calculated at several locations around Lake Pontchartrain. Figure 28 displays sample wind histories for Lake Pontchartrain at Lakefront (open water

roughness), Lake Pontchartrain at Lakefront (Whitaker et al. lake roughness), New Orleans Moisant Airport ($z_0 = .16$ m) and the U.S. Weather Bureau Office city office, New Orleans ($z_0 = 1$ m). No attempt is made to compare these calculated histories to measurements.

Anita

103. Hurricane Anita was one of the most intense hurricanes of historical record to cross the Gulf of Mexico. The storm formed in the east central Gulf of Mexico on August 28, 1977 and moved west-southwestward into Mexico on September 02, 1977, sparing populated areas from its fury. Anita passed about 50 n.mi. north of NOAA buoy EB04 on the 30th as a poorly organized but deepening tropical storm and about 10 n.mi. south of EB71 early on September 01. As the storm moved past EB71, it was much better organized and undergoing explosive development. The general path of the storm and the time history of central pressure are shown in Figure 29.

104. Four steady-state solutions were generated for Anita, corresponding to the storms' parameters at the times indicated in Figure 29. The radius to maximum wind in Anita contracted from 30 n.mi. at the time of the first solution to 15 n.mi. at the last solution. The four solutions were used to interpolate winds in space to the buoy locations over a 48 hour period.

105. The modelled wind series at the locations of the buoys are compared to the winds measured at 20 meter height in Figures 30 and 31. At EB04, the agreement is surprisingly good considering the poorly organized nature of the storm during the period shown. Agreement is generally very good also at EB71. As suggested by the Belle test, the steady-state model provides reasonably good simulations even when applied to storms undergoing rapid changes in intensity and structure.

PART III: THE COMPUTER PROGRAM

Program Description

. The program task which produces tropical storm wind histories at specified locations is divided into two main programs. The first, SNAP, produces snapshot wind fields on a nested grid and writes them onto an output data file from which the second program, HIST, obtains nested-grid wind fields for each hour of the storm's history, using linear interpolation if necessary. HIST then gets and prints the wind history at each measurement station specified, and, if requested, writes the wind history for a different grid onto an output data file.

. The programs were written in Fortran V and were run on a UNIVAC 1108 computer. Each snapshot takes approximately 6 minutes of computer time, and execution of program HIST usually takes less than 3 minutes. Some mass storage is required, the amount varying with the number of snapshots, the number of interpolations between snapshots, the length of the history, and whether or not winds are to be interpolated to an output grid; 250,000 words is sufficient for most storms. Substitution of tapes for mass storage is possible, but efficiency would be decreased.

. Program SNAP is composed of:

MAIN

- Together with its subprograms, produces one or more snapshot wind fields on a nested grid according to card input specifications. It prints the computed winds and writes them onto an output file, and it optionally prints corresponding pressure fields and initial guess winds. MAIN itself reads all input cards, calls subroutine CCROSS which sets up tables, calls BLOWUQ which controls computation of the winds, and writes the final snapshot wind fields onto the output file.

SUBROUTINE AANGEL - Converts grid components (UN , VN) of integrated wind to speed (VTN) and direction (ANG) for all points of the 21 x 21 x 5 wind grid. In addition, if

the switch variable $I20 \neq 0$, AANGEL reduces the speed (VTN) to a height of 19.5 m; TWIST, the necessary correction to ANG, is computed by interpolating the array TURN; u_* is computed by interpolating the array UXV containing u_*/V_m ; anemometer wind is computed from u_* (called UXX in the code) by the usual logarithmic profile.

Arguments: input, typing implicit
 I20: Flag, if non-zero winds are reduced to 19.5 meters.

- SUBROUTINE ABCC - Computes Arya's A_m , B_m , C_m (called AM, BM, CM in the FORTRAN program) and UV, the square of the integrated wind speed, all as functions of the friction velocity u_* . This is passed in common from CCROSS at location UX(K123), where $K123 = 1, 2, \text{ or } 3$ at various stages of the iteration. The code is slightly more general than needed in the hurricane model, catering for unstable, neutral, and stable wind profiles (indexed by the sign of HL). In computing A_m and B_m , the ratio fh/u_* is taken equal to unity.
- SUBROUTINE BLOWUQ - Controls computation and printing of all output on the nested grid. It is called once for each snapshot wind field.
- SUBROUTINE CCROSS - Computes the upwind and crosswind drag coefficients, the ratio u_*/V_m , and the angle between surface wind and integrated wind, for all $V_m = 0.8(0.8)80.0$. Values for intermediate V_m are linearly interpolated when required (lines 72-83 of COMQUT; lines 27-37 of AANGEL). The computation implements Arya's theory. The numerical method is an initial guess at u_* , followed by an iterative series of corrections by inverse interpolation. The iterations proper, and the computation of Arya's A_m , B_m , C_m , take place in subroutine ABCC.
- SUBROUTINE COMQUT - Solves equations which determine the final wind fields on the nested grid. For each snapshot, COMQUT is called as many times as specified in input NAME3. At each calling a grid level is specified, and computation is done on that level

and all finer-meshed levels only, so that wind computation on the innermost nest only is computed NM times.

Arguments: input, typing implicit

LEVEL: Input $1 \leq \text{LEVEL} \leq 5$.

Grid distance is doubled at each increase of LEVEL. Computation is done on all grid levels $\leq \text{LEVEL}$.

SUBROUTINE GRAD

- Computes the radial and tangential gradients $\partial P/\partial r$ and $r^{-1} \partial P/\partial \theta$ of an exponential pressure field and converts them to rectangular gradients $\partial P/\partial x$ and $\partial P/\partial y$.

Mathematical Method:

1. Compute polar coordinates $(r, \cos \theta, \sin \theta)$ of the $21 \times 21 \times 5$ grid points.
2. Convert direction of track to radians.
3. Convert forward speed to meters per second.
4. Compute x- and y- components of forward speed. The method here divides into two cases: circularly symmetric pressure field ($\text{JA}(6) = 0$) and quadrantal pressure field ($\text{JA}(6) \neq 0$).

A: Circularly symmetric pressure field.

The governing equation

$$P = P_0 + \Delta P \exp(-R/r) \quad (*)$$

yields on differentiation

$$\partial P/\partial r = \Delta P R r^{-2} \exp(-R/r).$$

5. Convert R to kilometers.
6. Compute P.
7. Compute $\partial P/\partial r$, $\partial P/\partial x$, $\partial P/\partial y$.

B: Quadrantal pressure field.

ΔP , prescribed in four quadrants, is expanded as the trigonometric polynomial

$$a_0 + a_1 \cos \theta + a_2 \sin \theta + [a_3 \cos 2\theta]$$

and then smoothed by removing the

bracketed term. R is similarly expanded and smoothed. Substituting these trigonometric polynomials in (*) yields

$$P = P_0 + (a_0 + a_1 \cos \theta + a_2 \sin \theta) \exp(-[b_0 + b_1 \cos \theta + b_2 \sin \theta]/r)$$

and the radial and tangential gradients

$$\begin{aligned} \partial P / \partial r = & (a_0 + a_1 \cos \theta + a_2 \sin \theta)(b_0 + b_1 \cos \theta + b_2 \sin \theta) r^{-2} \times \exp(-[b_0 + b_1 \cos \theta + b_2 \sin \theta]/r) \end{aligned}$$

$$\begin{aligned} r^{-1} \partial P / \partial \theta = & [r^{-1}(-a_1 \sin \theta + a_2 \cos \theta) + r^2(b_1 \sin \theta - b_2 \cos \theta)] \times \exp(-[b_0 + b_1 \cos \theta + b_2 \sin \theta]/r) \end{aligned}$$

8. Convert R to kilometers in each quadrant.
9. Compute ΔP to millibars in each quadrant.
10. Compute the coefficients in trigonometric polynomials.
11. Compute $\partial P / \partial r$ and $r^{-1} \partial P / \partial \theta$.
12. Compute $\partial P / \partial x$ and $\partial P / \partial y$.

Arguments: none

Variables (not in common):

AD	$\partial P / \partial r, r^{-1} \partial P / \partial \theta, \partial P / \partial x, \partial P / \partial y$
AE, AF, AG, AH	Temporary storage
AP, CR, CD	Coefficients in trigonometric polynomials
AT, CT	Direction cosines of motion of storm
BA, BC	JA, floated and converted to metric units
BP	Temporary storage
DEG	Radian measure of 1 deg.

IC, ID, IE, Do-loop indexes
IG, IH

LU Logical unit number of
standard print unit

S45 Circular sine of 45°

SUBROUTINE OUTBY1 - Sets outer boundary winds for the next time level. It is called once for each cycle of wind computation and grid level if the grid level is not the outermost computed at that time.

Arguments: typing implicit

NEST: Input - grid level at which boundary to be set.

SUBROUTINE OUTBY2 - Sets outer boundary winds for the same time level. It is called once for each cycle of wind computation for the coarsest meshed grid level being computed at that time unless that grid level is the outermost in the entire grid.

Arguments: typing implicit

NEST: Input - grid level at which boundary to be set.

SUBROUTINE OUTFLO - Operates on the entire field of $21 \times 21 \times 5$ wind vectors, rotating every vector clockwise (in the northern hemisphere) by 8° . Extensive numerical experiment with earlier versions of the hurricane wind model has indicated that the finite difference scheme used leads to excessive inflow; the 8° rotation approximately removes that bias.

SUBROUTINE OUTQUT - Controls printing of winds on nested grid.

Arguments: input, typing implicit

I20: Passed on to subroutine AANGEL.
If $I20 \neq 0$, wind speed will be adjusted to 19.5 meters.

NAME: 4-character name of storm

IDENT: 4-character identification of type of field (INIT or SNAP)

NSEQ: Snapshot sequence number.

SUBROUTINE PXYM - Receives the pressure gradients computed in GRAD, divides them by the density, and rearranges them in the order demanded by BLOWUQ. It then computes the gradient wind from the radial pres-

sure gradient to provide initial values for COMQUT.

Mathematical Method:

The gradient wind is given by Hess (1959, p. 183) as

$$C = -\frac{1}{2}fr + [(\frac{1}{2}fr)^2 + \rho^{-1}r \partial p/\partial r]^{\frac{1}{2}} (*)$$

For large r , (*) expresses C as the difference of two nearly equal terms, and so it is advisable to compute the equivalent expression

$$C = \frac{\rho^{-1}r \partial p/\partial r}{\frac{1}{2}fr + [(\frac{1}{2}fr)^2 + \rho^{-1}r \partial p/\partial r]^{\frac{1}{2}}}$$

where f is the Coriolis acceleration and ρ is the density of the atmosphere.

1. Coriolis, computed in SNAP, is passed in C_1 . Note that the latitude is taken as a constant throughout the cyclone; this approximation is inappropriate between $\pm 5^\circ$ of latitude.
2. Divide $\partial p/\partial x$ and $\partial p/\partial y$ by ρ . 1.15×10^{-3} is the density; 1×10^{-4} is a conversion factor from mb/km to newtons/m³.
3. Compute gradient wind. BC contains r in km, and the factor 1000 converts r to meters.
4. Resolve gradient wind into x- and y- components.
5. If steering flow is used, add $(W_c \times F)$ to the vector $\rho^{-1}\Delta P$.

Arguments: none

Variables (not in common):

AG,AH,AI	Temporary storage
I	Index variable for X
J, MJ	Index variable for Y
NEST	Index variable for nest (counted from inside out)
FADE	Attenuation factor for steering flow

SUBROUTINE SHORE - Sets the land/sea table for the nested grid. It is currently set to 'sea' throughout.

SUBROUTINE TVEL - Prints the contents of arrays VTN and ANG on the grid level indicated as well as on the next coarser grid level.
Arguments: Input, typing implicit

VTN: The top number in each pair of numbers printed is taken from this array. It is printed with the decimal moved one place to the right.

ANG: The bottom number in each pair of numbers printed is taken from this array.

NBASE: 4-character heading information

IDENT: 4-character heading information

KSEQ: Header information, 4-digit integer number.

LV: Finer-meshed (lower numbered) grid level to be printed at this call to TVEL.

I20: Flag, controlling printing of the legends "reduced" and "not reduced".

Note heading:

[NBASE] [IDENT] [KSEQ] LEVEL LV+1..

. Program HIST is composed of:

MAIN

- Produces winds at specified measurement stations for each hour of a storm's history. If requested, it will also interpolate winds to a grid. After card input has been read and tables have been set up, it writes all unique nested-grid winds (i.e. all snapshots plus all interpolated fields) on a temporary file in the order needed. It next loops through the list of stations and, using the temporary file just written, finds and prints the winds for each station throughout the storm's history. Then, if requested, it interpolates winds to another grid for each hour of the storm's history, prints the winds on the grid for any hours indicated, and writes the fields onto an output file.

SUBROUTINE ABCCC - (Called by UXXV) Operates exactly the same algorithm as ABCC (called by CCROSS). The only difference in coding is that ABCCC references the common block /C57/ , defined in program HIST.

SUBROUTINE BREEZE - Given LA0, LØ0, RØT, LA1, LØ1, DX, STHT, and LANSEA in common block D1, BREEZE determines the wind at point LA1, LØ1 at height STHT on the nested grid wind field in array XX in common block D2 and returns the wind data in W1, TH1, D, AL, and UST of common block D1.

Mathematical Method:

Let a , b , c be the sides of a spherical triangle, and α , β , γ the angles opposite; define $s = \frac{1}{2}(a + b + c)$.

Then

$$\begin{aligned} \text{hav } c &= \text{hav } (a - b) \\ &+ \sin a \sin b \text{ hav } \gamma; \end{aligned}$$

$$\tan^2 \frac{1}{2}\alpha = \frac{[\sin(s - b) \sin(s - c)]}{[\sin(s - a) \sin s]} (*)$$

1. Compute distance and bearing. If c is very small, $(s - a)$ and $(s - b)$ are nearly zero, and eq. (*) is unsuitable for computation; the bearing can then be computed without sen-

sible error by solving a plane triangle.

2. Reduce bearing to rectangular grid.
3. Reduce distance to kilometers.
4. Compute rectangular coordinates.
5. Search for the smallest rectangular grid in whose interior the point lies. If point lies without fifth nest, no wind has been computed; set wind to zero.
6. Interpolate components of wind, using bivariate linear interpolation:
$$\begin{aligned} &\phi(x + f_1 \Delta x, y + f_2 \Delta y) \\ &= (1 - f_1)(1 - f_2) \phi(x, y) \\ &+ (1 - f_1) f_2 \phi(x, y + \Delta y) \\ &+ f_1(1 - f_2) \phi(x + \Delta x, y) \\ &+ f_1 f_2 \phi(x + \Delta x, y + \Delta y) \end{aligned}$$
7. Compute wind speed and reduce to anemometer height. The factor 3600/1852 converts from m/sec to knots; the MIN function assures that the anemometer wind is never greater than the integrated wind.
8. Compute wind direction and reduce to true south.

Arguments: none

Variables: All variables except temporary storage are annotated in the program listing.

SUBROUTINE INVJD - Is the inverse of the function JULIAN. Given the Julian date, it returns the month, day, and year.

Arguments:

J: Input-Julian date, type integer

M: Output-Month, type integer

D: Output-Day, type integer

Y: Output-Year, type integer

FUNCTION JULIAN - Returns the Julian date.

Arguments:

MO: Month, type integer
DA: Day, type integer
YR: Year, type integer

SUBROUTINE PRLAKE - Is a grid-dependent subroutine and must be changed or replaced if the output grid is changed. It prints winds for each grid point, with speed on top, direction in the middle, and terrain code on the bottom.

Arguments: Input, typing implicit
NBASE: 4-character name of storm;
KHR: Integer sequence number of hour of storm;
ISTART: First hour of storm, corresponds to KHR = 1 . Format is YYYYDDHH;
IZONE: 3-character time zone of ISTART:
WIND: As on output file 20;
LSTAB: Terrain code table for output grid;
MAXI: Number of longitudes in output grid;
MAXJ: Number of latitudes in output grid.

Note: The grid currently used uses unequally spaced meridians and parallels; printed map is distorted.

SUBROUTINE RDGRID - Is a grid-dependent subroutine and must be replaced or altered if the output grid is changed. Its function is to read latitude, longitude, and terrain code for each grid point and store them in arrays ZLA, ZLØ, and LSTAB respectively. It is called only if winds are to be interpolated to an output grid.

Arguments: typing implicit
ZLA: Output - latitudes in radians ordered south to north.
ZLØ: Output - west longitudes in radians, ordered west to east.
LSTAB: Output - terrain codes for all grid points; the first subscript increases eastward, the second increases northward.
MAXI: Input - number of longitudes in grid.

MAXJ : Input - number of latitudes
in grid

SUBROUTINE UPDOWN - Computes the ratio u_*/V_m and the angle between surface wind and integrated wind, all for $V_m = 0.8(0.8)80.0$, for terrains other than open ocean. The program consists of two parts: "UP" (lines 8-19) and "DOWN" (the rest of the code). UP computes U_m and V_{TOP} (components of wind at the top of the boundary layer), $VW2$ (squared wind speed at top), and $TARN$ (tan of angle between integrated wind and wind at top). The computation in UP uses quantities computed in UXXV (open ocean) and is consistent with Arya's theory. The assumption is now made that wind at the top of the boundary layer in a hurricane does not "see" the terrain below, so that the surface wind over any terrain can be computed by working UP and then DOWN. DOWN follows a logic similar to UXXV: Arya's A_o and B_o are constants (neutral wind profile); the roughness length is computed as

$$Z_o = AZ/u_* + BZu_* + CZ.$$

SUBROUTINE UXXV - Computes the ratio u_*/V_m , the angle between surface wind and integrated wind and the cosine and sine of this angle, all for $V_m = 0.8(0.8)80.0$. Values for intermediate V_m are linearly interpolated when required (line 73-82 of BREEZE). The computation implements Arya's theory. The numerical method is an initial guess at u_* , followed by an iterative series of corrections by inverse interpolation. The iteration proper, and the computation of Arya's A_m , B_m , C_m , take place in subroutine ABCCC. UXXV works the part of the algorithm of CCROSS (called from SNAP) pertaining to sea, i.e. $LS = 2$. The computations in UXXV are valid for open ocean only; all other terrains are treated in subroutine UPDOWN.

Remarks

. In all arrays dimensioned $21 \times 21 \times N$, where N is a multiple of 5, the 1st dimension increases eastward, the 2nd dimension increases northward, and the 3rd dimension, grid nest, increases with grid spacing. Grid spacing doubles with each increasing nest level.

. Logical unit numbers for the card reader and printer are 5 and 6, respectively, on the system under which these programs were run. These unit numbers are set by a DATA statement into variables LR and LP in programs HIST and SNAP, and the printer unit is set into LU in subroutines GRAD and TVEL.

. Equivalences between snapshot input parameters and array JA in COMMON block C2 of program SNAP:

<u>JA</u>	<u>NAME</u>	<u>TYPE</u>
1	ITRACK	I
2	EYELAT	R
3	EYLONG	R
4	DIREC	R
5	SPEED	R
6	IQUAD	I
7	EYPRES	R
8	RADIUS(1)	R
9	RADIUS(2)	R
10	RADIUS(3)	R
11	RADIUS(4)	R
12	PFAR(1)	R
13	PFAR(2)	R
14	PFAR(3)	R
15	PFAR(4)	R

Explanation of program organization charts:

- Rectangular box - program element
- Cut-off corner - punched card image
- Diamond - printer
- Barrel - mass storage
- Rounded ends - program stop

Table 2

Files

<u>Description</u>	<u>Unit Number</u>	<u>Size</u>	<u>Program SNAP</u>	<u>Program HIST</u>	<u>Save</u>
Card Reader	5		Input	Input	
Printer	6		Output	Output	
Snapshot Wind Fields on Nested Grid	13	4436 Words each Record (Snapshot)	Output	Input	✓
Ordered Unique Wind Fields on Nested Grid	10	4411 Words each Record (Wind Field)		Work	
Hourly Wind Fields on Output Grid	20	Grid-dependent, 3855 Words each Record (Hour) for Test Grid		Output	✓

Records in files 10, 13, and 20 are written with Fortran unformatted WRITE statements. There are file marks after the last data records in output files 13 and 20.

Table 3
Card Input

Description and order within programs of card input groups

<u>Program</u>	<u>Seq. Number</u>	<u>Name* (If Namelist)</u>	<u>Number/Remarks</u>	<u>Description</u>
SNAP	1	NAME1	1	Processing control
SNAP	2	NAME2	1	Parameters in roughness law (usually constant)
SNAP	3	NAME3	1 for each wind snapshot	Parameters describing wind field
HIST	1	NAME4	1	Storm identification, also grid parameters if winds are to be inter- polated to an output grid
HIST	2	NAME5	1	Terrain coefficients and number of types of terrain other than open ocean
HIST (RDGRID)	3		Only if grid conversion	Longitudes and latitudes of grid points. Card count, format and ordering of data must agree with subroutine RDGRID.
HIST (RDGRID)	4		Only if grid conversion	Code for type of terrain at each grid point. Card count, format, and ordering of data must agree with subroutine RDGRID.

* Namelist is not a construction recognized by the current FORTRAN standard (ANSI X3.9-1978).
Appendix A contains an account of Namelist as used in this program.

Table 3 (concluded)

<u>Program</u>	<u>Seq. Number</u>	<u>Name (If Namelist)</u>	<u>Number/Remarks</u>	<u>Description</u>
HIST	5(or 3)		One card for each station where wind history is needed, terminated by end-of-file	Station location and height at which measurements taken.
HIST	6(or 4)		One card for each hour of storm history, terminated by end-of-file	Location of eye of storm, snapshot identification

Table 4
Program SNAP namelist input

<u>Namelist Name</u>	<u>Variable Name</u>	<u>Size in Words</u>	<u>Units</u>	<u>Type</u>	<u>Default Value</u>	<u>Description</u>
NAME1	IB	1		I		Switch variable: 0 suppresses printing of pressures and initial winds.
	NZ	1		I		Number of snapshot wind fields to compute
NAME2	DTH	2	°K	R	0,-2.	1: Air-land temperature difference 2: Air-sea temperature difference
	HH	1	m	R	650.	Boundary layer height over water
	ZOLAND	1		R	.08	Roughness length over land
	GARR	1		R	.0144	Charnock's constant
	PTH	1	°K	R	300.	Potential temperature
	K35	1		R	.35	Karman's constant

Table 4 (continued)

<u>Namelist Name</u>	<u>Variable Name</u>	<u>Size in Words</u>	<u>Units</u>	<u>Type</u>	<u>Default Value</u>	<u>Description</u>
NAME3	SGW	1	m/sec	R		Surface geostrophic wind of ambient flow
	AN1	1	deg	R		Direction of SGW, counterclockwise from snapshot x-axis
	NAME	1		H		4-character name of storm
	EYELAT	1	deg	R		North latitude of eye of storm
	EYLONG	1	deg	R		West longitude of eye of storm; for reference only
	DIREC	1		R		Direction of track of storm, clockwise from north. See ITRACK for units.
	SPEED	1	kn	R		Forward speed of storm
	EYPRES	1	mb	R		Pressure at eye of storm
	RADIUS	4	nm	R		Exponential pressure profile scale radius in 4 quadrants. If the pressure field is circularly symmetric (IQUAD = 0) input is required for the first quadrant only
	PFAR	4	mb	R		Far field pressure in 4 quadrants. If the pressure field is circularly symmetric (IQUAD = 0) input is required for first quadrant only.
	NM	1		I	800	Number of times to cycle wind computation in innermost grid nest
	DX	1	km	R	5.	Grid spacing of innermost nest
	ST12	1	km	R	0.	Distance from axis to $\frac{1}{2}$ magnitude of SGW

(continued)

Table 4 (concluded)

<u>Namelist Name</u>	<u>Variable Name</u>	<u>Size in Words</u>	<u>Units</u>	<u>Type</u>	<u>Default Value</u>	<u>Description</u>
NAME3	ITRACK	1		I	0	If 0, DIREC in degrees; if 1, DIREC in points of 11.25 degrees
	IQUAD	1		I	0	Indicator for quadrants of pressure field: 0, circularly symmetric pressure field; 1, 1st quadrant is right front; 2, 1st quadrant if forward

Table 5
Program HIST Namelist Input

<u>Namelist Name</u>	<u>Variable Name</u>	<u>Size in Words</u>	<u>Type</u>	<u>Description</u>
NAME4	NBASE	1	H	4-character name of storm - must be same as 1st SNAP namelist NAME3, item NAME
	ISTART	1	I	Starting time of storm, format YYMMDDHH
	IZONE	1	H	3-character time zone of ISTART
	ICNVRT	1	I	Flag: if non-zero, winds will be interpolated to an output grid, and grid data must be input
	NPRT	1	I	Interval in hours at which to print winds on output grid. If zero, winds will be printed only for hours so flagged in the history table
NAME5	LAKE	1	I	Number of types of terrain in addition to open ocean. $0 \leq \text{LAKE} \leq 5$
	ZCOEFF	15	R	3 coefficients in formula relating Z_o to U^* for all terrains except open ocean. Dimensioned (3,5).

Table 6

Program HIST Fixed Format Card Input

- 1) Station location and data: One card for each measurement station, format (5I4,F6.1,1X,I3)
 1. Degrees of north latitude
 2. Minutes of latitude
 3. Degrees of west longitude
 4. Minutes of longitude
 5. Terrain code, same codes as grid terrain code table
 6. Station height in meters
 7. Station number (for identification only)

- 2) History: One card for each hour, format (6I4,F8.4,2I4)
 1. Degrees of north latitude of eye of storm
 2. Minutes of latitude of eye
 3. Degrees of west longitude of eye
 4. Minutes of longitude of eye
 5. Sequence number of 1st snapshot wind field to be used for this hour
 6. Sequence number of 2nd snapshot wind field to be used for this hour (blank if no interpolation this hour)
 7. Interpolation distance between 1st and 2nd snapshots (blank if (6) is blank)
 8. Clockwise rotation of snapshot in degrees
 9. Flag: non-zero if output grid wind field is to be printed

Table 7

Input Cards with Data Defining Program HIST Test Output Grid

- 1) 5 cards with 62 west longitudes in the form DDMM and progressing from west to east. Each card, except the last has 15 longitudes and a sequence number in format 16I5. The last card is blank filled between the last data field and the sequence number.
- 2) 3 cards with 31 latitudes progressing from south to north. Form and format are the same as those of the longitude cards.
- 3) 31 cards of terrain code. Each card is for one latitude, and cards are ordered from south to north. The format is 2I3, for degrees and minutes of latitude, then 2X,62I1, where the 62I1's are one-digit numeric terrain codes for each longitude and progress from west to east. As used in the test grid for Lake Pontchartrain, the codes are as follows -
 - 1: open ocean
 - 2 lake
 - 3: marsh
 - 4: plains
 - 5: woods
 - 6: cities

Table 8

COMMON BlocksProgram SNAP

<u>Block Name</u>	<u>Variable Name</u>	<u>Size in Words</u>	<u>Units</u>	<u>Source</u>	<u>Disposition</u>	<u>Description</u>
C1	NAME	1		Input NAME3	Snapshot wind data file	4-character name of storm
	NSNAP	1				Sequence number of wind snapshot
	DX	1	km	Input NAME3	Snapshot wind data file	Grid spacing of innermost nest
	DT	1	sec			Time increment for computation of winds in innermost nest
	F	1				Coriolis force
	SGW	1	m/sec	Input NAME3	Snapshot wind data file	Surface geostrophic wind of ambient flow
	AN1	1	deg	Input NAME3	Snapshot wind data file	Direction of SGW counterclockwise from snapshot x-axis
	UC	1	m/sec			X-component of velocity of storm movement
	VC	1	m/sec			Y-component of velocity of storm movement
	UG	1	m/sec			X-component of surface geostrophic wind
	VG	1	m/sec			Y-component of surface geostrophic wind
	CS	1	m/sec			Speed of storm movement
	NM	1		Input NAME3		Number of times to cycle wind computation in innermost grid nest
	IB	1		Input NAME1		Flag: if zero, do not print pressure field or initial wind

Table 8 (continued)

Block Name	Variable Name	Size in Words	Units	Source	Disposition	Description
[C1]	ST12	1	km	Input NAME3	Snapshot wind data file	Distance from axis to $\frac{1}{2}$ magnitude of SGW
C2	JA	15		Input NAME3	Snapshot wind data file	See program SNAP output data file record description, page . Also note equivalence list in remarks, page .
	AB	6615				Work array, 1st third, $\partial\rho/\partial x$; 2nd third, $\partial\rho/\partial y$; last third, $\partial\rho/\partial r$
	AC	3087				Dimensioned $21 \times 7 \times 21$. Location in grid defined by 1st and 3rd subscripts. If 2nd subscript, N, is 1, value is cosine of angle of grid point; if 2, value is sine of angle of grid point; if 3-7, value is radius in meters of point in nest N-2.
C3	U	2205	m/sec			Work array, x-component of boundary layer wind at previous time level
	V	2205	m/sec			Work array, y-component of boundary layer wind at previous time level
	UN	2205	m/sec		Snapshot wind data file	X-component of boundary layer wind
	VN	2205	m/sec		Snapshot wind data file	Y-component of boundary layer wind
	PX	2205				Work array, $\partial\rho/\partial x$
	PY	2205				Work array $\partial\rho/\partial y$
	VTN	2205	kn			Work array, holds wind speeds to be printed
	ANG	2205	deg			Work array, holds wind directions to be printed

(Continued)

Table 8 (continued)

Block Name	Variable Name	Size in Words	Units	Source	Disposition	Description
[C3]	LW	2205				Land/sea table: 1 for land, 2 for sea
C4	CDR	400				Work array, dimensioned 100 × 2 × 2. Drag coefficients: CDR(I,1,1) is upwind component of drag coefficients over land, when integrated wind speed is (.8*I) m/sec. CDR(I,2,1) is crosswind component over land CDR(I,1,2) is upwind component over ocean CDR(I,2,2) is crosswind component over ocean
	UXV	200				Work array, dimensioned 100 × 2. UXV(I,1) is $\frac{U_*}{V_m}$ over land, when $V_m = (.8*I) \text{ m/sec}$ UXV(I,2) is the same over ocean
	TURN	200	rad			Work array, dimensioned 100 × 2. TURN(I,1) is the angle between surface wind and integrated wind, over land, when integrated wind speed is (.8*I) m/sec. TURN(I,2) is the same over ocean
C5	FLAT	1				Coriolis force
	PTH	1	°K	Input NAME2	Snapshot wind data file	Potential temperature
	DTH	2	°K	Input NAME2	Snapshot wind data file	(1) Air-land temperature difference (2) Air-sea temperature difference

(continued)

Table 8 (continued)

Block Name	Variable Name	Size in Words	Units	Source	Disposition	Description
[C5]	HH	1	m	Input NAME2	Snapshot wind data file	Boundary layer height over water
	ZOLAND	1		Input NAME2		Roughness length over land
	LS					Index variable
	VV	100	m/sec			Vertically integrated wind speeds. VV(I) at point I = .8m/sec × I
	UX	3	m/sec			Latest 3 values of U _x in an iterative loop
	UV	3	m ² /sec ²			Latest 3 values of integrated wind speed corresponding to U _x
	DUV	3	m ² /sec ²			Interpolated value of wind speed squared minus desired value squared
	K35	1		Input NAME2	Snapshot wind data file	Karman's constant, type real
	K2	1				K35 ² , type real
	G	1				Acceleration of gravity = 9.806 m/sec ²
	GA	1	sec ² /m			Charnock's constant divided by G
	DEN	1				Used in stability length computation
	VV2	1	m ² /sec ²			VV(I) ² for current I
	HL	1				HH/stability length
	K123	1				Index variable
	Z0	1	m			Roughness length

(continued)

Table 8 (continued)

<u>Block Name</u>	<u>Variable Name</u>	<u>Size in Words</u>	<u>Units</u>	<u>Source</u>	<u>Disposition</u>	<u>Description</u>
[C5]	ZLOG	1				Log (ZO/HH)
	AM	1				Constant in Arya's logarithmic scale law
	BM	1				Constant in Arya's logarithmic scale law
	CM	1				Constant in Arya's logarithmic scale law
	FF	1	sec ⁻¹			Coriolis parameter. Retained for consistency with other versions of CCROSS; not used in this program.

Program HIST

C57	PTH	1	°K	Snapshot wind data file		Potential temperature
	DTH	1	°K	Snapshot wind data file		Air-sea temperature difference
	HH	1	m	Snapshot wind data file		Boundary layer height over water
	ZCOEFF	15		Input NAME5		3 coefficients in formula relating Z_0 to U_* for all terrains except open ocean, where Garratt's formula is used
	LAKE	1		Input NAME5		Number of terrains other than open ocean. Integer, 0-5
	VV	100	m/sec			Vertically integrated wind speeds at point I: $(VV(I) = I \times .8 \text{ meters/sec})$
	UX	3	m/sec			Latest 3 values of U_* in an iterative loop

(continued)

Table 8 (continued)

Block Name	Variable Name	Size in Words	Units	Source	Disposition	Description
[C57]	UV	3	m ² /sec ²			Latest 3 values of square of integrated wind speed corresponding to U*
	DUV	3	m ² /sec ²			Difference between squares of interpolated value of wind speed and desired value
	K35			Snapshot wind data file		Karman's constant, type real
	K2					K35 ² , type real
	G	1	m/sec ²			Acceleration of gravity: 9.806 constant
	GA	1	sec ² /m			Charnock's constant divided by G
	DEN		mKsec ⁻²			Temporary variable used in stability length computation
	VV2		m ² /sec ²			VV(I) ² for current I
	HL					HH/stability length
	K123					Index variable
	Z0		m			Roughness length
	ZLOG					LOG(Z0/HH)
	AM					Correction terms in Arya's logarithmic scaling law
	BM					Correction terms in Arya's logarithmic scaling law
	CM					Correction terms in Arya's logarithmic scaling law
	UXV	600				U*/VV for each I, terrain type

(continued)

Table 8 (continued)

<u>Block Name</u>	<u>Variable Name</u>	<u>Size in Words</u>	<u>Units</u>	<u>Source</u>	<u>Disposition</u>	<u>Description</u>
[C57]	TURN	600	rad			Turning angle between surface wind and integrated wind for each I, terrain type
	COST	100				Cosine of TURN for current terrain
	SINT	100				Sine of TURN for current terrain
D1	LA0	1	rad			Latitude of storm eye at current hour, type real
	LO0	1	rad			West longitude of storm eye at current hour, type real
	ROT	1	deg			Clockwise angle to rotate snapshot wind field
	LA1	1	rad			Latitude of 1 point at which wind is wanted, type real
	LO1	1	rad			West longitude of point of which wind is wanted, type real
	DX	1	km	Snapshot wind data file		Grid spacing of innermost nest
	STHT	1	m			Height of measurement at current location
	LANSEA	1				Indicated sea or type of terrain for current location
	W1	1	kn			Wind speed at current location
	TH1	1	deg			Meteorological wind direction
	D	1	km			Distance between locations LA0,L00 and LA1,L01

(continued)

Table 8 (concluded)

Block Name	Variable Name	Size in Words	Units	Source	Disposition	Description
[D1]	AL	1	deg			Bearing of point LA1,L01, from point LA0,L00, clockwise from north
	UST	1	m/sec			Friction velocity at current location
D2	XX	4410		Snapshot wind data file		Winds on nested grid at current hour
D3	NSNAP1	100				1st wind snapshot sequence number
	NSNAP2	100				2nd wind snapshot sequence number (0 if none)
	PCT	100				Interpolation distance between snapshots NSNAP1 and NSNAP2
	IPI	100				Flag: non-zero if listing of winds on output wanted
	NHT	1				Number of hours in storm history
	INTVN	1				Not used
	INTVI	1	hours			Interval at which to print winds on output grid
LGRID*	ILAT	31				List of output grid latitudes, south to north, in the format DDMM
	ILONG	62				List of output grid west longitudes, west to east, in the format DDMM

*Not in main program, in subroutines RDGRID and PRLAKE only.

Table 9

Description of Program HIST arrays not in COMMON

Station data arrays - all dimensioned 100

MAD	Location, from card input - degrees of north latitude
MAM	Location, from card input - minutes of latitude
MMOD	Location, from card input - degrees of west longitude
MOM	Location, from card input - minutes of longitude
LLAKE	Terrain code, from card input
STAHT	Height in meters, from card input
KSTA	Station number (identification), from card input
YLA	Latitude in radians
YLO	Longitude in radians

History table arrays - all dimensioned 100

NAD	Location of eye of storm, from card input - degrees of north latitude
NAM	Location of eye of storm, from card input - minutes of latitude
NOD	Location of eye of storm, from card input - degrees of west longitude
NOM	Location of eye of storm, from card input - minutes of longitude
IROT	Grid rotation angles, from card input
KDATE	Date in form YYMMDD
KTIME	Hour of KDATE
JSEQ	Sequence numbers of nested grid winds on work file

Output grid data arrays as used with test grid

ZLA	List of latitudes of grid points, south to north, in radians
ZLO	List of west longitudes of grid points, west to east, in radians

Table 9 (concluded)

ZANG Deviation between true north and grid north for
each grid point - zero throughout test grid

LSTAB List of terrain codes of grid points.

Other arrays

XY Dimensioned $21 \times 21 \times 10$. Contains 2nd snapshot
wind field when needed

Table 10

Program Stops

<u>Program</u>	<u>Stop Number</u>	<u>Interpretation</u>
SNAP	999*	Normal completion of run
HIST	999*	Normal completion of run
HIST	5	Error in reading station or history input card
HIST	146	Error in reading mass storage work file of wind fields on nested grid
HIST	444	Snapshot interpolation distance out of range (< 0 or > 1).
HIST	515	Input card and snapshot data file storm identifications are different
HIST	516	Too many station input cards (> 100)
HIST	517	Too many history input cards (> 100)
HIST (RDGRID)	21	Error in reading grid longitude card
HIST (RDGRID)	23	Error in reading grid latitude card
HIST (RDGRID)	51	Error in reading grid terrain code card

* If running a FORTRAN that requires STOP number to be octal, substitute 777.

Table 11

Output Data File Record DescriptionSnapshot wind field record from program SNAP

<u>Variable Name</u>	<u>(Dimension)</u>	<u>Size</u>	<u>Accumulated Word Count</u>	<u>Units</u>	<u>Applicable Format*</u>	<u>Description</u>
UN	(21,21,5)	2205	2205	m/sec	F4.1	X-component of boundary layer wind 1st dimension increases with increasing x 2nd dimension increases with increasing y
VN	(21,21,5)	2205	4410	m/sec	F4.1	Y-component of boundary layer wind 3rd dimension (grid nest) increases with grid spacing
NAME		1	4411		A4	4-character name of storm
DX		1	4412	km	F3.0	Grid spacing of innermost nest
JA	(15)	15	4427		I1	1: Indicator for coding of (4) If 0, (4) in degrees; if 1, (4) in points of 11.25 degrees.
				deg	F5.1	2: North latitude of eye of storm
				deg	F6.1	3: West longitude of eye of storm
				see JA(1)	F4.0	4: Direction of track of storm, clockwise from north
				kn	F5.1	5: Forward speed of storm
					I1	6: Indicator for quadrants of pressure field

* Format appropriate for printing this variable or array.

Table 11 (continued)

Variable Name	(Dimension)	Size	Accumulated Word Count	Units	Applicable Format	Description
[JA]						0 - circularly symmetric pressure field 1 - 1st quadrant is right front 2 - 1st quadrant is forward
				mb	F6.1	7: Pressure at eye of storm
				nm	F4.0	8-11: Exponential pressure profile scale radius in four quadrants. If JA(6) is zero, JA(9) - JA(11) may not contain valid data
				mb	F5.0	12-15: Far field pressure in four quadrants. If JA(6) is zero, JA(13) - JA(15) may not contain valid data
SGW		1	4428	m/sec	F3.0	Surface geostrophic wind of ambient flow
AN1		1	4429	deg	F4.0	Direction of SGW counterclockwise from snapshot x-axis
ST12		1	4430	km	F5.1	Distance from axis to $\frac{1}{2}$ magnitude of SGW
DTH		2	4432	$^{\circ}$ K		(1) Air-land temperature difference (2) Air-sea temperature difference
HH		1	4433	m		Boundary layer height over water
GARR		1	4434			Charnock's constant
PTH		1	4435	$^{\circ}$ K		Potential temperature
K35		1	4436			Karman's constant, type real

(continued)

Table 11 (concluded)

Test output grid wind field record from program HIST

<u>Variable Name</u>	<u>(Dimension)</u>	<u>Size</u>	<u>Accumulated Word Count</u>	<u>Units</u>	<u>Applicable Format</u>	<u>Description</u>
NBASE		1	1		A4	4-character name of storm
KHR		1	2		I3	Sequence number of hour of storm
ISTART		1	3		I8	Starting time of storm in format YYMMDDHH (Time at which KHR=1)
IZONE		1	4		A3	Time zone of ISTART
IMAX		1	5		I2	Longitudinal dimension of output grid
JMAX		1	6		I2	Latitudinal dimension of output grid
GRIDHT		1	7	m	F6.1	Height to which wind speeds are scaled
NAD		1	8		I3	Location of eye of storm - degrees of north latitude
NAM		1	9		I2	Location of eye of storm - minutes of latitude
NOD		1	10		I4	Location of eye of storm - degrees of west longitude
NOM		1	11		I2	Location of eye of storm - minutes of longitude
WIND	(2, MAX1, MAXJ) (3844 for test grid)		11+2*MAX1*MAXJ (3855 for test grid)			Wind at specified height on wave grid. If 1st subscript is 1, value is wind speed in knots. If 1st subscript is 2, value is direction in degrees toward which wind blows counterclockwise from north

Printed Output

. Program SNAP initially prints card input data and finally prints an end-of-job message. For each snapshot it prints card input data pertinent to that snapshot, a pressure field and an initial guess wind field if requested, and a final snapshot wind field on the nested grid. Snapshot wind speeds are printed in tenths of knots, directions are meteorological, and west is at the top of the page. Each snapshot is printed both with wind speeds as computed and with wind speeds scaled to 19.5 meters.

. Program HIST prints card input data, the wind history at each requested station, wind fields on the output grid for hours requested, and an end-of-job message. Output grid wind speeds are in knots and directions are meteorological. Terrain types are indicated by blank for type 1, '*' for 2, '=' for 3, '-' for 4, '+' for 5 and '\$' for 6.

Table 12

Program Changes Needed for a New Output Grid

- 1) Subroutine RDGRID
- 2) Subroutine PRLAKE
- 3) COMMON block LGRID (used in RDGRID and PRLAKE only)
- 4) In program Hist:
 - a) Parameters MAXI, MAXJ, and IGRDHT, where MAXI is the longitudinal dimension of the grid, MAXJ is the latitudinal dimension, and IGRDHT is its height in tenths of meters.
 - b) ZLA, ZLO become two-dimensional if rows and columns do not fall on latitude, longitude lines, and the settings of LA1 and LO1 in the DO 111 and DO 110 loops will be affected
 - c) Array ZANG, the angle between true meridian and grid meridian, may become non-zero.

PART IV: CONCLUSIONS AND RECOMMENDATIONS

. A method is developed to specify the surface stress and the wind speed and direction in the planetary boundary layer of a tropical cyclone from meteorological storm parameters available for historical hurricanes. The method is based upon a numerical primitive-equation model of the planetary boundary layer in a moving tropical cyclone. The complete time history of the evolution of the surface wind field is described from a series of characteristic wind field states calculated at discrete times in a storm's history by the steady-state model.

. A surface drag formulation, based upon a contemporary similarity model (Arya, 1977) coupled with a roughness parameter specification for a water surface consistent with Cardone's (1969) law, is incorporated into the numerical model. As a result, the model was found to produce a consistent description of the integrated planetary boundary layer wind, the magnitude and direction of the surface stress, and the wind speed and direction at anemometer level, without recourse to arbitrary, empirical calibration schemes. The surface winds calculated in several recent hurricanes are found to be in excellent agreement with available, representative surface wind measurements made from offshore platforms and data buoys.

. Transformations based upon an equilibrium planetary-boundary-layer similarity model are developed to specify the surface wind over terrain of specified roughness, including lake surfaces, from the over-water wind-field solution. Calculated over-land and over-lake winds are compared to the limited measurements available for several recent storms. Agreement is generally good.

. The principal limitation of the model is the neglect of fetch effects in the adjustment of the PBL across roughness discontinuities. Adjustments in near-surface wind speed, however, are believed to occur sufficiently rapidly that accuracy over homogeneous terrain and lakes the size of Pontchartrain and Okeechobee should not be significantly limited. The adjustment scale for wind direction, however, might be much larger.

. The principal obstacle to further development and evaluation of the method developed here is the lack of high-quality measurements of surface winds over the lakes of interest in well documented storms. As part of an intensive field program conducted in Lake Pontchartrain by the U.S. Army Corps of Engineers during the past year, wind data was apparently collected at several points in the lake during the passage of two hurricanes (Bob and Frederick, 1979). Even though only the peripheral parts of those storms were sampled, it is strongly recommended that those measurements be carefully processed and that the method developed in this study be applied to those storms.

LITERATURE CITED

- Anthes, R.A. 1974. The dynamics and energetics of mature tropical cyclones. Reviews of Geophysics and Space Physics. (Vol. 12, No. 3): 495-522.
- Anthes, R.A. and S. Chang. 1978. Response of the hurricane boundary layer to changes of sea-surface temperature Proc. of 11th Technical Conference on Hurricanes and Tropical Meteorology, Dec. 13-16, 1977. Miami, Florida. 568-573.
- Arya, S.P.S. 1977. Suggested revisions to certain boundary layer parameterization schemes used in atmospheric circulation models. Mon. Wea. Rev. (Vol. 105, No. 2): 215-227.
- Blackadar, A.K. and H. Tennekes. 1968. Asymptotic similarity in neutral barotropic PBL. J. Atmos. Sci. (Vol. 25): 1015-1022.
- Bretschneider, C.L. and E. Tamage. 1976. Hurricane wind and wave forecasting techniques, Look Lab/Hawaii Report, Jan. 1976. Ocean Engineering. Univ. of Hawaii, Hawaii.
- Cardone, V.J. 1969. Specification of the wind field distribution in the marine boundary layer for wave forecasting, Report TR-69-1, Geophys. Sci. Lab., Available from NTIS AD# 702-490. New York University, N.Y.NY.
- Cardone, V.J., W.J. Pierson, and E.G. Ward. 1976. Hindcasting the directional spectra of hurricane generated waves. J. of Petrol. Technol. (Vol. 28): 385-394.
- Cardone, V.J., D.B. Ross and M. Ahrens. 1978. An experiment in forecasting hurricane generated sea states, In 11th Technical Conference on Hurricanes and Tropical Meteorology, Dec. 13-16, 1977. Miami Beach, Florida. 688-695.
- Cardone, V.J. and D. Ross. 1979. "State-of-the-art wave prediction methods and data requirements." Ocean Wave Climate. Edited by M.D. Earle and A. Malahoff, (1979). Plenum Publishing Corporation, N.Y. N.Y. 61-91.
- Chang, S. 1977. The mutual response of the tropical cyclone and the ocean as revealed by an interacting atmospheric and oceanic model, Doctoral Dissertation, May 1977. Pennsylvania State Univ., University Park, Penn.
- Chow, S. 1971. A study of the wind field in the planetary boundary layer of a moving tropical cyclone, Masters Thesis, Dec. 1971, New York University, New York, N.Y.
- Deardoff, J.W. 1972. Parameterization of the planetary boundary layer for use in general circulation models. Mon. Wea. Rev. (Vol. 100):93-106.
- Deardoff, J.W. 1972b. Numerical investigation of neutral and unstable planetary boundary layers. J. Atmos. Sci. (Vol. 29): 91-115.
- Elliott, W.P. 1958. The growth of the atmospheric internal boundary layer. Trans. Amer. Geophys. Union. (Vol. 39): 1048-1054.

- Elsberry, R.L., N.A. Pearson and L.J. Corngate. 1974. A quasi-empirical model of the hurricane boundary layer. J. of Geophys. Res. (Vol. 79): 3033-3040.
- Forristall, G.Z. 1974. Three-dimensional structure of storm-generated currents. J. of Geophys. Res. (Vol. 79): 2721-2729.
- Forristall, G.Z., E.G. Ward, V.J. Cardone, and L.E. Borgman. 1978. The directional spectra and kinematics of surface waves in Tropical Storm Dalia. J. Phys. Oceanogr. (Vol. 8): 888-909.
- Garratt, J.R. 1977. Review of drag coefficients over oceans and continents. Mon. Wea. Rev. (Vol. 105): 915-929.
- Graham, H.E. and G.N. Hudson. 1960. Surface winds near the center of hurricanes (and other cyclones), National Hurricane Research Project Report No. 39. U.S. Weather Bureau, 1960. 200 pp. Washington, D.C.
- Hess, S.L. 1959. Introduction to Theoretical Meteorology. Holt, Rinehart and Winston. 362 pp. New York, N.Y.
- Jelesnianski, C. 1967. Numerical computation of storm surges with bottom stress. Mon. Wea. Rev. (Vol. 95): 740-756.
- Jensen, N.O. 1978. Change of surface roughness and the planetary boundary layer. Quart. J.R. Met. Soc. (Vol. 104): 351-356.
- Jones, W.L., F.J. Wentz, L.C. Schroeder. 1978. Algorithm for inferring wind stress from SEASAT-A. J. of Spacecraft and Rockets. (Vol. 15): 368-374.
- Moss, M.S. and S.L. Rosenthal. 1975. On the estimation (from bulk data) of boundary layer variables and cloud base mass flux in mature hurricanes, NOAA Technical Memorandum ERLWMP0-23. U.S. Dept. of Commer., Nat. Oceanic and Atmos. Admin. Environmental Research Lab., Oct. 1975. Wash. DC.
- Moss, M.S. 1978. Low level turbulence structure in the vicinity of a hurricane. Mon. Wea. Rev. (Vol. 106): 841-849.
- Moss, M.S. and R.W. Jones. 1978. A numerical simulation of hurricane landfall, NOAA Tech. Mem. NHGML-3 NOAA Environmental Research Lab. Boulder, Colo.
- Myers, V.A. and W. Malkin. 1961. Some properties of hurricane wind field as deduced from trajectories, National Hurricane Research Project, No. 49, U.S. Weather Bureau. Washington, D.C.
- Patterson, M.M. 1972. Hurricane hindcasting in the Gulf of Mexico. J. of Soc. of Petrol. Eng. (Vol. 12): 321-328.
- Phillips, D.W. and J.G. Irbe. 1977. Lake to land ratios of wind, temperature and humidity during IFYGL, CLI2-77, Atmospheric and Environmental Service. Downsview, Ontario.
- Richards, T.L., H. Dragert, and D.R. McIntyre. 1966. Influence of atmospheric stability and over water fetch on winds over the lower great lakes. Mon. Wea. Rev. (Vol. 94, No. 17): 454-458.

- Ross, D.B. and W.L. Jones. 1977. On the relationship of radar backscatter to wind speed and fetch. Boundary-Layer Meteorology. (Vol. 13): 151-163.
- Ross, D.B. and V.J. Cardone. 1978. "A comparison of parametric and spectral hurricane wave prediction products." In Turbulent Fluxes through the Sea Surface, Wave Dynamics, and Prediction. Editors A. Faure, K. Hasselmann. Plenum Press. 647-665.
- Schauss, C.E. 1962. Reconstruction of the surface pressure and wind fields of Hurricane Helene, Nat. Hurricane Res. Proj. Rep 59. U.S. Dept. of Commer., Washington, D.C. 45 pp.
- Shea, D.J. and W.M. Gray. 1973. The hurricanes inner core region I, symmetric and asymmetric structure. J. Atmos. Sci. (Vol. 30): 1544-1564.
- Smagorinsky, J. 1963. General circulation experiments with the primitive equations: I. The Basic Experiment. Mon. Wea. Rev. (Vol. 91): 99-164.
- Sperry Univac Series 1100, Fortran V Level 4 R1 programmer reference, edition April 1979. Available from, UNIVAC, P.O. Box 500, Blue Bell, PA. 19422, ATTN. Systems Publications Dept.
- Taylor, P.A. 1968. The planetary boundary layer above a change in surface roughness. J. Atmos. Sci. (Vol. 26): 432-440.
- U.S. Weather Bureau, Hydrometeorological Section. 1954. Analysis and synthesis of hurricane wind pattern over Lake Okeechobee Florida. Hydrometeorological Report #31. Washington, D.C.
- Wanstrath, J.J., R.E. Whitaker, R.O. Reid, and A.C. Vastano. 1976. Storm surge simulation in transformed coordinates Vol. I, Theory and Application Technical Report No. 76-3. Prepared for U.S. Army Corps of Engineers Coastal Engineering Research Center, Kingman Building, Fort Belvoir, VA., Nov. 1976.
- Wanstrath, J.J. 1978. An open-coast mathematical storm surge model with coastal flooding for Louisiana, Report 1, Theory and Application, Miscellaneous Paper H-78-5, Hydraulics Lab. U.S. Army Engineer Waterways Experiment Station, P.O. Box 631, Vicksburg, Miss. 39180, Feb. 1978.
- Ward, E.G., L.E. Borgman, and V.J. Cardone. 1979. Statistics of hurricane waves in the Gulf of Mexico. J. of Petrol. Technol. (Vol. 31): 632-642.
- Whitaker, R.E., R.O. Reid, A.C. Vastano. 1973. Drag coefficient at hurricane wind speeds as deduced from numerical simulation of dynamic water level changes in Lake Okeechobee. Ref. 73-13-T, Dept. of Oceanography, Texas A&M University, College Station, Texas.
- Zilitinkevich, S.S. 1970. Dynamics of the Atmospheric Boundary Layer. Hydrometeorological Press, 290 pp. (in Russian).

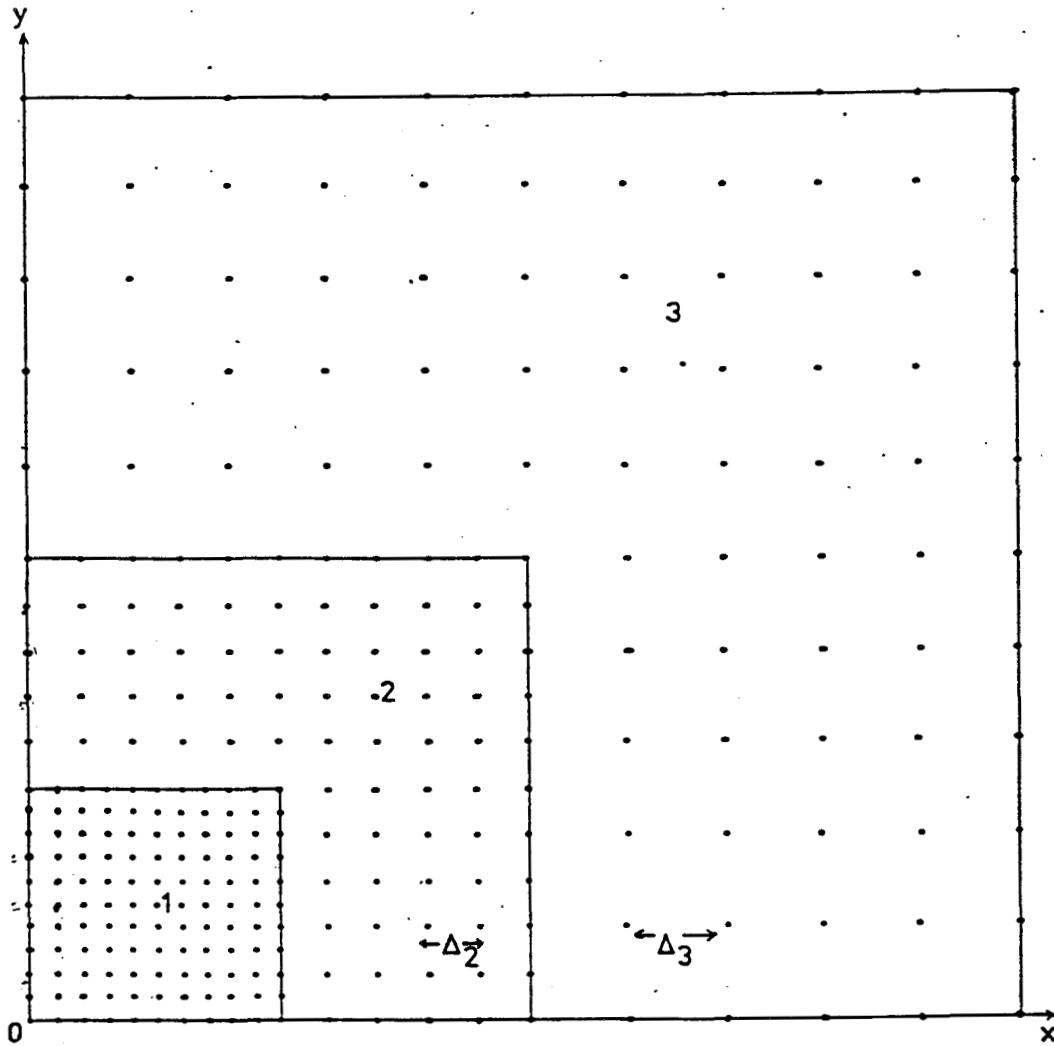


Figure 1. Grid points of the inner three grids in one quadrant of the nested grid system. The center of the grid system is indicated by 0 (from Chow 1971)

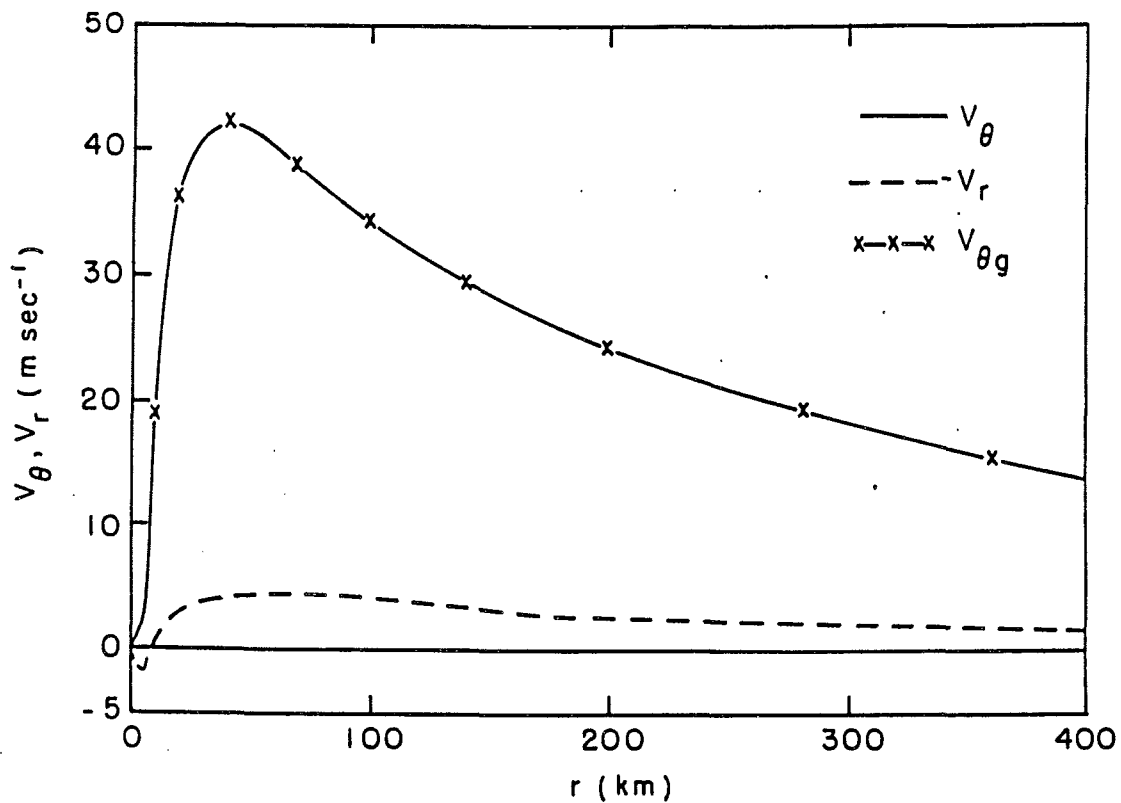


Figure 2. Radial distribution of tangential velocity (V_θ) and radial velocity (V_r) for a frictionless, symmetrical, stationary storm given by $\Delta p = 50$ mb and $R = 40$ km, computed from Chow's numerical model. Analytical (gradient wind solution) solution ($V_{\theta g}$) for specified pressure field is shown (from Chow 1971)

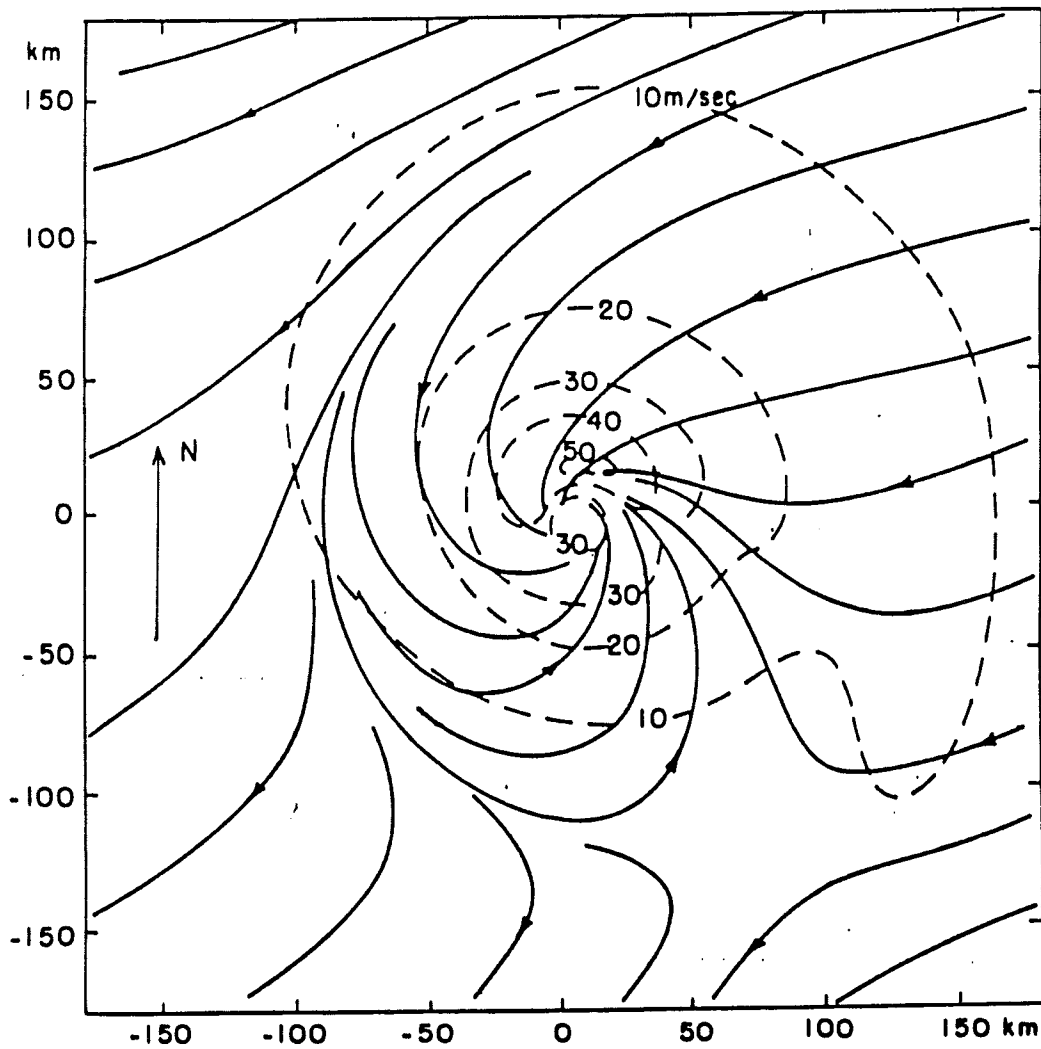


Figure 3. Streamlines (solid lines) and isotachs (dashed lines) of the steady-state solution for the vertically integrated boundary layer wind in a mature tropical cyclone moving westward at 10 m/sec, in a westerly steering flow (10 m/sec), from the model of Chow (1971)

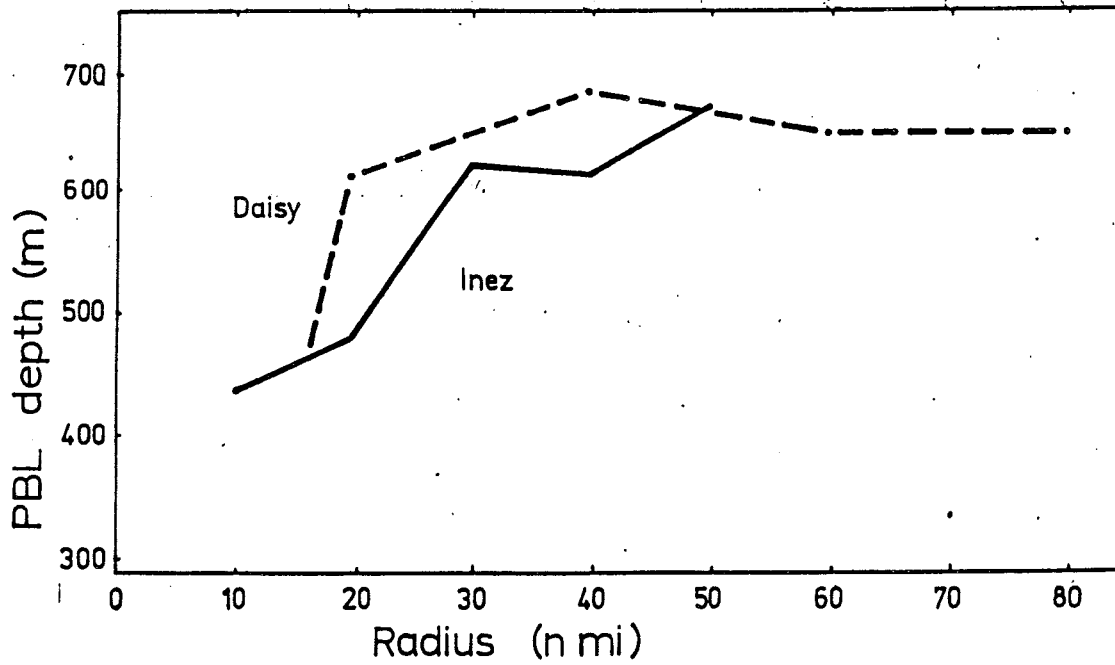


Figure 4. Computed depth of the planetary boundary layer versus radial distance from the eye for Hurricanes Daisy (1958) and Inez (1966) (from Moss and Rosenthal 1975)

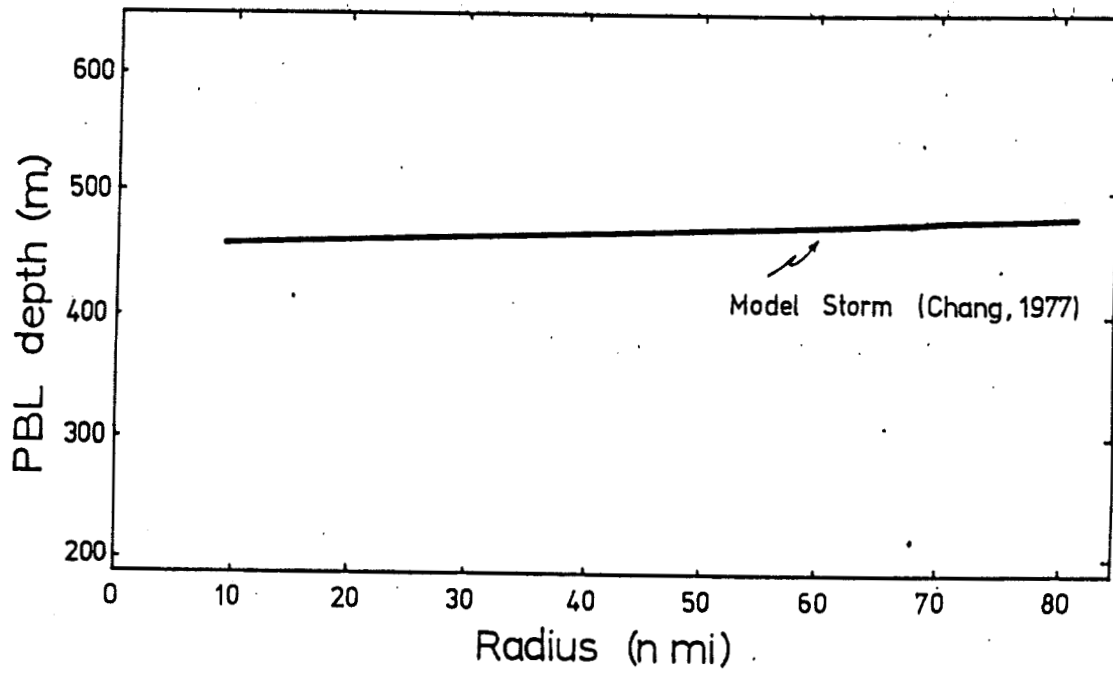


Figure 5. Computed depth of the planetary boundary layer in a mature, steady-state tropical cyclone (from Chang 1977)

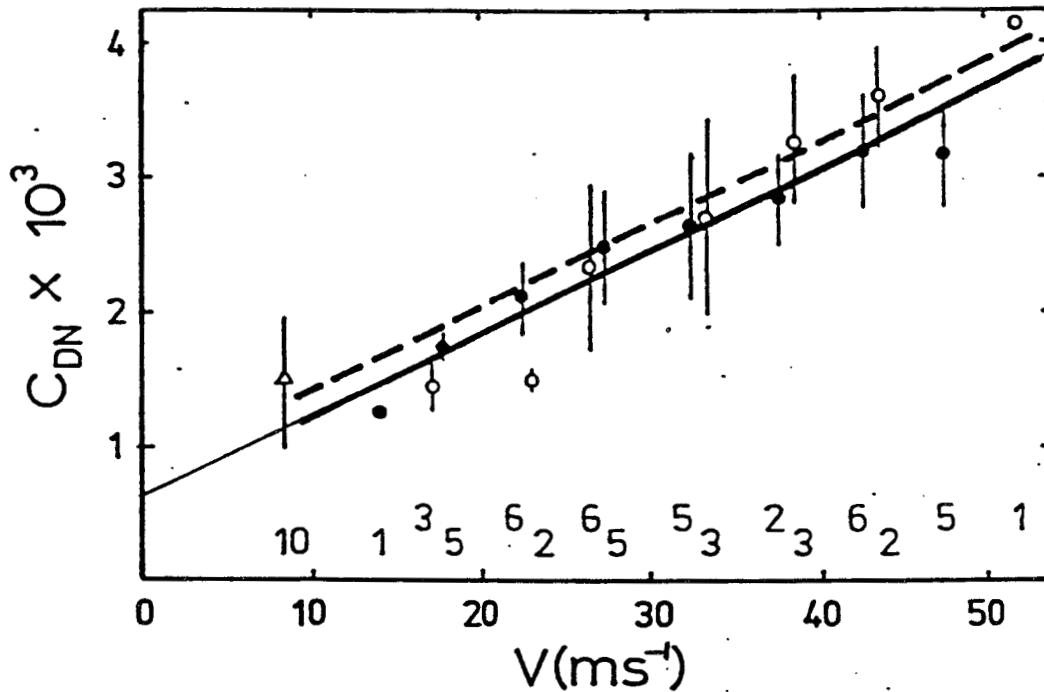


Figure 6. Garratt's (1977) collection of mean values of the drag coefficient as a function of wind speed at the 10-m height for 5-m/sec intervals, based on individual data from hurricane studies (O), wind flume experiments (•), and vorticity/mass budget analysis (Δ). Vertical bars refer to the standard deviation of individual data for each mean, with the number of data used in each mean shown below each mean value immediately above the abscissa scale. The dashed curve represents the variation of the 10-m neutral drag coefficient C_{DN} with wind speed based on

$$z_o = a \frac{u_*^2}{g}$$

with $a = 0.0144$ and a value of the barrier constant k of 0.41. The solid curve represents the variation with $a = 0.035$ and $k = 0.35$

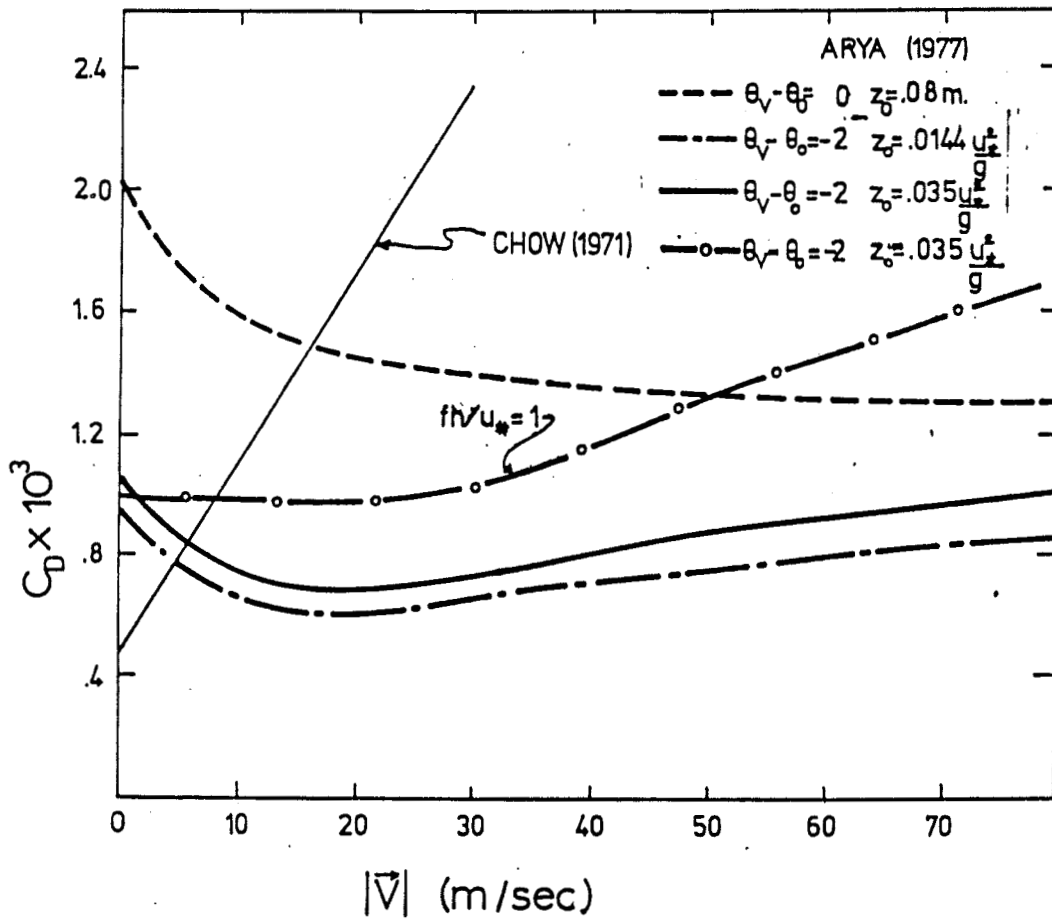


Figure 7. Drag coefficient with respect to the vertically integrated planetary boundary layer wind versus integrated boundary layer wind from Arya's model for alternate air-sea temperature and roughness parameter specifications and/or the case of restricted scale/height ratio. The form used by Chow (1971) is shown for comparison

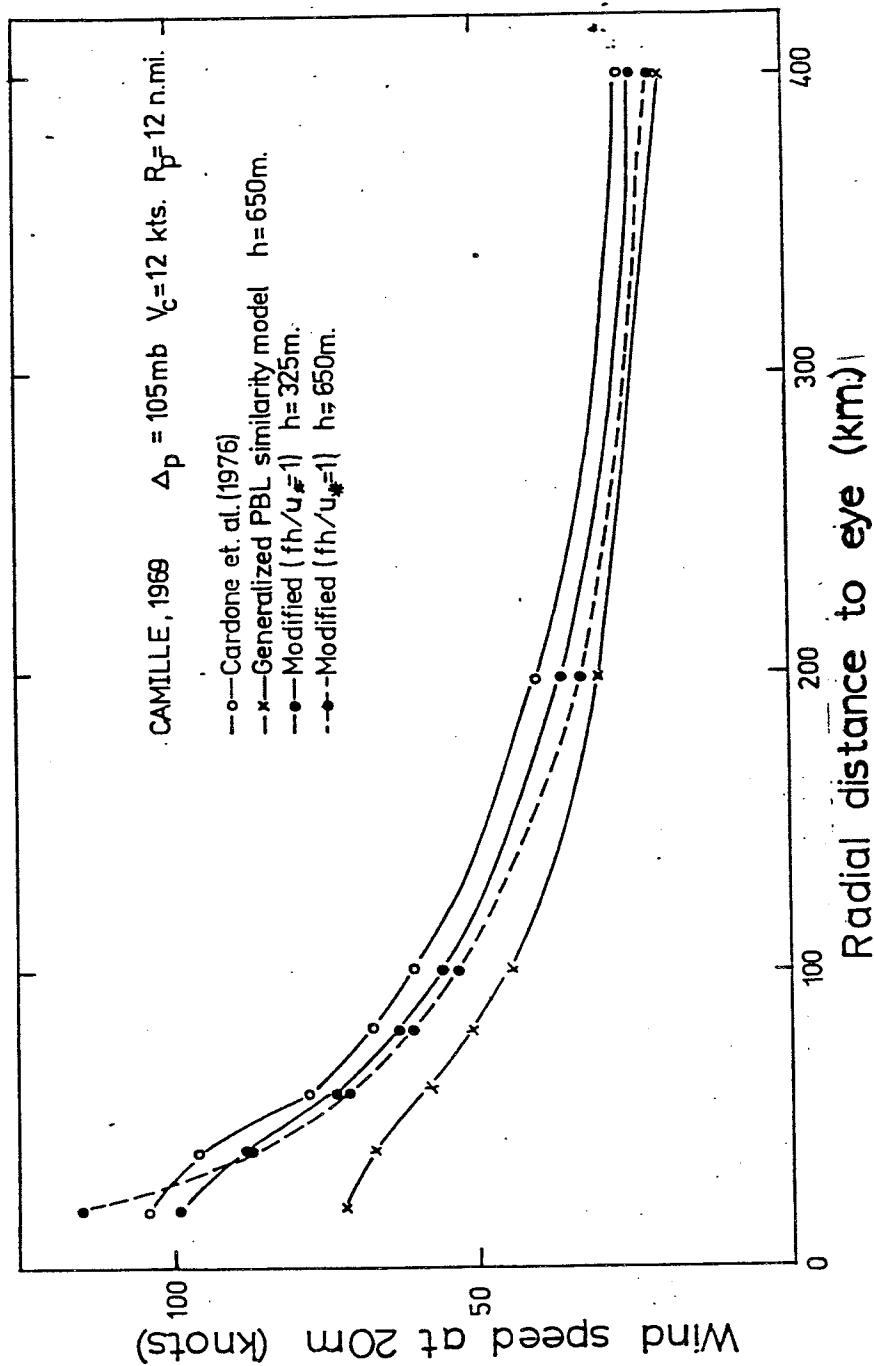


Figure 8. Predictions of 20-m wind speed versus radial distance to eye in Camille from the model of Cardone et al. (1976) and from the model with revised PBL stress law

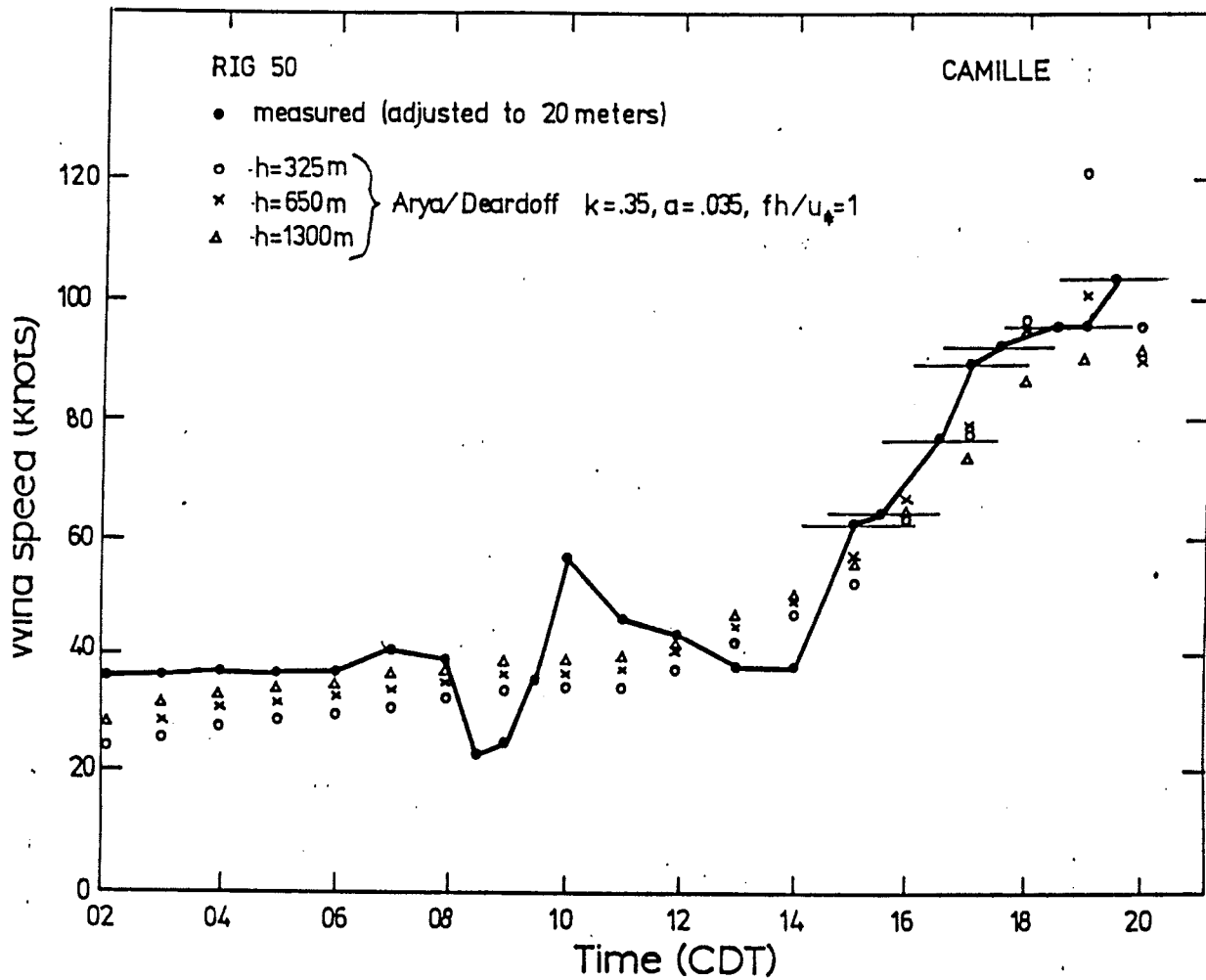


Figure 9. Comparison of modelled and measured surface wind speed at Rig 50 in Camille for vortex model with modified similarity model drag law and alternate boundary layer heights

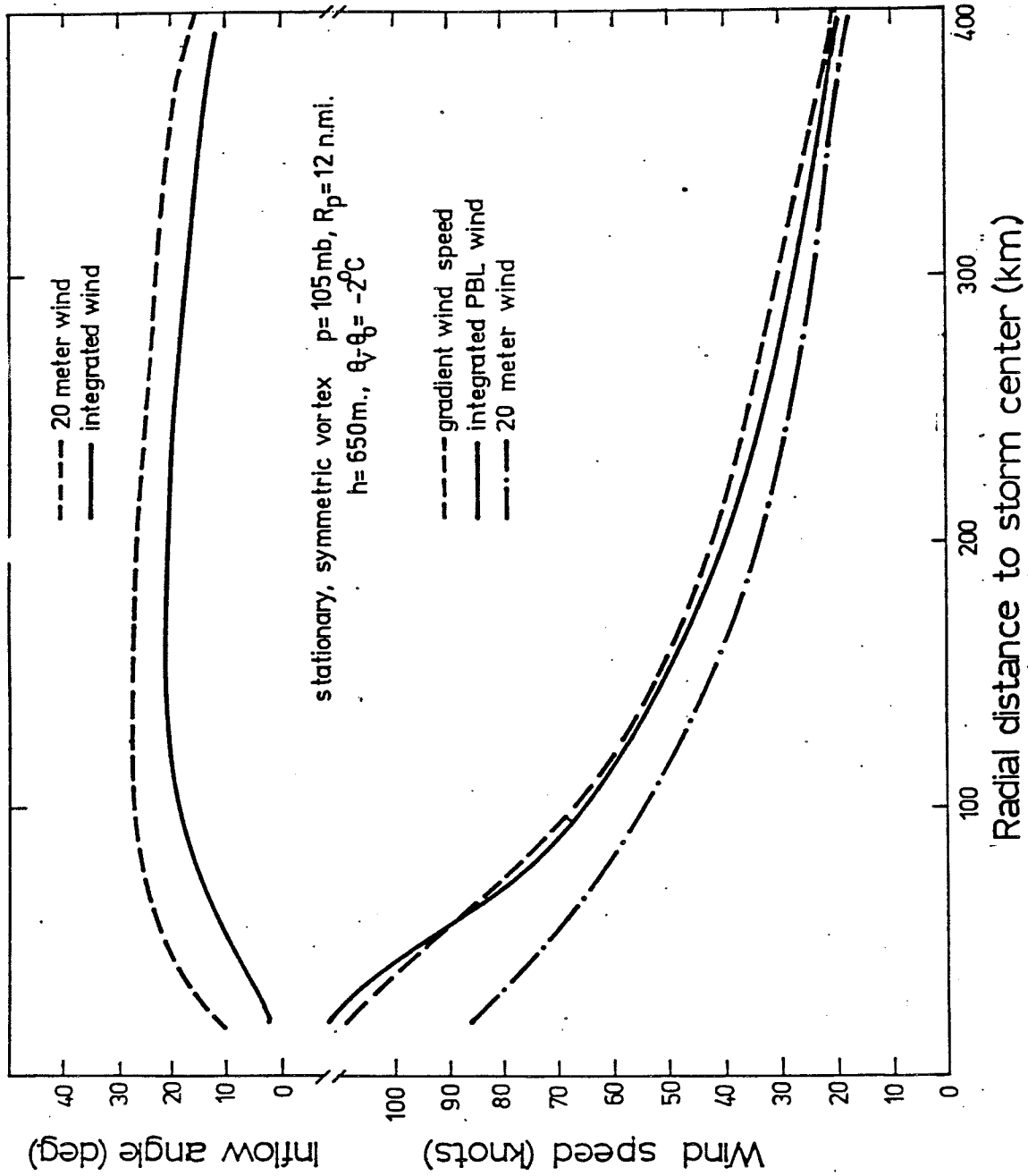


Figure 10. Radial profile of gradient wind speed, integrated PBL wind speed, 20-m wind speed, inflow angle of integrated and surface wind for a severe, stationary, symmetric hurricane

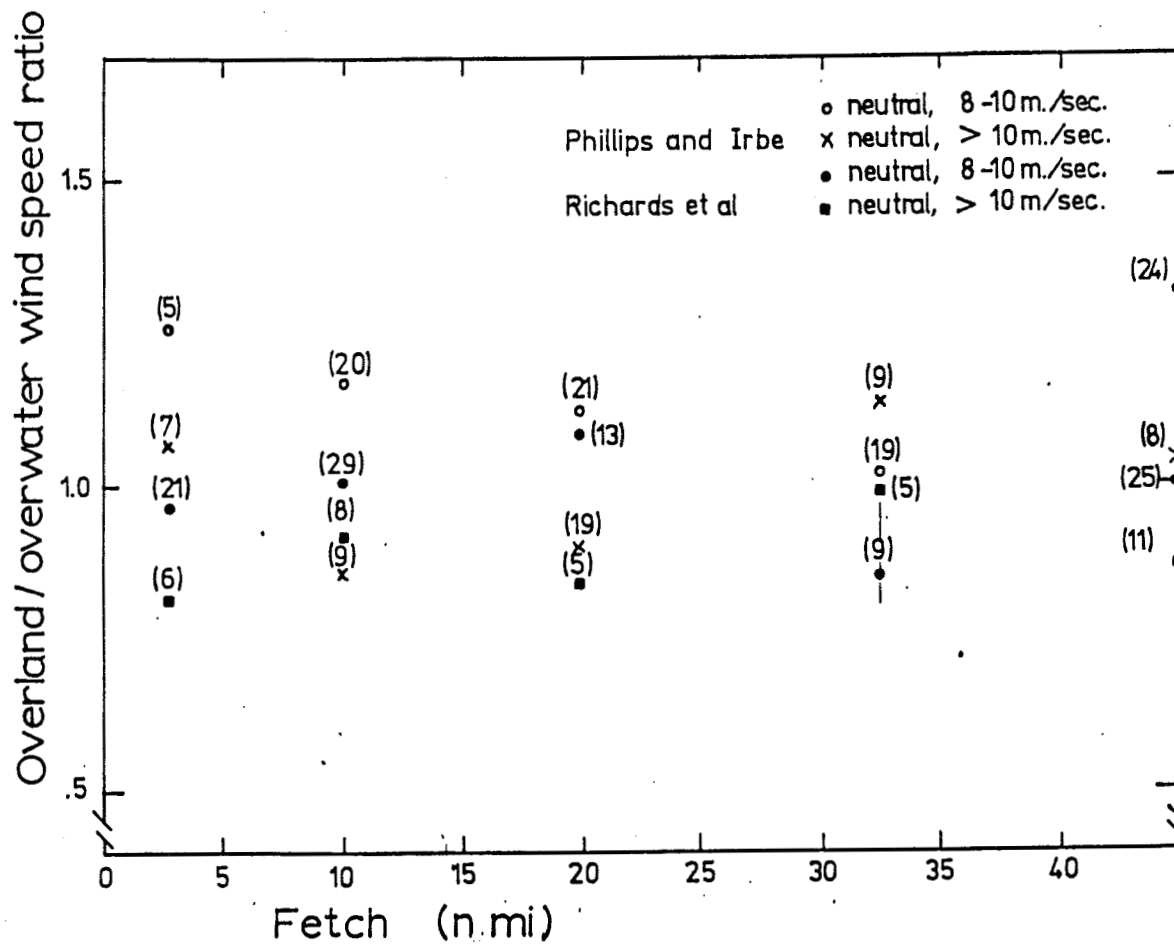
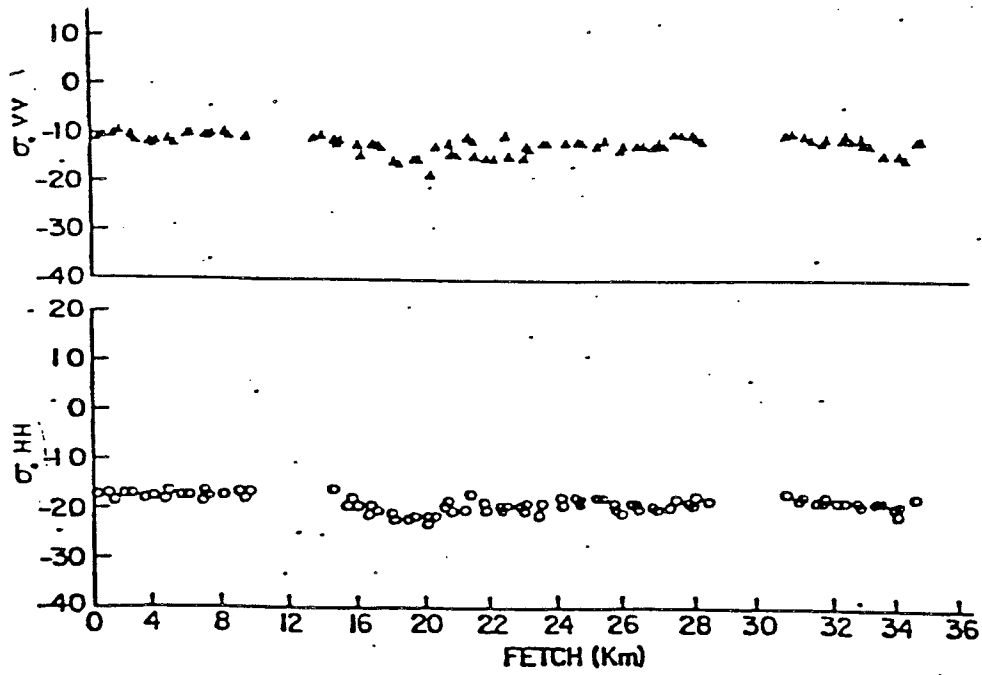
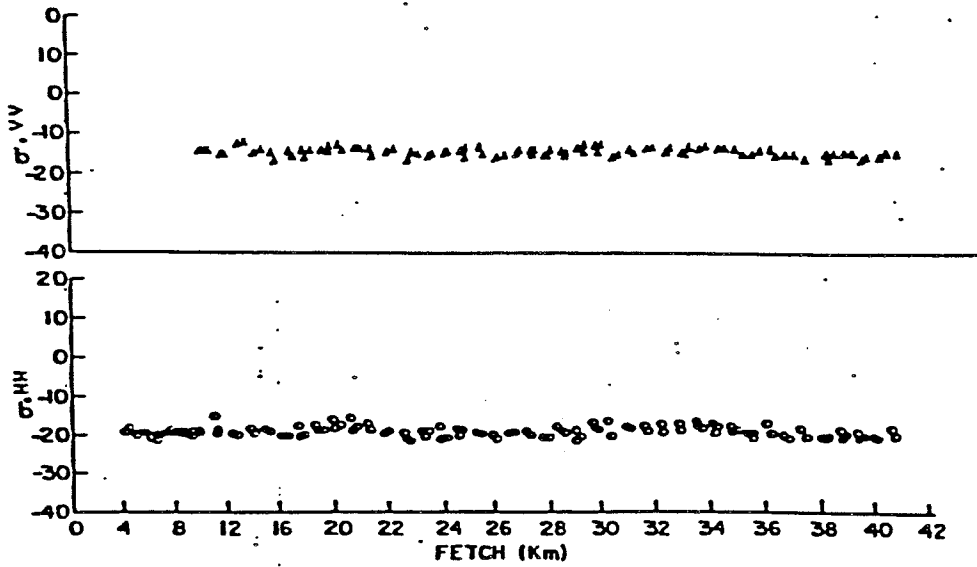


Figure 11. Ratio of overland/over-water wind speed versus fetch for near neutral moderate-high wind speed data of Richards et al. (1966) and Phillips and Irbe (1977)



Radar scattering cross section σ_0 as a function of fetch at an incidence angle of 40° . Surface wind speeds were 9.0 m s^{-1} .



Radar scattering cross section σ_0 as a function of fetch at an incidence angle of 53° . Surface wind speeds were 13.0 m s^{-1} .

Figure 12. Radar scattering cross section σ_0 as a function of fetch at an incidence angle of 40° for wind speeds of 9.0 m/sec (above) and an incidence angle of 53° for wind speeds of 13.0 m/sec (below)

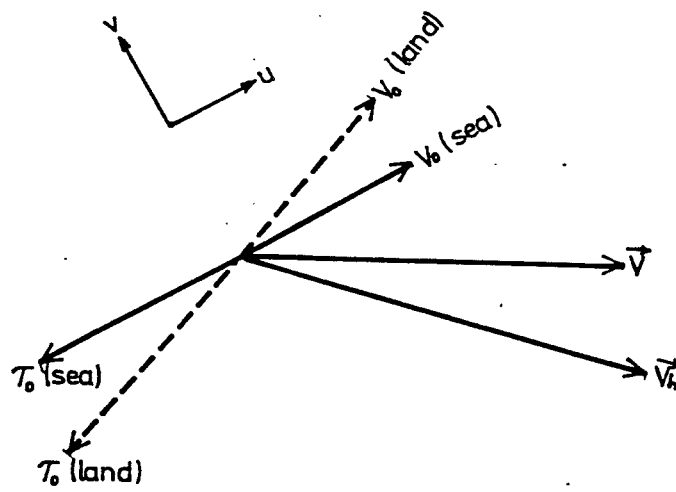


Figure 13. Coordinate system and relationship of wind stress components in the equilibrium model PBL over rough and smooth (sea) terrain

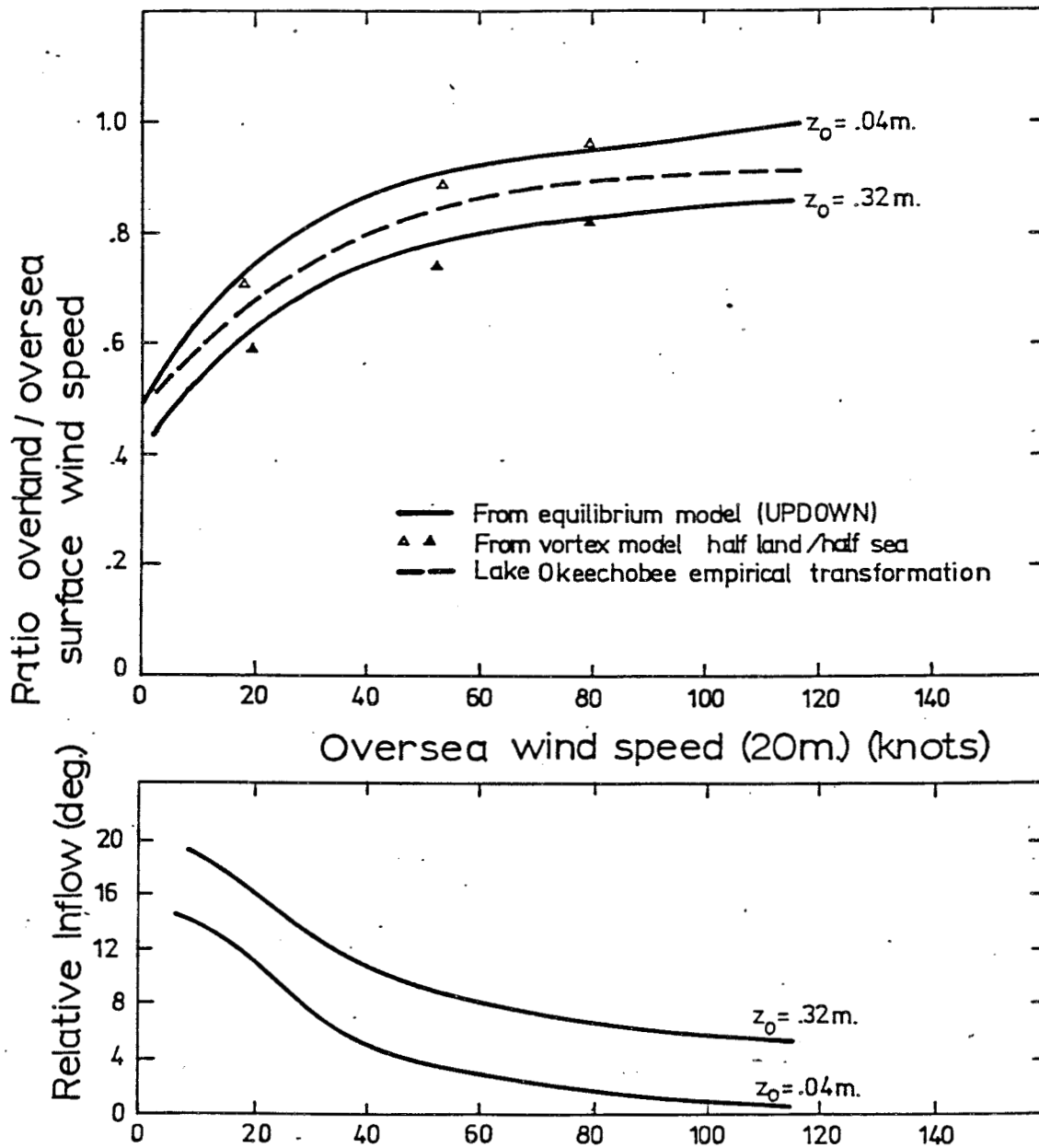


Figure 14. Ratio of the surface wind speed at the 20-m height overland to over sea (above) and the difference between the overland and over-sea inflow angle (below) from the equilibrium PBL model for two terrain roughnesses, from the numerical vortex model and the empirical wind speed ratio derived from measurements in hurricanes at Lake Okeechobee

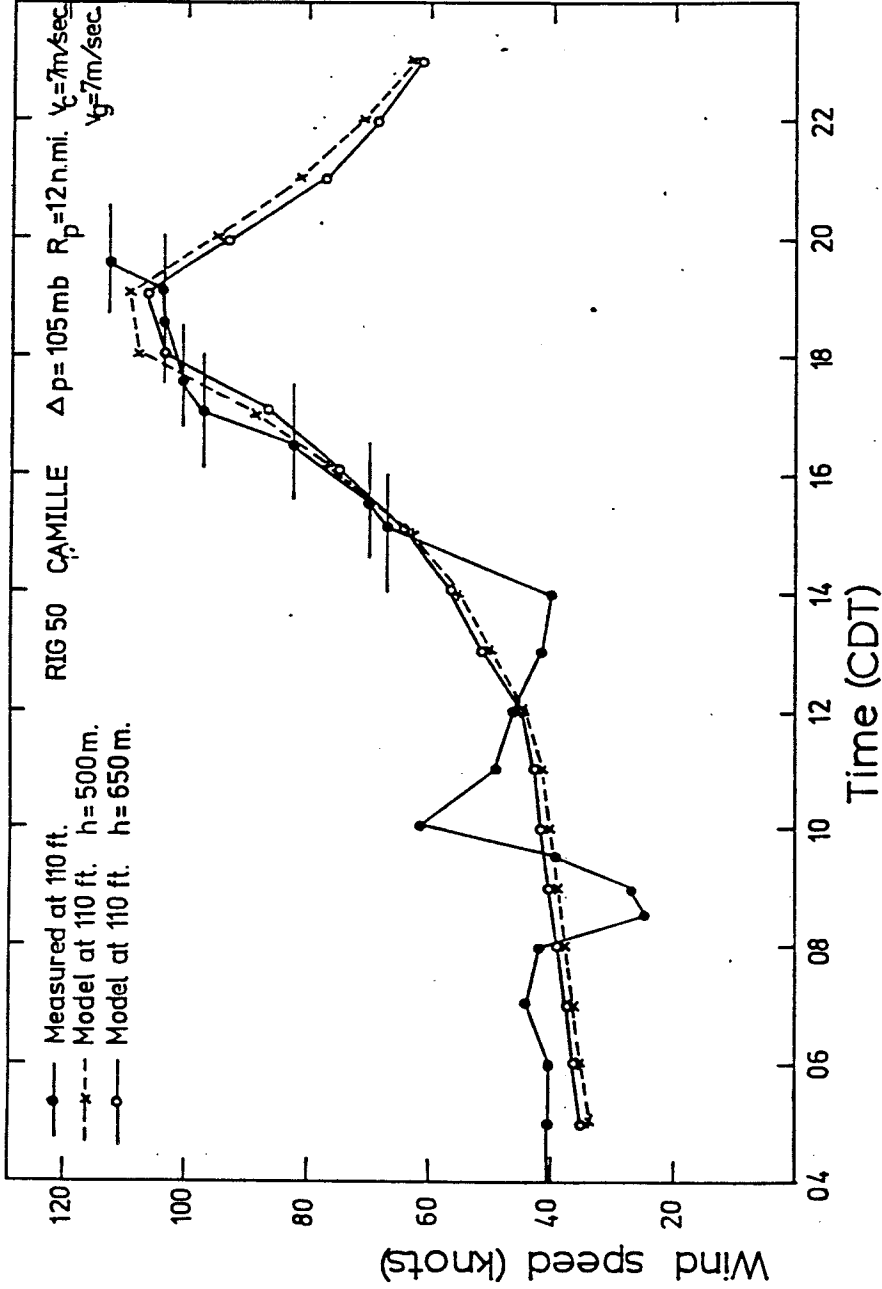


Figure 15. Comparison of measured and modelled wind speed at Rig 50 at measurement height in Camille

16 Z_0 Values for Typical Terrain Types (After ESDU 72026, 1972)

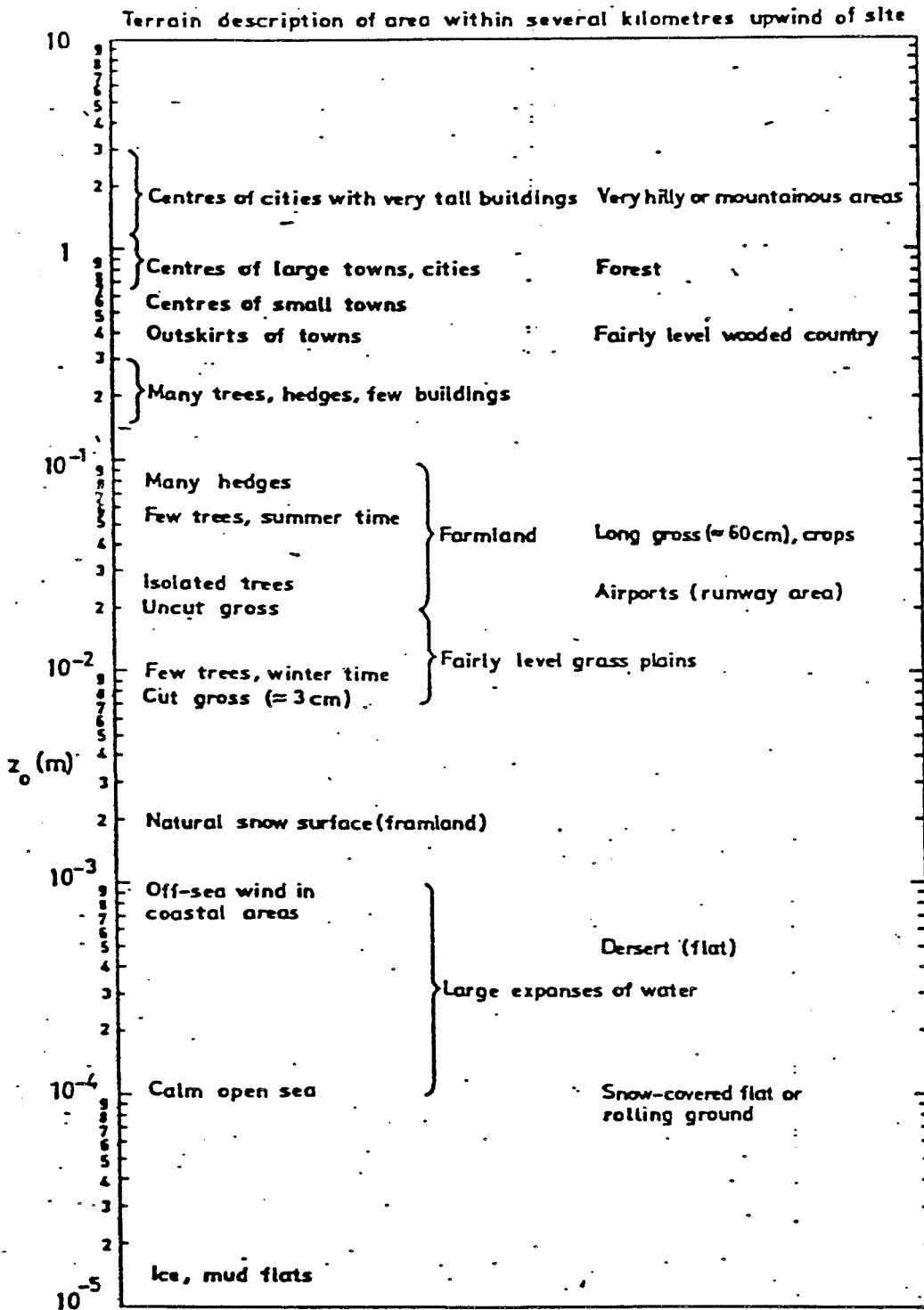


Figure 16. Roughness parameter values for typical terrain types (after ESDU 72026, 1972)

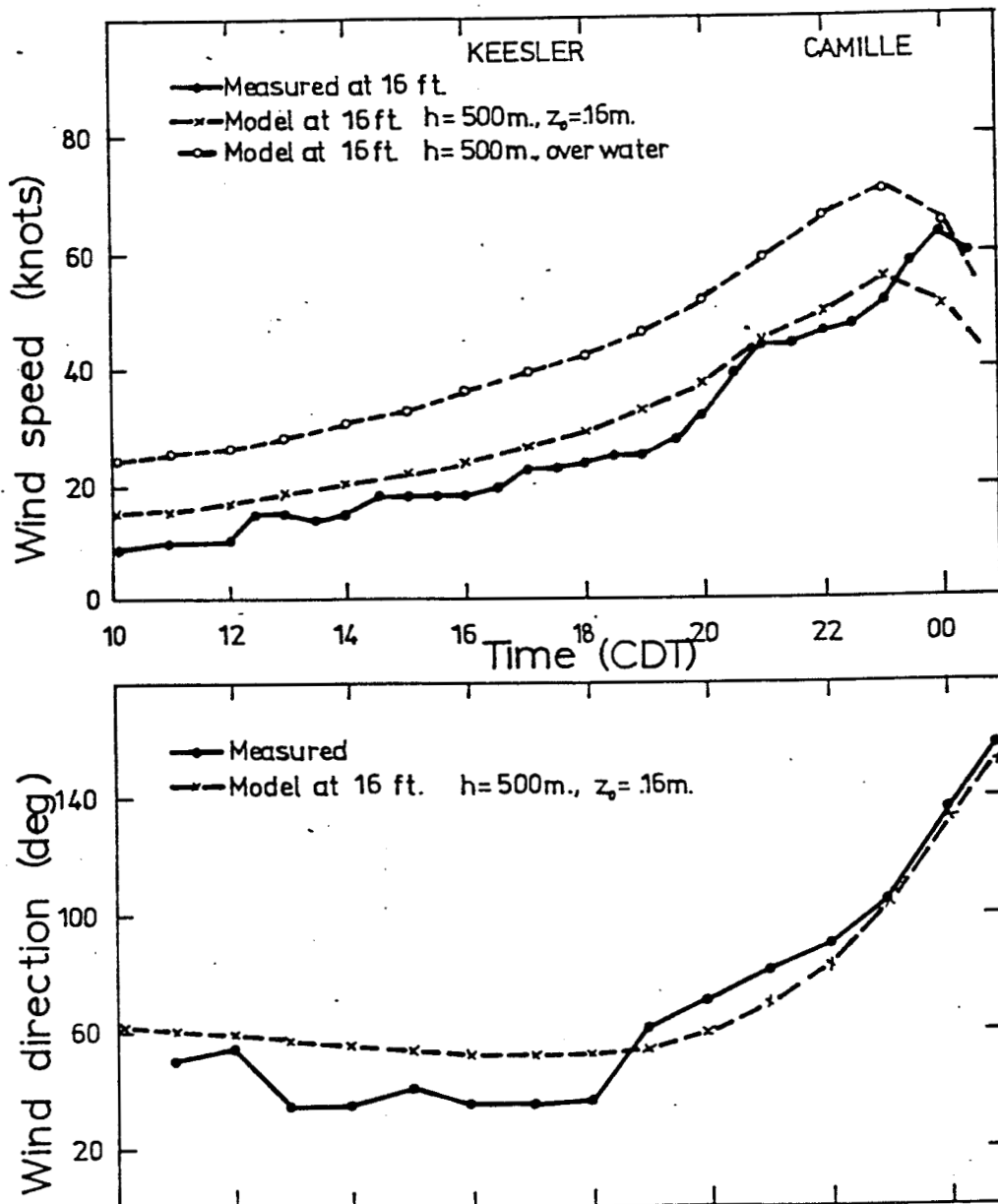


Figure 17. Comparison of measured and modelled winds at Keesler Air Force Base, Biloxi, MS, in Camille

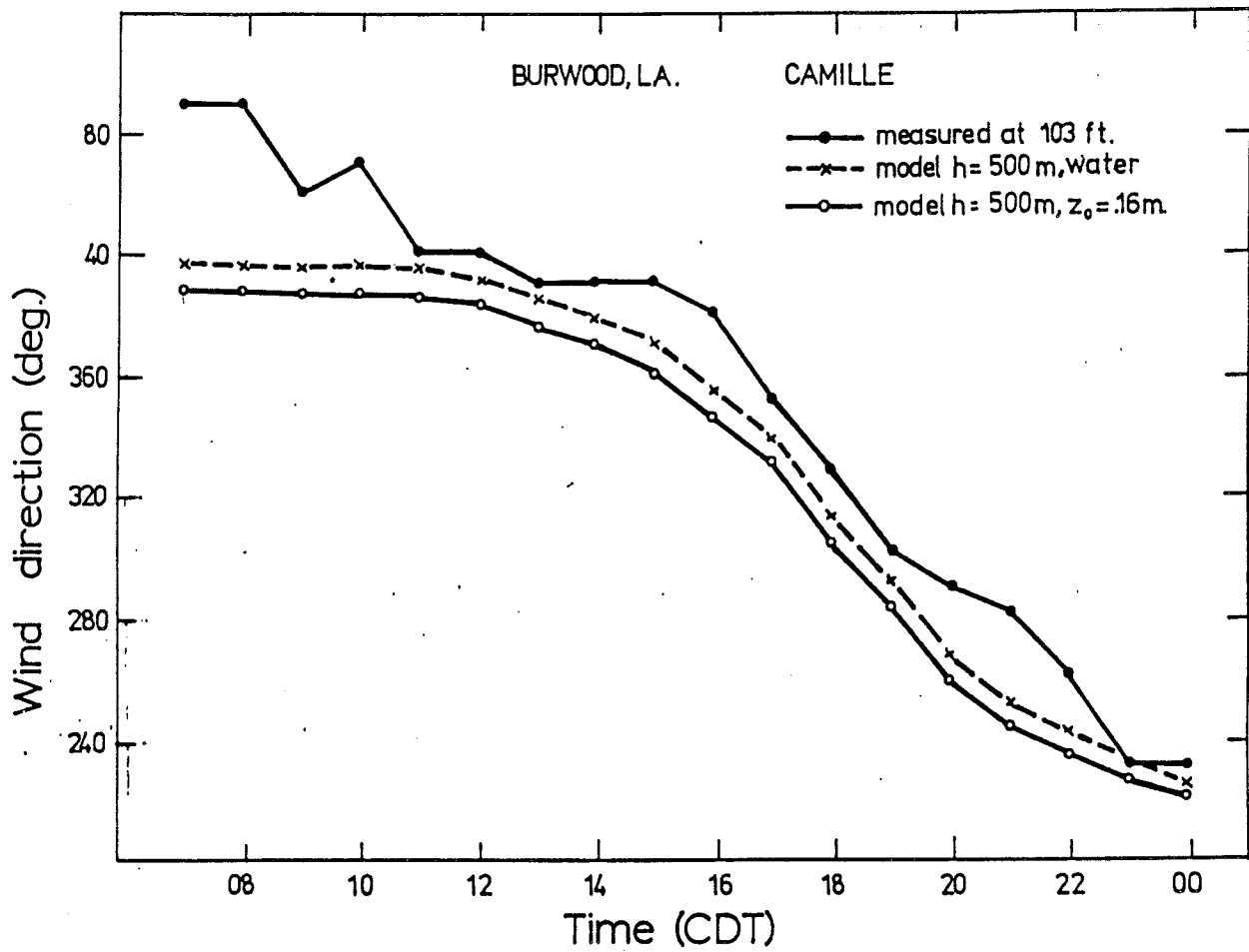


Figure 18. Comparison of measured and modelled wind direction at Burwood, LA, in Camille

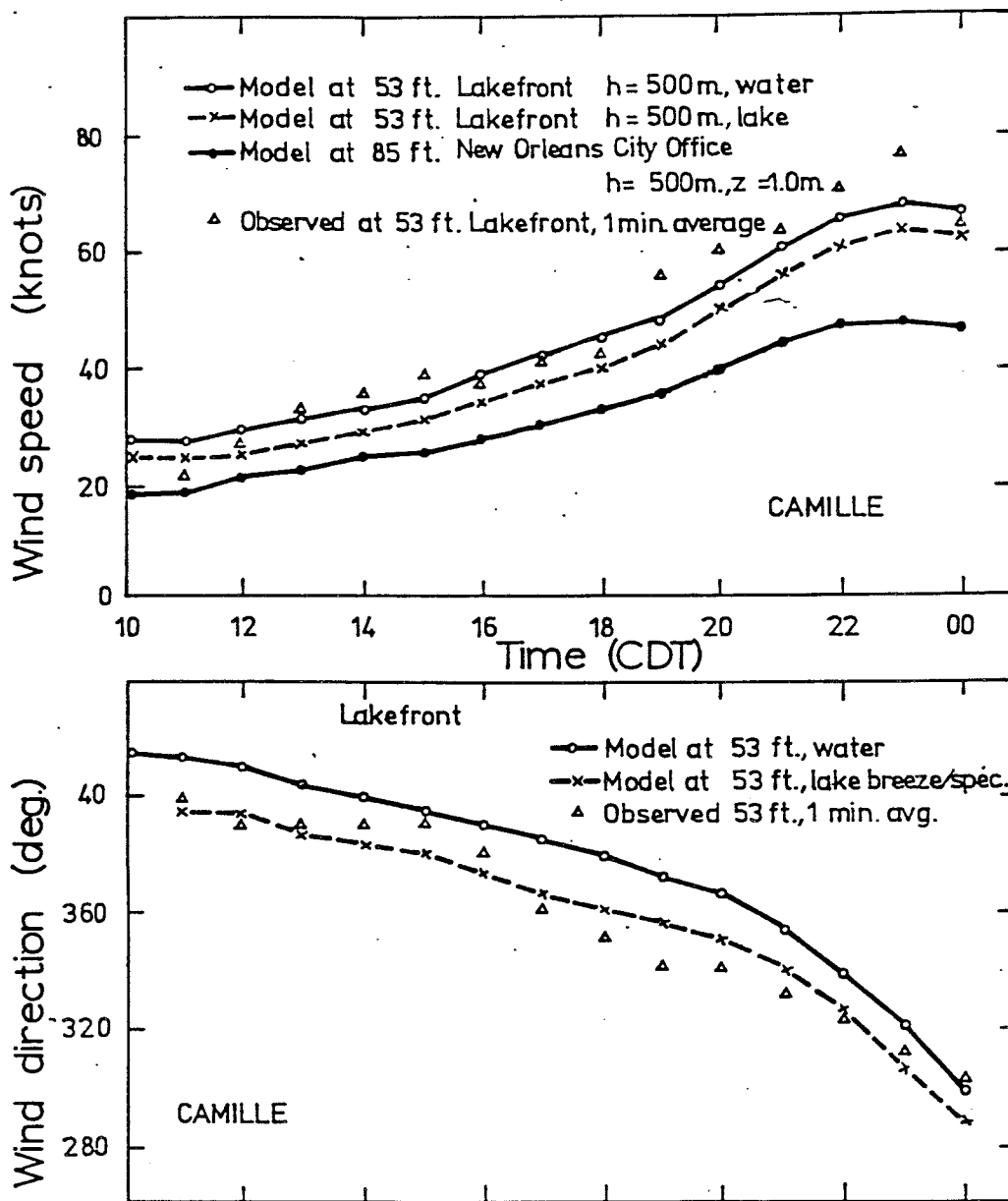


Figure 20. Comparison of measured and modelled wind speed (above) and wind direction (below) at New Orleans Lakefront Airport in Camille. Modelled wind at New Orleans for roughness parameter of 1 m shown

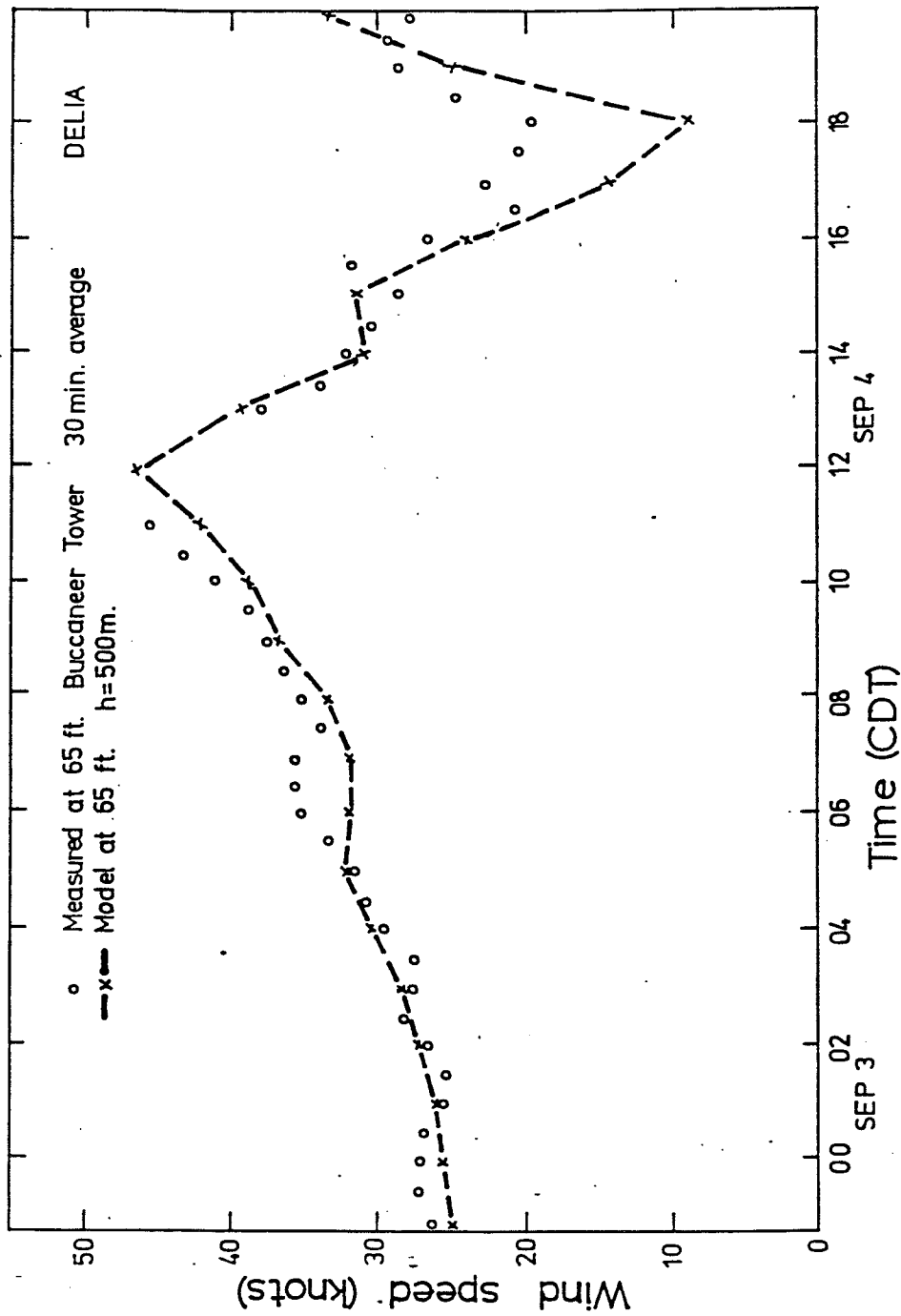


Figure 21. Comparison of measured and modelled wind speed at Buccaneer Tower in Delia

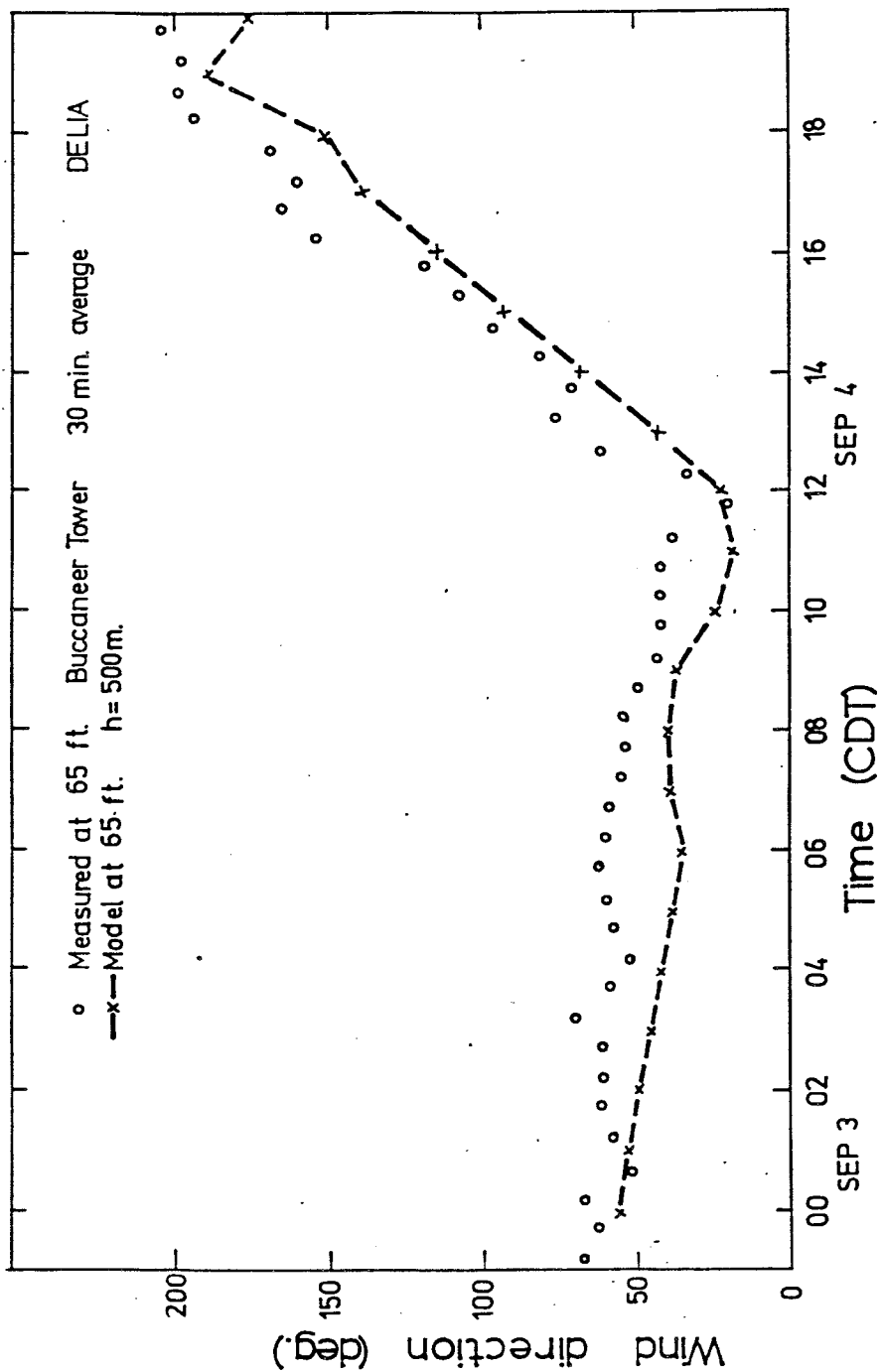


Figure 22. Comparison of measured and modelled wind direction at Buccaneer Tower in Delia

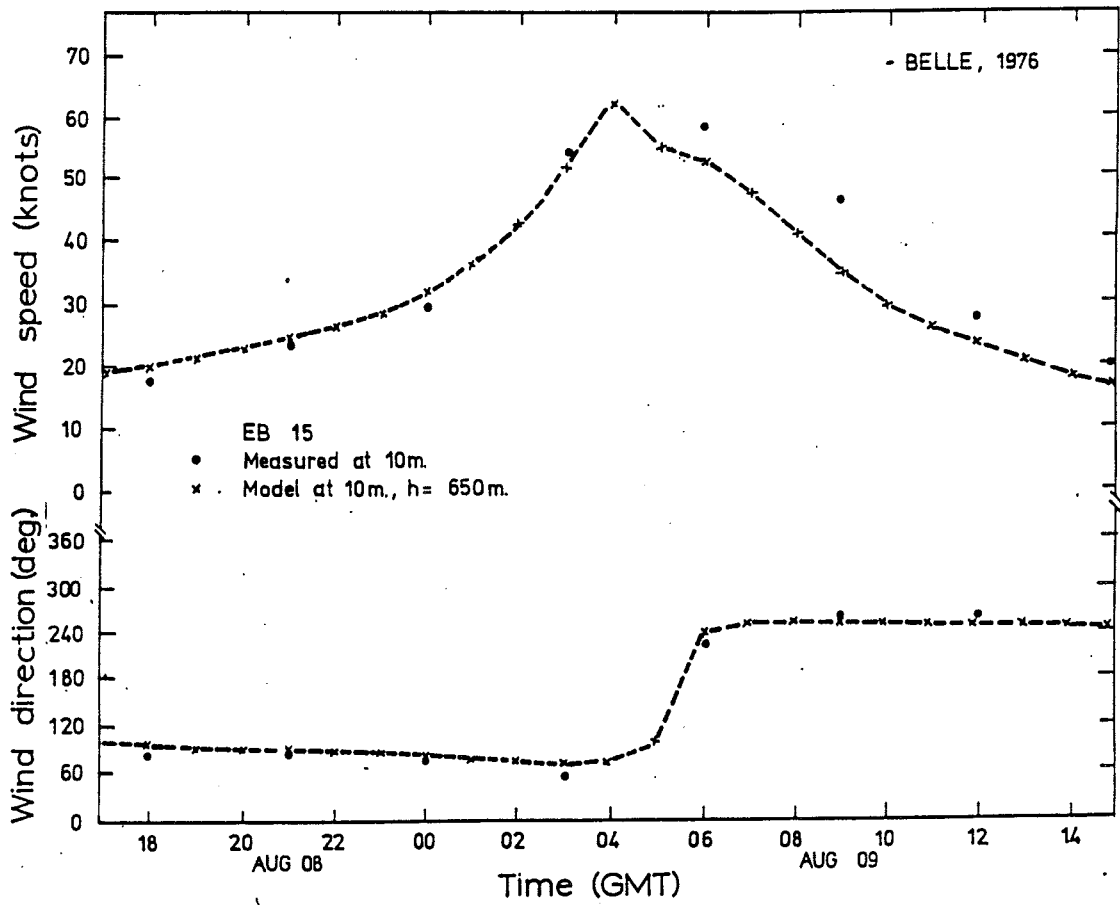


Figure 23. Comparison of measured and modelled wind speed and direction at buoy EB15 in Belle

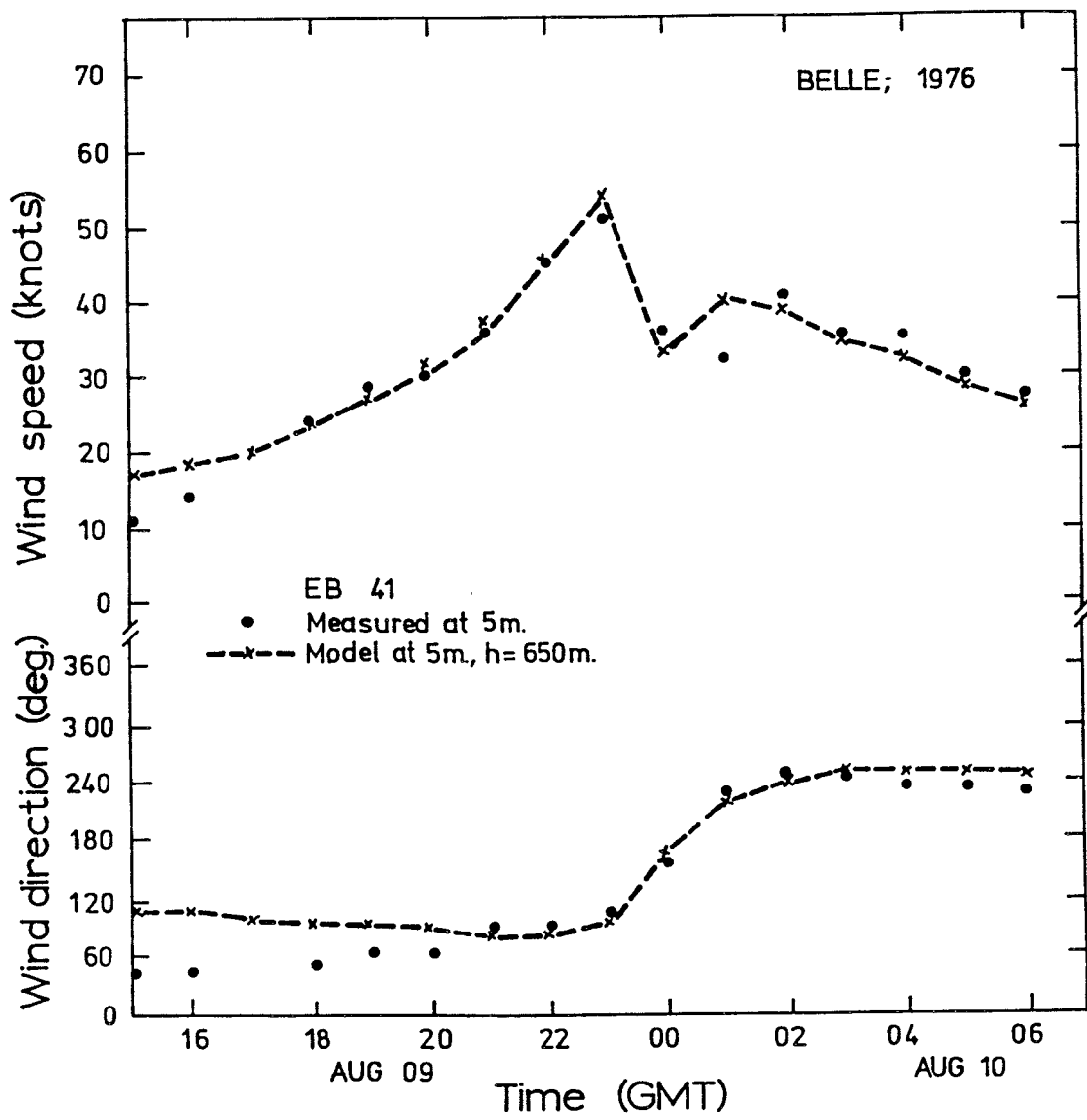


Figure 24. Comparison of measured and modelled wind direction at buoy EB41 in Belle

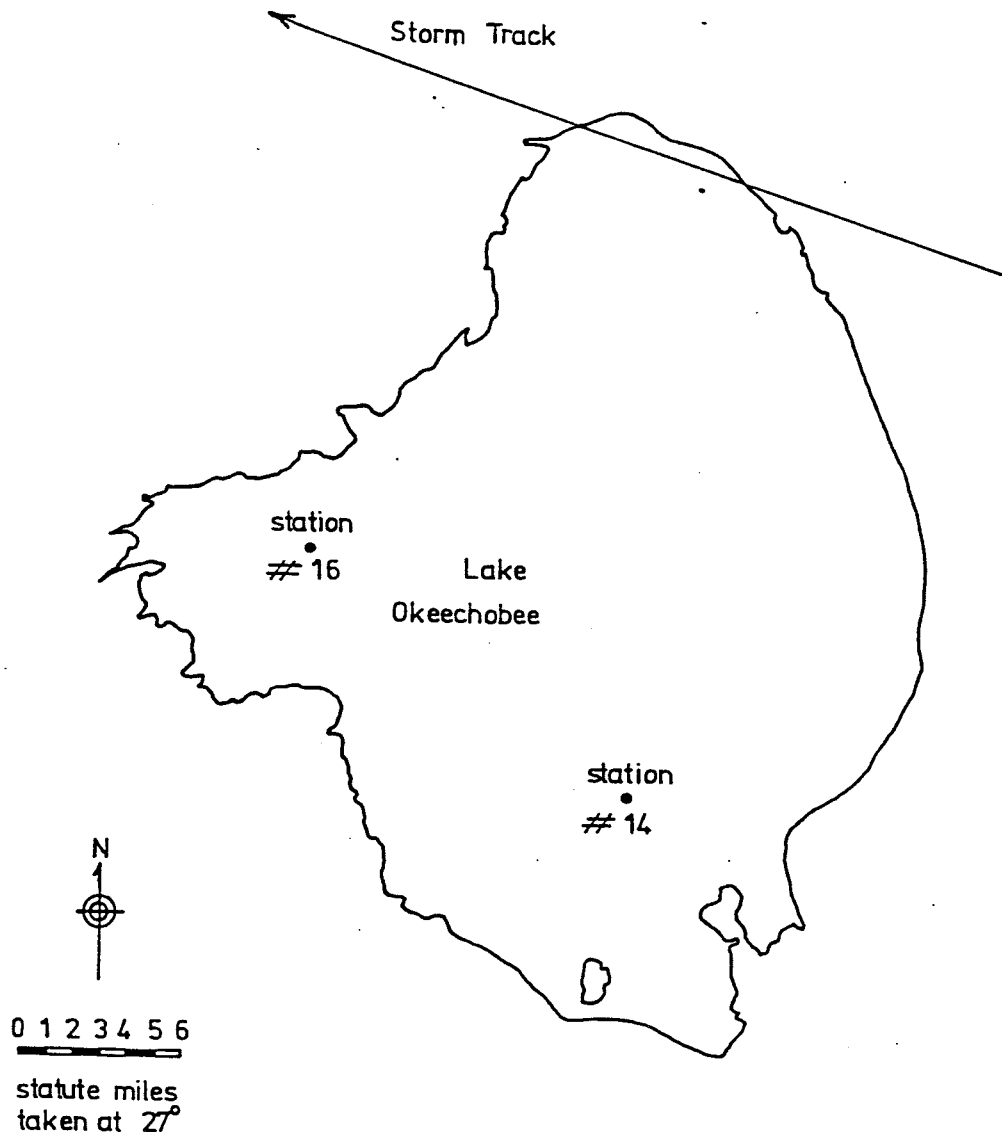


Figure 25. Location of measurement stations in Lake Okeechobee and path of the 1949 Lake Okeechobee hurricane

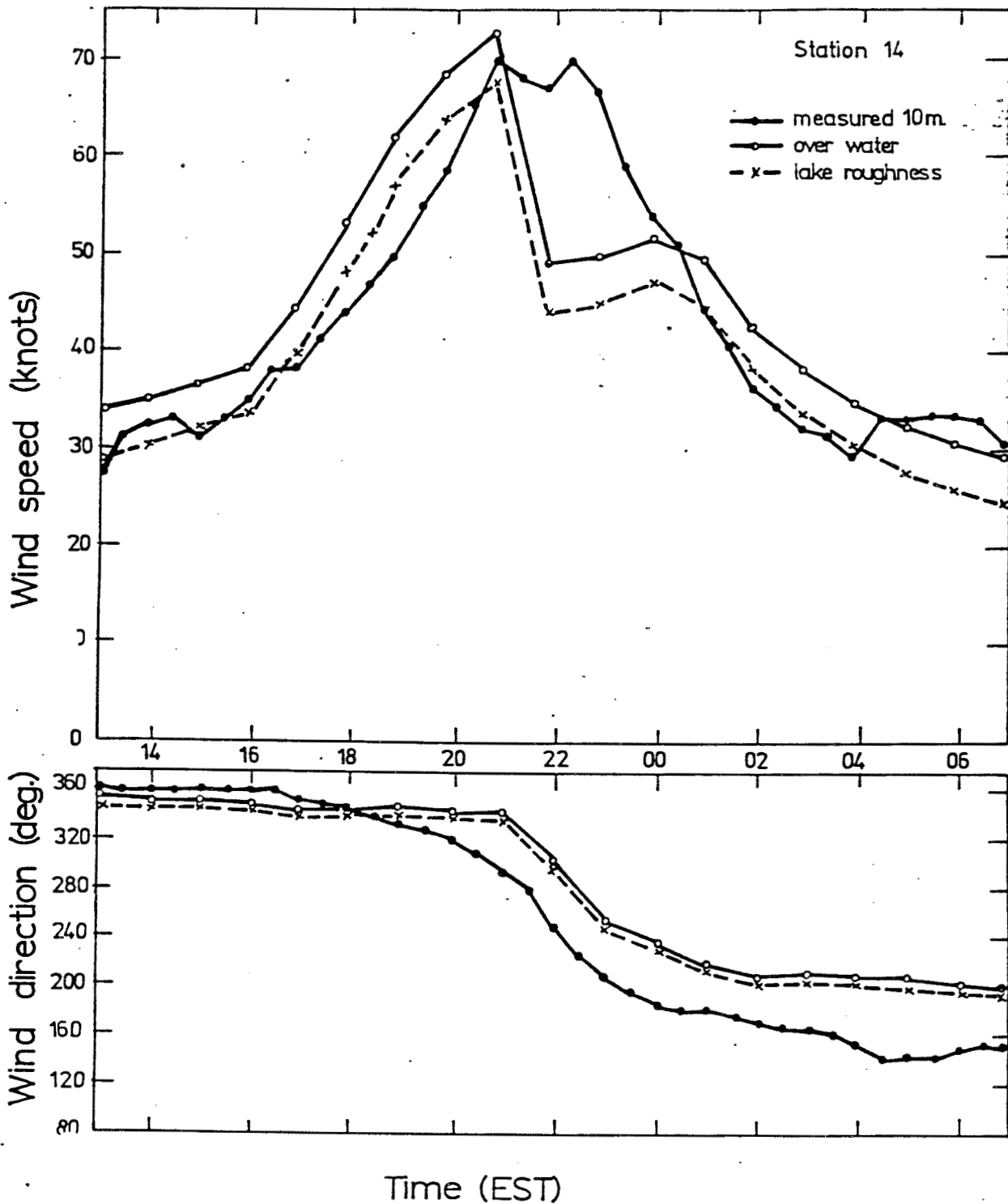


Figure 26. Comparison of measured and modelled wind speed and direction at station 14 in the 1949 Lake Okeechobee hurricane

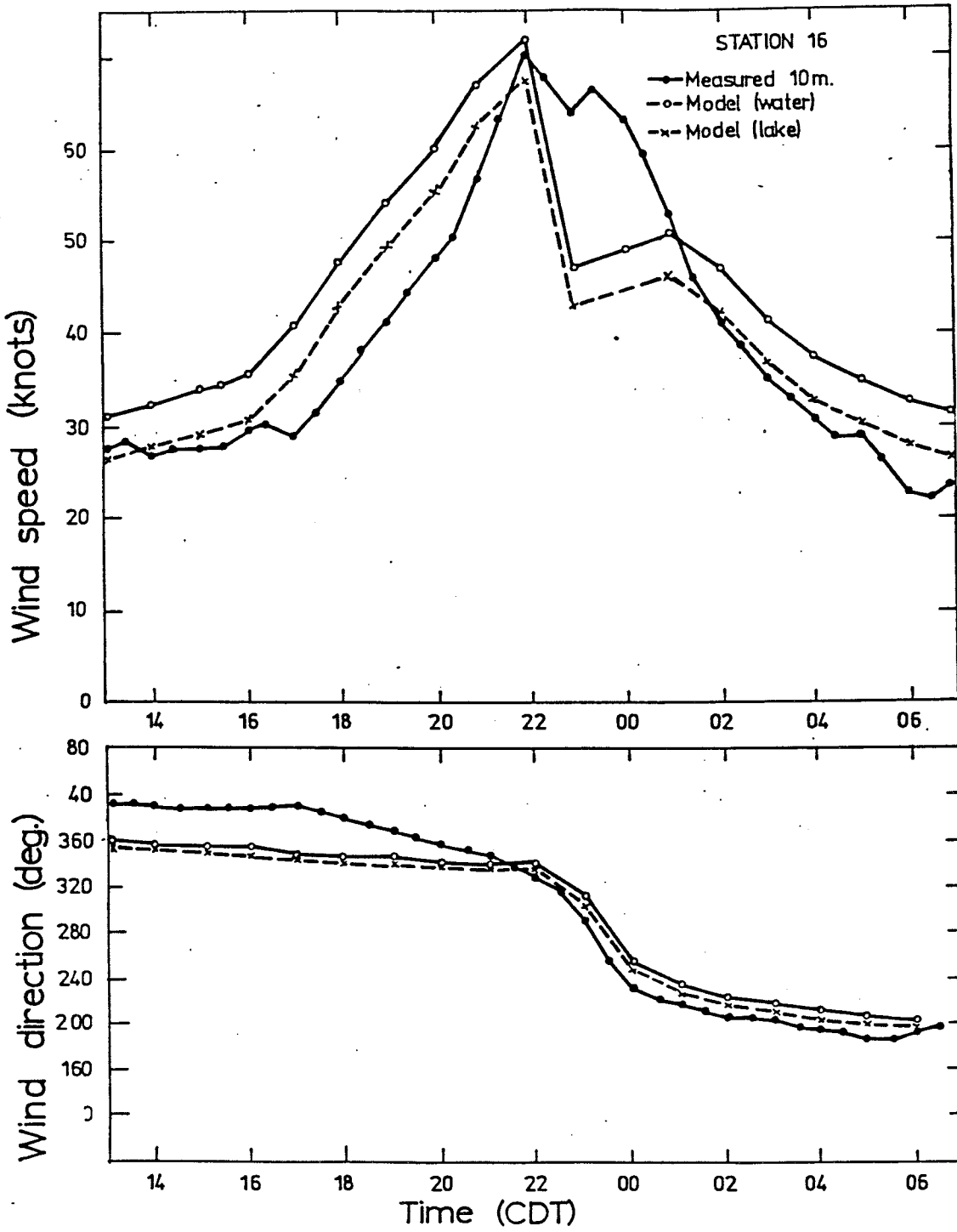


Figure 27. Comparison of measured and modelled wind speed and direction at station 15 in the 1949 Lake Okeechobee hurricane

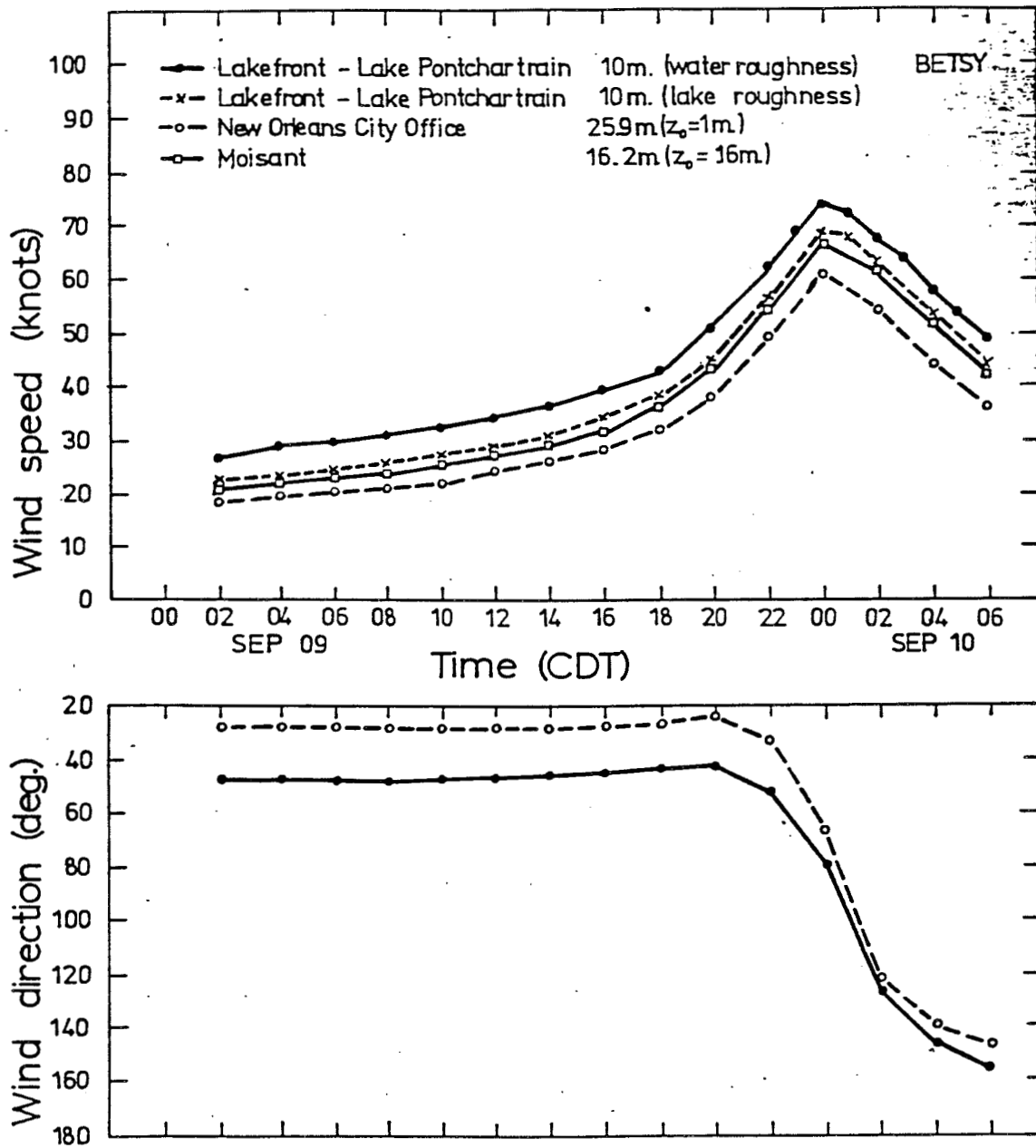


Figure 28. Modelled wind speed and direction for various terrain roughnesses in Hurricane Betsy

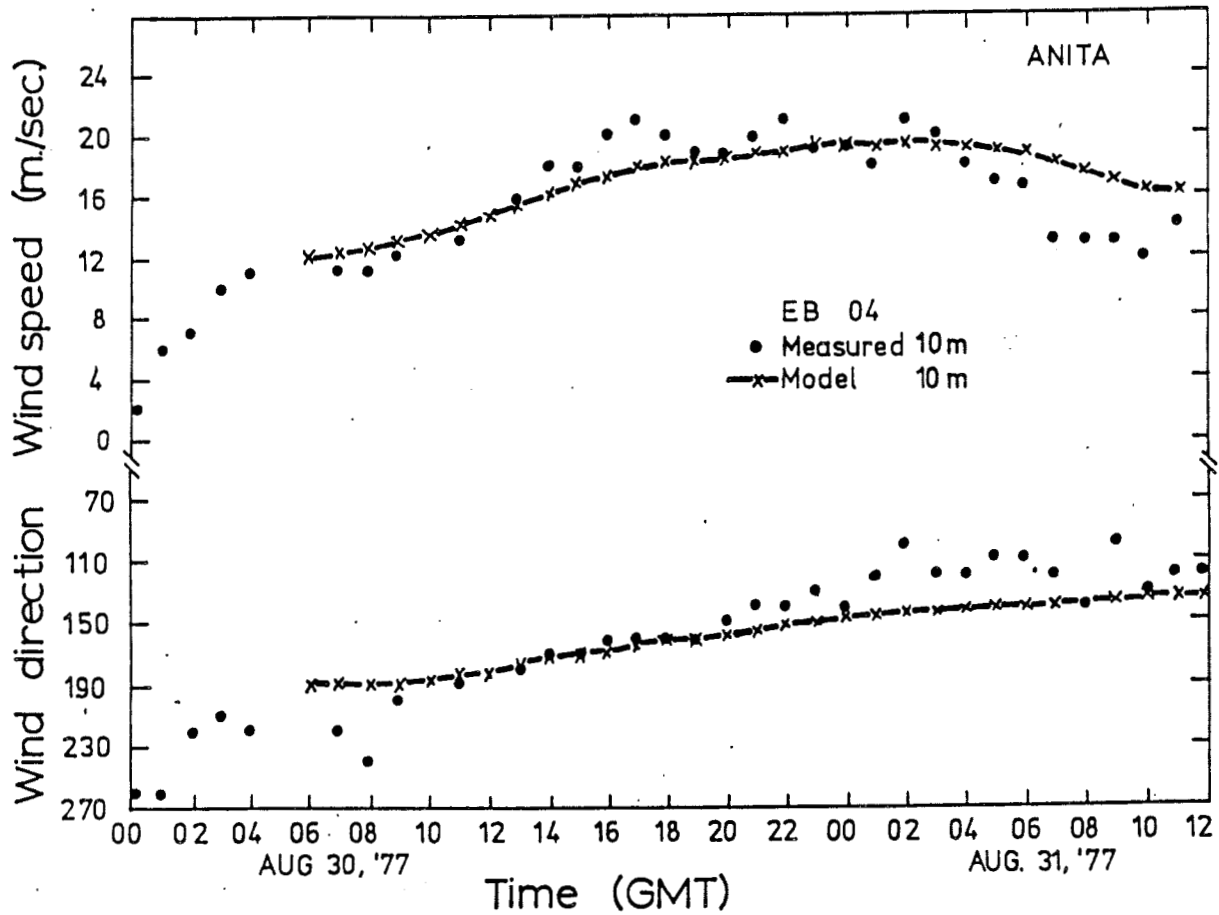


Figure 30. Comparison of measured and modelled wind speed and direction at buoy EB04 in Hurricane Anita

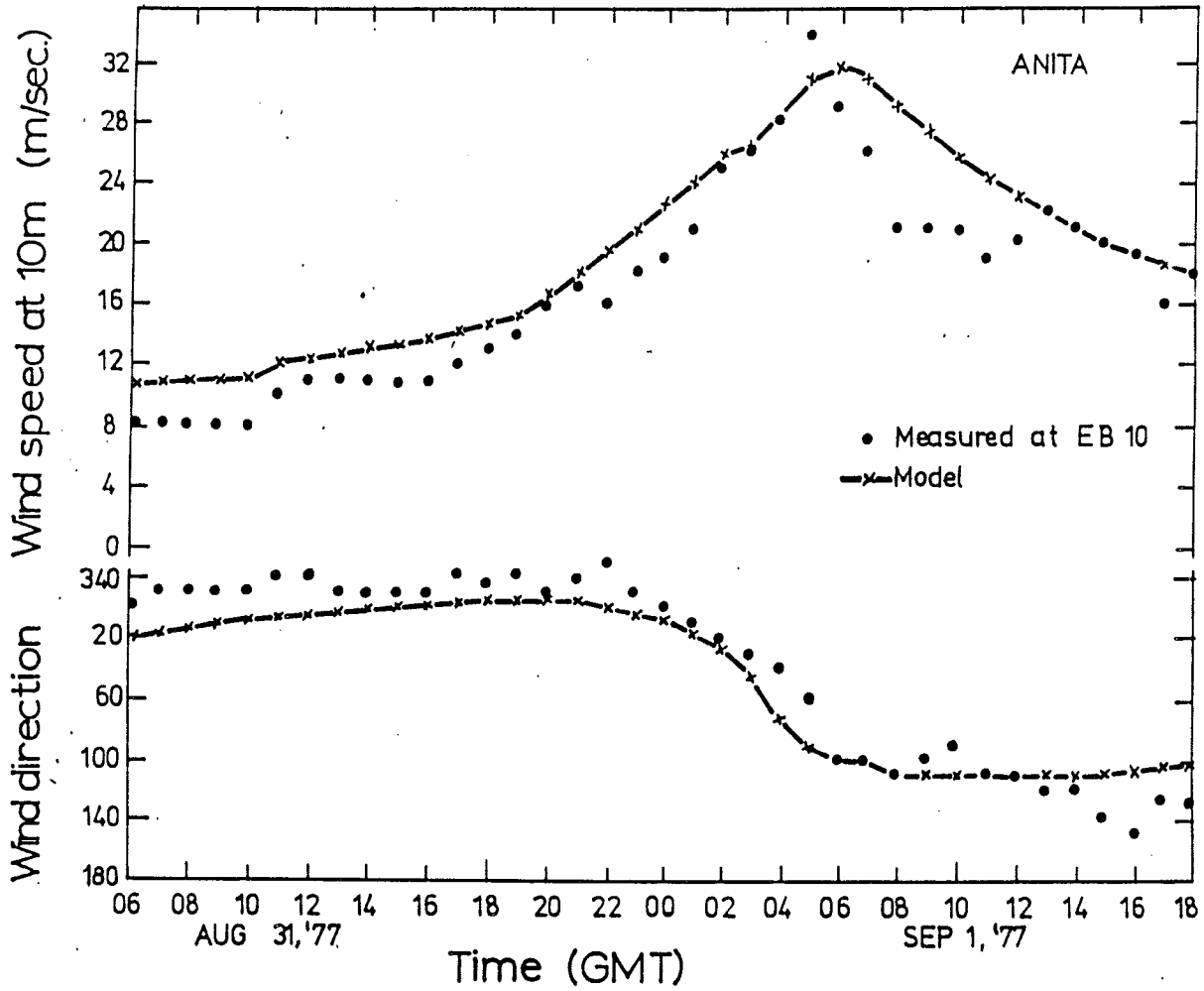


Figure 31. Comparison of measured and modelled wind speed and direction at buoy EB71 in Hurricane Anita

APPENDIX A: NAMELIST

1. Source. The material below is abridged from §6.4 of "Sperry Univac Series 1100, FORTRAN V Level 4 R1, programmer reference", edition of April 1979.

2. The nonexecutable NAMELIST statement and the associated forms of the formatted input/output statements provide a simplified means of transmitting an annotated list of data to and from peripheral units. The input/output statements take the form

```
      READ (unit, x)
           and
      WRITE (unit, x)
```

where *x* is a namelist name. The list of items in the namelist is used on input to specify those items which may have their values defined in the records to be read. Not all items of the namelist list need be used in the input records nor must the input fields be in the same order as the list items. On output, each list item of the designated namelist is formatted in a standard fashion for output in the order specified by the list.

3. Namelist Statement. The general form of the statement is

```
NAMELIST /X/A,B,....,C/Y/D,E,....,F/Z/G,H,....,I
```

where X, Y, Z,.... are namelist names and A, B, C, D,.... are simple variables, subscripted variables, or array names. An array must be dimensioned before appearing in a namelist. The following rules apply to defining and using a namelist:

- a. A namelist name consists of from one to six alphanumeric characters, the first of which must be alphabetic.
- b. Within a NAMELIST statement, a namelist name is enclosed in slashes. The list of variables associated with a namelist name ends when a new namelist name enclosed in slashes is encountered or with the end of the NAMELIST statement.
- c. A namelist name may be defined only once in a routine by its appearance in a NAMELIST statement. In the routine in which it is defined, a namelist name may appear only in

input/output statements and in the defining NAMELIST statement.

- d. A namelist name must not be the same as any other name in the routine in which it appears.
- e. A variable name, array element name, or an array name may be assigned to one or more namelist names. Array names must have been previously declared.
- f. The subscript(s) of an array element must consist of constants.

4. Namelist Input. The READ (i,X) statement causes the records that contain the input data for the variables and arrays that belong to the namelist name X to be read from input unit i. For READ (i,X) , the first character in each data record to be read is always ignored. The second character of the first record of a group of data records to be read must be a \$ immediately followed by the namelist name and a blank. The remainder of the first record and following records may contain any combination of the legal data items which are separated by commas (a comma after the last data group is ignored). The last input record is terminated by a blank followed by \$END.

5. The forms the data items may take are:

- a. Variable Name= Constant. Variable name is a simple variable name.
- b. Subscripted Variable=Constant. The array element appears in the NAMELIST statement. The subscripts in the input record must be constants.
- c. Array Name=Set of Constants. The set is represented by constants separated by commas, or k*constant may represent k constants (k is an unsigned integer). The number of constants must be less than or equal to the number of elements in the array.

6. Constants used in the data items may take any of the following forms:

- a. Integer constants.
- b. Real constants. These are written with a decimal point, and, optionally, they are written with an exponent consisting of E , + , or - , or a combination of E and sign (for example, E+2, E2, +2).
- c. Hollerith constants. These are written as nHhhh...h where hh...h is a string of n alphanumeric characters, including blanks. Six characters can be stored in one

location. If less than six characters remain they are stored left-justified with the rest of the computer word filled out with blanks.

7. Hollerith constants may only be associated with integer or real variables. The data items that appear on the input records need not appear in the same order as the corresponding variable or array names in the namelist. All variable or array names of the namelist need not have a corresponding data item in the input records; if none appears, the contents of the variable or array are unchanged. Names that are equivalenced to these names may not be used in the input records unless they are part of the namelist. Blanks must not be embedded in a constant or a repeat constant field, but may be used freely elsewhere in a data record. The name of an array and the value of its first elements must appear on the same record. The last item on each record that contains data items must be a constant followed by a comma. The comma is optional in the record that contains or precedes the \$END sentinel.

8. Namelist Output. The WRITE (i,X) statement causes all names of variables and arrays (as well as their values) that belong to the namelist name X to be written on the output unit i. In the WRITE (i,X) statement, all variables and arrays, and their values belonging to the namelist name, are written out according to their types. The output data is written such that:

- a. The name of a variable and its value are written on one line.
- b. The name of an array is written, with the values of the elements of the array written in a convenient number of columns, in the order of the array in main storage, that is, with the left dimension [varying fastest].
- c. The data fields are large enough to contain all the significant digits.
- d. The output can be read by an input statement referencing the namelist name.

APPENDIX B: PROGRAM LISTING

```

SUBROUTINE ANGEL (I20)
C CONVERTS U,V TO SPEED(KN), DIRECTION.
C COMPUTES SPEED AT 20 MTRS ALTITUDE IF I20 NE 0.
COMMON /C3/ U(21,21,5),V(21,21,5),UN(21,21,5),VN(21,21,5)
1 ,PX(21,21,5),FY(21,21,5),VTN(21,21,5),ANG(21,21,5)
2 ,LW(21,21,5)
COMMON
$/C4/ CUR(100,2,2),UXV(100,2),TURN(100,2)
$/C5/ FLAT,PTH,PTH(2),HH,ZOLAND,LS,VV(100),UX(3),UV(3),
$ DUV(3),K35,K2,G,GA,DEN,VV2,HL,K123,Z0,ZLOG,AM,BM,CM,FF
REAL K35,K2
DO 1000 NEST=1,5
DO 1000 I=1,21
DO 1000 J=1,21
C COMPUTE VTN
VTN(I,J,NEST)=SQRT(UN(I,J,NEST)**2+VN(I,J,NEST)**2)
IF(VTN(I,J,NEST)) 860,840,860
840 ANG(I,J,NEST)=0.0
GO TO 1000
860 AN=57.29578*ATAN2(VN(I,J,NEST),UN(I,J,NEST))
ANG(I,J,NEST)=AMOD(270.-AN,360.)
C REDUCE SPEED TO 20 MTRS IF I20 NE 0
C REDUCE SPEED TO KNOTS IF I20 EQ 0
IF (I20 .NE. 0) GO TO 900
VTN(I,J,NEST) = VTN(I,J,NEST)*(.3600./1852.)
GO TO 1000
900 SPP = 1.25*VTN(I,J,NEST)
KPP = SPP
SPP = SPP-KPP
LS = LW(I,J,NEST)
IF (KPP .NE. 0) GO TO 910
UXX =VTN(I,J,NEST)*UXV(I,LS)
TWIST = TURN(I,LS)
GO TO 930

```

```

910 IF (KPP .GE. 100) GO TO 920
    UXX = VTN(I,J,NEST)*((1.-SPP)*UXV(KPP,LS)+SPP*UXV(KPP+1,LS))
    TWIST = (1.-SPP)*TURN(KPP,LS)+SPP*TURN(KPP+1,LS)
    GO TO 930
920 UXX = VTN(I,J,NEST)*UXV(100,LS)
    TWIST = TURN(100,LS)
930 Z20 = 19.5/ZOLAND
    IF (LS .EQ. 2) Z20 = 19.5/(GA*UXX**2)
    VTN(I,J,NEST) = (3600./1852.)*AMIN1
    $ (UXX/K35*ALOG(Z20),VTN(I,J,NEST))
    ANG(I,J,NEST) = ANG(I,J,NEST)+57.29578*TWIST
    IF (ANG(I,J,NEST).LT. 0.) ANG(I,J,NEST) = ANG(I,J,NEST)+360.
1000 CONTINUE
    RETURN
    END

```

```

SUBROUTINE ABCC
COMMON
$/C4/ CDR(100,2,2),UXV(100,2),TURN(100,2)
$/C5/ FLAT,PTH,DTH(2),HH,ZOLAND,LS,VV(100),UX(3),UV(3),
$ DUV(3),K35,K2,G,GA,DEN,VV2,HL,K123,Z0,ZLOG,AM,BM,CM,FF
REAL K35,K2
IF (LS.EQ. 1) GO TO 53
Z0 = GA*UX(K123)**2/HH
ZLOG = ALOG(Z0)
53 HL = -HH*DEN/(UX(K123)**2*PTH*(ZLOG+CM))
IF (HL+2.) 54,55,56
54 HLOG = ALOG(-HL)
AM = AMIN1(HLOG+1.5,-.875*ZLOG)
BM = 1.8*EXP(.2*HL)
CM = AMIN1(HLOG+3.7,-.875*ZLOG)
GO TO 60
55 AM = 2.1931472
BM = 1.2065761
CM = 4.3931472
GO TO 60

```



```

56  IF (HL-2.) 57,58,59
57  AM = 1.3865736-.4032868*HL
    BM = 1.953288+.37335598*HL
    CM = 2.5465736-HL*.9232868
    GO TO 60
58  AM = .58
    BM = 2.70
    CM = .7
    GO TO 60
59  YLOG = ZLOG+4.7
    HL = .25*(YLOG+SQRT(YLOG**2+8.*HH*DEN/(UX(K123)**2*PTH)))
    AM = AMAX1(2.5-.96*HL,-99.)
    BM = AMIN1(1.1+.8*HL,99.)
    CM = 4.7-2.*HL
60  UV(K123) = UX(K123)**2/K2*((ZLOG+AM)**2+BM**2)
    DUV(K123) = UV(K123)-VV2
    RETURN
    END

```

```

SUBROUTINE ABCCC
COMMON /C57/ PTH,DTH,HH,ZCOEFF(3,5),LAKE,VV(100),UX(3),UV(3),
$ DUV(3),K35,K2,G,GA,DEN,VV2,HL,K123,Z0,ZLOG,AM,BM,CM,UXV(100,6),
$ TURN(100,6),COST(100),SINT(100)
REAL K2,K35
Z0 = GA*UX(K123)**2/HH
ZLOG = ALOG(Z0)
53 HL = -HH*DEN/(UX(K123)**2*PTH*(ZLOG+CM))
IF (HL+2.) 54,55,56
54 HLOG = ALOG(-HL)
AM = AMIN1(HLOG+1.5,-.875*ZLOG)
BM = 1.8*EXP(.2*HL)
CM = AMIN1(HLOG+3.7,-.875*ZLOG)
GO TO 60
55 AM = 2.1931472
BM = 1.2065761
CM = 4.3931472
GO TO 60
56 IF (HL-2.) 57,58,59
57 AM = 1.3665736-.4032868*HL
BM = 1.953288+.37335598*HL
CM = 2.5465736-HL*.9232868
GO TO 60
58 AM = .58
BM = 2.70
CM = .7
GO TO 60
59 YLOG = ZLOG+4.7
HL = .25*(YLOG+SQRT(YLOG**2+8.*HH*DEN/(UX(K123)**2*PTH)))
AM = AMAX1(2.5-.96*HL,-99.)
BM = AMIN1(1.1+.8*HL,99.)
CM = 4.7-2.*HL
60 UV(K123) = UX(K123)**2/K2*((ZLOG+AM)**2+BM**2)
DUV(K123) = UV(K123)-VV2
RETURN
END

```

```

SUBROUTINE BLOWUG
C BLOWUP PRODUCES THE WIND FIELD FOR MOVING VORTEX IN THE PLANETARY
C BOUNDARY LAYER. ITS U(EASTWARD) AND V(NORTHWARD) COMPONENTS
C ARE IN ARRAYS UN,VN RESPECTIVELY UPON EXIT.
C SGW IS MAGNITUDE OF SURFACE GEOSTROPHIC WIND
C AN1 IS ANGLE BETWEEN SGW AND EAST, COUNTERCLOCKWISE FROM EAST
C ST12 IS DISTANCE IN KM FROM AXIS OF STORM TO HALF MAGNITUDE OF SGW
C (UG,VG) IS THE SFC GEOSTROPHIC WIND.
C CS IS SPEED OF STORM MOVEMENT.
COMMON/C1/NAME,NSNAP,DI(2),F,SGW,AN1,UC,VC,UG,VG,CS,NM,IB
,ST12
COMMON /C3/ U(21,21,5),V(21,21,5),UN(21,21,5),VN(21,21,5)
1 ,PX(21,21,5),PY(21,21,5),VTN(21,21,5),ANG(21,21,5)
2 ,LW(21,21,5)
COMMON
$/C4/ CDR(100,2,2),UXV(100,2),TURN(100,2)
$/C5/ FLAT,PTH,DTH(2),HH,ZOLAND,LS,VV(100),UX(3),UV(3),
$ DUV(3),K35,K2,G,GA,DEN,VV2,HL,K123,Z0,ZLOG,AM,BM,CM,FF
REAL K35,K2
DIMENSION LEVEL(16)
REAL CDH2(2)
DATA LEVEL/1,5,1,2,1,3,1,2,1,4,1,2,1,3,1,2/
DEGG = AN1/57.29578
UG=SGW*COS(DEGG)
VG=SGW*SIN(DEGG)
CALL SHORE
CALL PXYH
IF (IB.NE.0) CALL OUTOUT(0,NAME,4HINIT,NSNAP)
SPP = 1.25*SGW
KPP = SPP
SPP = SPP-KPP
DO 1020 LS = 1,2
CDH2(LS) = ((1.-SPP)*UXV(KPP,LS)+SPP*UXV(KPP+1,LS))**2/HH)**2
CONTINUE
1020 CS=SQRT(UC**2+VC**2)
DC 1026 I = 1,21

```

```

DO 1026 J = 1,21
IF (I .EQ. 1) GO TO 1025
IF (I .EQ. 21) GO TO 1025
IF (J .EQ. 1) GO TO 1025
IF (J .EQ. 21) GO TO 1025
GO TO 1026

1025 CONTINUE
LS = LW(I,J,5)
AA = CDH2(LS)*(PX(I,J,5)**2+PY(I,J,5)**2)
F2=F**2/2.0
SK=AA/(F2+SQRT(F2**2+AA))
BK=SQRT(SK)
V(I,J,5)=(F+PX(I,J,5)-BK*PY(I,J,5))/(F**2+SK)
U(I,J,5)=-PY(I,J,5)/F-V(I,J,5)*BK/F
V(I,J,5)=V(I,J,5)-VC
U(I,J,5)=U(I,J,5)-UC

1026 CONTINUE
DO 1028 I = 1,21
DO 1028 J = 1,21
UN(I,J,5)=U(I,J,5)
VN(I,J,5)=V(I,J,5)

1028 CONTINUE
DO 1030 NEST = 1,5
DO 1030 I = 1,21
DO 1030 J = 1,21
PX(I,J,NEST)=PX(I,J,NEST)-F*VC
PY(I,J,NEST)=PY(I,J,NEST)+F*UC

C
DO 1430 K=1,NM
KCK = MOD(K,16)
CALL COMOUT (LEVEL(KCK+1))
1430 CONTINUE
CALL OUTFLO
C SOLUTION OF WIND FIELD ON COORDINATE SYSTEM MOVING
C WITH STORM IS NOW COMPLETE.

```

```
C      COMPUTE SOLUTION WITH RESPECT TO SEA SURFACE.
      DO 1450 NEST=1,5
      DO 1450 I=1,21
      DO 1450 J=1,21
      UN(I,J,NEST)=UN(I,J,NEST)+UC
      VN(I,J,NEST)=VN(I,J,NEST)+VC
      1450 CONTINUE
      CALL OUTPUT(1,NAME,4HSNAP,NSNAP)
      CALL OUTPUT(0,NAME,4HSNAP,NSNAP)
      RETURN
      END
```

```

SUBROUTINE BREEZE
REAL LA0,LA1,L00,L01,LB,LL
COMMON /C57/ PTH,DTH,HH,ZCOEFF(3,5),LAKE,VV(100),UX(3),UV(3),
$ DUV(3),K35,K2,G,GA,DEN,VV2,HL,K123,Z0,ZLOG,AM,BM,CM,UXV(100,6),
$ TURN(100,6),COST(100),SINT(100)
REAL K2,K35
COMMON /D1/LA0,L00,ROT,LA1,L01,DX,STHT,LANSEA,W1,TH1,D,AL,UST
COMMON /D2/ XX(21,21,10)
EQUIVALENCE (U1,XY), (V1,XY(2)), (UX,X,UST)      INPUT (RADIANS)
LA0,L00 ARE LAT,LON OF EYE(PT0)
LA1,L01 ARE LAT,LON OF POINT AT WHICH WIND IS WANTED(PT1)-INPUT(RAD)
      LONGITUDE IS POSITIVE WEST.
C   DX IS GRID SPACING OF INNERMOST NEST - INPUT(KILOMETERS)
C   W1 IS WIND SPEED AT PT1,20 METERS - OUTPUT(KNOTS)
C   D IS DISTANCE BETWEEN PT0 AND PT1 - OUTPUT(KM)
C   ROT IS ANGLE FROM TRUE NORTH TO Y-AXIS OF NESTED RECTANGULAR
C   GRID WIND FIELD (CLOCKWISE,DEGREES).
C   TH1 IS DIRECTION TO WHICH WIND BLOWS, CLOCKWISE FROM SOUTH(DEG)
C   AL IS BEARING OF POINT 1 FROM POINT 0, CLOCKWISE FROM NORTH(DEG)
C   LANSEA IS TERRAIN CODE AT POINT 1
C   1 IS OCEAN, 2 TO 6 ARE VARIOUS GROUNDS AND LAKES
DIMENSION XY(2)
NAMELIST/DBG2/I,J,F1,F2,XY,SPP,LANSEA,UX,X,TWIST,STHT,GA,K35
HAV(X) = (SIN(.5*X))**2
AHAV(X) = 2.*ASIN(SQRT(X))
SGRU(X) = SQRT(ABS(X))
LL = LA0+LA1
LB = LA0-LA1
R = AHAV(HAV(LB)+COS(LA0)+COS(LA1))*HAV(L00-L01))
IF(R.EQ.0.) GO TO 16
IF (R.LT.1E-4) AB = ATAN2((L00-L01)*COS(.5+LL),-LB)
AB = AB*.5
IF(R.GE.1E-4) AB = ATAN2(SGRU(COS(.5*(LL+R)))+SIN(.5*(R+LB))),
1 SGRU(COS(.5*(LL-R)))*SIN(.5*(R-LB)))
IF (L01 .GT. L00) AB = -AB
AL = 2.*57.29578*AB

```

```

IF (AL .LT. 0.) AL = AL+360.
DE = (AL-ROT)/57.29578
D = R+1.852*3437.7468
AA = 10.0+DX
IZ = 1
XY(1) = D*SIN(DE)
XY(2) = D*COS(DE)
AB = AMAX1(ABS(XY(1)),ABS(XY(2)))
10 IF (AB .LT. AA) GO TO 11
AA = AA+AA
IZ = IZ+1
GO TO 10
11 IF (I7 .LC. 5) GO TO 12
U1 = 0.
V1 = 0.
W1 = 0.
TH1 = 0.
RETURN
110
DO 13 IA = 1,2
XY(IA) = (AA+XY(IA))*10./AA
I = XY(1)
J = XY(2)
F1 = XY(1)-I
F2 = XY(2)-J
G11 = (1.-F1)*(1.-F2)
G12 = (1.-F1)*F2
G21 = F1*(1.-F2)
G22 = F1*F2
DO 14 IA = 1,2
IB = 5*IA+IZ-5
XY(IA) = G11*XX(I+1,J+1,IB)+G12*XX(I+1,J+2,IB)+G21*
*XX(I+2,J+1,IB)+G22*XX(I+2,J+2,IB)
W1 = U1+V1+W1
15 IF (W1.EQ.0.) GO TO 110
W1 = SORT(W1)

```

```

C          REDUCE W1 TO STATION HEIGHT
900      SPP = 1.25*W1
        KPP = SPP
        SPP = SPP-KPP
        IF (KPP .NE. 0) GO TO 910
        UXX = W1*UXV(1,LANSEA)
        TWIST = TURN(1,LANSEA)
        GO TO 930
910      IF (KPP .GE. 100) GO TO 920
        UXX = W1*((1.-SPP)*UXV(KPP,LANSEA)+SPP*UXV(KPP+1,LANSEA))
        TWIST = (1.-SPP)*TURN(KPP,LANSEA)+SPP*TURN(KPP+1,LANSEA)
        GO TO 930
920      UXX = W1*UXV(100,LANSEA)
        TWIST = TURN(100,LANSEA)
930      IF (LANSEA .EQ. 1) Z0 = CA*UST**2
        IF (LANSEA .NE. 1) Z0 = ZCOEFF(1,LANSEA-1)/UST+
        $ ZCOEFF(2,LANSEA-1)*UST**2+ZCOEFF(3,LANSEA-1)
        Z20 = STHT/Z0
C          WRITE(6,DBG2)
        W1 = (3600./1852.)*AMIN1
        $ (UXX/K35*ALOG(Z20),W1)
        TH1 = (ATAN2(-UI,-V1)+TWIST)*57.29578+ROT
        IF (TH1 .LT. 0.) TH1 = TH1+360.
        RETURN
16      U1=XX(11,11,1)
        V1=XX(11,11,6)
        D=0.
        AL=0.
        GO TO 15
        END

```



```

IF (R.GE.1E-4) AB = ATAN2(SQRU(COS(.5*(LL+R))*SIN(.5*(R+LB))),
1  SQRU(COS(.5*(LL-R))*SIN(.5*(R-LB))))
IF (L01 .GT. L00) AB = -AB
AL = 2.*57.29578*AB
IF (AL .LT. 0.) AL = AL+360.
DE = (AL-ROT)/57.29578
D = R*1.852*3437.7468
AA = 10.0*DX
IZ = 1
XY(1) = D*SIN(DE)
XY(2) = D*COS(DE)
AB = AMAX1(ABS(XY(1)),ABS(XY(2)))
10 IF (AB .LT. AA) GO TO 11
AA = AA+AA
IZ = IZ+1
GO TO 10
11 IF (IZ .LE. 5) GO TO 12
U1 = 0.
V1 = 0.
W1 = 0.
TH1 = 0.
110 RETURN
DO 13 IA = 1,2
13 XY(IA) = (AA+XY(IA))*10./AA
I = XY(1)
J = XY(2)
F1 = XY(1)-I
F2 = XY(2)-J

```

```

- G11 = (1.-F1)*(1.-F2)
  G12 = (1.-F1)*F2
  G21 = F1*(1.-F2)
  G22 = F1*F2
  DO 14 IA = 1,2
    IB = 5*IA+IZ-5
14  XY(IA) = G11*XX(I+1,J+1,IB)+G12*XX(I+1,J+2,IB)+G21*
    *XX(I+2,J+1,IB)+G22*XX(I+2,J+2,IB)
15  W1 = U1*U1+V1*V1
    IF (W1.EQ.0.) GO TO 110
    W1 = SQRT(W1)
C   REDUCE W1 TO STATION HEIGHT
900 SPP = 1.25*W1
    KPP = SPP
    SPP = SPP-KPP
    LSSUB=LANSEA
    IF(LSSUB.EQ.2) LSSUB=6
    IF (KPP .NE. 0) GO TO 910
    UXX =W1*UXV(1,LANSEA)
    TWIST = TURN(1,LSSUB)
    GO TO 930
910 IF (KPP .GE. 100) GO TO 920
    UXX = W1*((1.-SPP)*UXV(KPP,LANSEA)+SPP*UXV(KPP+1,LANSEA))
    TWIST = (1.-SPP)*TURN(KPP,LSSUB)+SPP*TURN(KPP+1,LSSUB)
    GO TO 930
920 UXX = W1*UXV(100,LANSEA)
    TWIST = TURN(100,LSSUB)
930 IF (LANSEA .EQ. 1) Z0 = GA*UST**2
    IF (LANSEA .NE. 1) Z0 = ZCOEFF(1,LANSEA-1)/UST+
    $ ZCOEFF(2,LANSEA-1)*UST**2+ZCOEFF(3,LANSEA-1)
    Z20 = STHT/Z0

```

```
C      WRITE(6,DBG2)
      W1 = (3600./1852.)*AMIN1
      $ (UXX/K35*ALOG(Z20),W1)
      TH1 = (ATAN2(-U1,-V1)+TWIST)*57.29578+ROT
      IF (TH1 .LT. 0.) TH1 = TH1+360.
      RETURN
16     U1=XX(11,11,1)
      V1=XX(11,11,6)
      D=0.
      AL=0.
      GO TO 15
      END
```

```

SUBROUTINE CCROSS
COMMON
$/C4/ CDR(100,2,2),UXV(100,2),TURM(100,2)
$/C5/ FLAT,PTH,DTH(2),HH,ZOLAND,LS,VV(100),UX(3),UV(3),
$ DUV(3),K35,K2,G,GA,DEN,VV2,HL,K123,Z0,ZLOG,AM,BM,CM,FF
REAL K35,K2
FF = AMAX1(ABS(FLAT),1.832E-6)
DO 10 IA = 1,100
  VV(IA) = .8*FLOAT(IA)
CONTINUE
DO 41 LS = 1,2
  DEN = G*K2*DTH(LS)
  DO 40 IA = 1,100
    IB = 101-IA
    VV2 = VV(IB)**2
    IF (IA .NE. 1) GO TO 20
    CM = 2.55
    K123 = 1
    UX(1) = 2.74
    IF (LS .EQ. 1) UX(1) = 3.38
    Z0 = ZOLAND/HH
    ZLOG = ALOG(Z0)
    CALL ABCC
    K123 = 2
    UX(2) = UX(1)*80./SQRT(UV(1))
    GO TO 30
  UX(1) = UX(3)
  UV(1) = UV(3)
  DUV(1) = UV(1)-VV2
  K123 = 2
  UX(2) = UX(1)*VV(IB)/VV(IB+1)
  CALL ABCC
  KSTOP = 0
  K123 = 3

```

10

20

30

```

31      IF (DUV(1).EQ. DUV(2)) GO TO 32
        UX(3) = AMAX1(.5*AMIN1(UX(1),UX(2)),
        $   AMIN1(2.*AMAX1(UX(1),UX(2)),
        $   (UX(1)*DUV(2)-UX(2)*DUV(1))/(DUV(2)-DUV(1)))
        CALL ABCC
        IF (KSTOP .NE. 0) GO TO 32
        IF (ABS(DUV(3)).LT..1E-4*VV2) KSTOP = 1
        UX(1) = UX(2)
        UX(2) = UX(3)
        DUV(1) = DUV(2)
        DUV(2) = DUV(3)
        GO TO 31
32      AB = SQRT((ZLOG+AM)**2+BM**2)
        UXV(IB,LS) = K35/AB
        AB = UXV(IB,LS)**2/AB
        CDR(IB,LS,1) = (ZLOG+AM)*AB
        CDR(IB,LS,2) = BM*AB
        TURN(IB,LS) = ATAN(BM/(ZLOG+AM))
        CONTINUE
40      CONTINUE
41      RETURN
        END

```

```

SUBROUTINE COMQUT (LEVEL)
COMMON/C1/DM1(2),DX,DT,F,DM2(2),UC,VC,DM3(5)
,ST12
COMMON /C3/ U(21,21,5),V(21,21,5),UN(21,21,5),VN(21,21,5)
1 ,PX(21,21,5),PY(21,21,5),VTN(21,21,5),ANG(21,21,5)
2 ,LW(21,21,5)
COMMON
$/C4/ CDR(100,2,2),UXV(100,2),TURN(100,2)
$/C5/ FLAT,PTH,DTH(2),HH,ZOLAND,LS,VV(100),UX(3),UV(3),
$ DUV(3),K35,K2,G,GA,DEN,VV2,HL,K123,Z0,ZLOG,AM,BM,CM,FF
DIMENSION HKL(21,21),DRAG(2)
DATA E1,E2/0.5,0.5/
DATA VONK/0.4/
C SQQ IS APPROXIMATION TO SQRT OF SUM OF SQUARES
SQQ(A,B) = (ABS(A)+ABS(B))/2.51 + (ABS(A+B)+ABS(A-B))/0.7071/2.51
DO 800 NC = 1,LEVEL
NEST = LEVEL-NC+1
DO 720 I = 1,21
DO 720 J = 1,21
U(I,J,NEST) = UN(I,J,NEST)
V(I,J,NEST) = VN(I,J,NEST)
720 CONTINUE
IF(NEST.NE.LEVEL) GO TO 721
IF(NEST.NE.5) CALL OUTBY2(NEST)
GO TO 722
721 CALL OUTBY1(NEST)
722 CONTINUE
DXL = 2.0**(NEST-1)*DX*1000.0
DXL2=DXL**2
DTL=2.0**(NEST-1)*DT
FTL=F*DTL
FTL1=FTL**2+1.0
FCL=2.0*VONK**2*(DXL/2.0)**2
C INNER BOUNDARY
IF(NEST .EQ. 1) GO TO 730
DO 724 J=1,10

```

```

U(7,J+6,NEST)=UN(3,2*J+1,NEST-1)
V(7,J+6,NEST)=VN(3,2*J+1,NEST-1)
V(15,J+6,NEST)=VN(19,2*J+1,NEST-1)
U(15,J+6,NEST)=UH(19,2*J+1,NEST-1)
724 CONTINUE
DO 726 I=1,10
U(1+6,7,NEST)=UN(2*I+1,3,NEST-1)
V(1+6,7,NEST)=VN(2*I+1,3,NEST-1)
U(1+6,15,NEST)=UN(2*I+1,19,NEST-1)
V(1+6,15,NEST)=VN(2*I+1,19,NEST-1)
726 CONTINUE
C COMPUTATION OF INTERIOR POINT
730 DO 734 I=1,20
DO 734 J=1,20
IF (NEST .EQ. 1) GO TO 733
IF(I .LE. 6 .OR. I .GE. 15) GO TO 733
IF(J .LE. 6 .OR. J .GE. 15) GO TO 733
HKL(I,J)=0.0
GO TO 734
733 D1=0.5*(U(I+1,J,NEST)-U(I,J,NEST))+U(I+1,J+1,NEST)-U(I,J+1,NEST)
1 -V(I,J+1,NEST)+V(I,J,NEST)-V(I+1,J+1,NEST)+V(I+1,J,NEST))/DXL
1 +U(I,J+1,NEST)-U(I,J,NEST)+U(I+1,J+1,NEST)-V(I+1,J,NEST))/DXL
HKL(I,J) = FCL*SQ(D1,D2)
734 CONTINUE
DO 775 I=2,20
DO 775 J=2,20
IF(NEST .EQ. 1) GO TO 736
IF(I .LE. 6 .OR. I .GE. 16) GO TO 736
IF(J .LE. 6 .OR. J .GE. 16) GO TO 736
UN(I,J,NEST)=U(I,J,NEST)
VN(I,J,NEST)=V(I,J,NEST)
GO TO 775
736 U1=U(I,J,NEST)+UC
V1=V(I,J,NEST)+VC

```



```

C DRAG(1) IS TANGENTIAL DRAG CORRECTION TERM
C DRAG(2) IS NORMAL DRAG CORRECTION TERM
LS=LW(I,J,NEST)
SPP=SQ3(U1,V1)
SPPI = AMAX1(1.,AMIN1(99.99,1.25*SPP))
KPP=SPPI
SPPI=SPPI-KPP
SPH = SPP/HH
DO 737 IA = 1,2
    DRAG(IA) = SPH*(CDR(KPP,LS,IA)+
$      SPP1*(CDR(KPP+1,LS,IA)-CDR(KPP,LS,IA)))
737 CONTINUE
    IF(NEST .NE. 5) GO TO 741
    IF(I .NE. 2 .AND. I .NE. 20) GO TO 741
    IF(I-2) 738,738,740
738 IF(U(I,J,NEST)) 739,739,741
739 UKX=0.0
    VKX=0.0
    GO TO 742
740 IF(U(I,J,NEST)) 741,739,739
741 UKX=0.5*((HKL(I,J-1)+HKL(I,J))+(U(I+1,J,NEST)-U(I,J,NEST)))/DXL2
1   -(HKL(I-1,J-1)+HKL(I-1,J))+(U(I,J,NEST)-U(I-1,J,NEST)))/DXL2
    VKX=0.5*((HKL(I,J-1)+HKL(I,J))+(V(I+1,J,NEST)-V(I,J,NEST))
1   -(HKL(I-1,J-1)+HKL(I-1,J))+(V(I,J,NEST)-V(I-1,J,NEST)))/DXL2
    IF(NEST .NE. 5) GO TO 746
742 IF(J .NE. 2 .AND. J .NE. 20) GO TO 746
743 IF(J-2) 743,743,745
744 IF(V(I,J,NEST)) 744,744,746
    UKY=0.0
    VKY=0.0
    GO TO 747
745 IF(V(I,J,NEST)) 746,744,744
746 UKY=0.5*((HKL(I-1,J)+HKL(I,J-1))+(U(I,J+1,NEST)-U(I,J,NEST)))/DXL2
1   -(HKL(I-1,J-1)+HKL(I,J-1))+(U(I,J,NEST)-U(I,J-1,NEST)))/DXL2
    VKY=0.5*((HKL(I-1,J)+HKL(I,J))+(V(I,J+1,NEST)-V(I,J,NEST))
1   -(HKL(I-1,J-1)+HKL(I,J-1))+(V(I,J,NEST)-V(I,J-1,NEST)))/DXL2

```

```

747 IF(U(I,J,NEST)) 748,750,750
748 UX=-U(I,J,NEST)*(U(I,J,NEST)-U(I+1,J,NEST))/DXL
    VX=-U(I,J,NEST)*(V(I,J,NEST)-V(I+1,J,NEST))/DXL
    GO TO 752
750 UX= U(I,J,NEST)*(U(I,J,NEST)-U(I-1,J,NEST))/DXL
    VX= U(I,J,NEST)*(V(I,J,NEST)-V(I-1,J,NEST))/DXL
752 IF(V(I,J,NEST)) 754,756,756
754 UY=-V(I,J,NEST)*(U(I,J,NEST)-U(I,J+1,NEST))/DXL
    VY=-V(I,J,NEST)*(V(I,J,NEST)-V(I,J+1,NEST))/DXL
    GO TO 758
756 UY= V(I,J,NEST)*(U(I,J,NEST)-U(I,J-1,NEST))/DXL
    VY= V(I,J,NEST)*(V(I,J,NEST)-V(I,J-1,NEST))/DXL
758 UR=0.5*(U(I,J,NEST)+V(I,J,NEST))
    VR=0.5*(-U(I,J,NEST)+V(I,J,NEST))
    IF(UR) 760,762,762
760 UY1=-UR*(U(I,J,NEST)-U(I+1,J+1,NEST))/DXL
    VX1=-UR*(V(I,J,NEST)-V(I+1,J+1,NEST))/DXL
    GO TO 764
762 UX1= UR*(U(I,J,NEST)-U(I-1,J-1,NEST))/DXL
    VX1= UR*(V(I,J,NEST)-V(I-1,J-1,NEST))/DXL
764 IF(VR) 766,768,768
766 UY1=-VR*(U(I,J,NEST)-U(I-1,J+1,NEST))/DXL
    VY1=-VR*(V(I,J,NEST)-V(I-1,J+1,NEST))/DXL
    GO TO 770
768 UY1= VR*(U(I,J,NEST)-U(I+1,J-1,NEST))/DXL
    VY1= VR*(V(I,J,NEST)-V(I+1,J-1,NEST))/DXL
770 UXY=E1*(UX+UY)+E2*(UX1+UY1)
    VXY=E1*(VX+VY)+E2*(VX1+VY1)

```

```

775      B1 = U(I,J,NEST)+DTL*
          $ (UKX+UKY-PX(I,J,NEST)-UXY+U1*DRAG(1))+V1*DRAG(2)
          B2 = V(I,J,NEST)+DTL*
          $ (VKX+VKY-PY(I,J,NEST)-VXY+V1*DRAG(1))-U1*DRAG(2)
          UN(I,J,NEST)=(B1+FTL*B2)/FTL1
          VN(I,J,NEST)=(B2-FTL*B1)/FTL1
          CONTINUE
800      CONTINUE
          RETURN
          END

```

SUBROUTINE GRAD
GRAD COMPUTES PRESSURE GRADIENT
COMPLEX CD,CR,CT
COMMON/C1/DM1(2),DX,DM2(4),UC,VC,DM3(4),IB
,ST12
COMMON/C2/JA(15),AB(21,21,15),AC(21,7,21)
DIMENSION AD(21,4),AP(3,2),AT(2),BA(15),BC(4,2),BP(2,2)
EQUIVALENCE (CR,AP(2,1)),(CD,AP(2,2)),(CT,AT),(BC,BA(8))
IB IS SWITCH VARIABLE. IB = 0 TO SUPPRESS PRINTING.
ITRACK IS INDICATOR FOR CODING OF DIREC
EYELAT IS NORTH LATITUDE OF EYE IN DEGREES
(SOUTH LATITUDE MUST HAVE MINUS SIGN)
EYLONG IS EAST LONGITUDE OF EYE IN DEGREES
(WEST LONGITUDE MUST HAVE MINUS SIGN)
DIREC IS DIRECTION OF TRACK OF HURRICANE, CLOCKWISE FROM NORTH
ITRACK = 0, DIREC IN DEGREES
ITRACK = 1, DIREC IN POINTS OF 11.25 DEG
SPEED IS FORWARD SPEED OF HURRICANE IN KNOTS
IQUAD IS INDICATOR FOR QUADRANTS OF PRESSURE FIELD
IQUAD = 0, CIRCULARLY SYMMETRIC PRESSURE FIELD
IQUAD = 1, FIRST QUADRANT IS RIGHT FRONT
IQUAD = 2, FIRST QUADRANT IS FORWARD
QUADRANTS FOLLOW CLOCKWISE FROM FIRST
LYPRES IS PRESSURE AT EYE IN MILLIBARS
RADIUS(1,2,3,4) ARE R IN FOUR QUADRANTS IN UNITS OF 1.0 NM
(1852 METERS)
PFAR(1,2,3,4) ARE FAR FIELD PRESSURE IN FOUR QUADRANTS,
IN MILLIBARS
IF IQUAD = 0, ENTER RADIUS(1) AND PFAR(1) ONLY
AB(I+11,J+11,K+1) IS DP/DX (EAST) IN MB/KM AT 5*I+2**K KM EAST OF EYE
AND 5*J+2**K KM SOUTH OF EYE
AB(I+11,J+11,K+6) IS DP/DY (NORTH) IN MB/KM AT SAME POINT
AB(I+11,J+11,K+11) IS DP/DR (OUTWARD) IN MB/KM AT SAME POINT
AC(I+11,1,J+11) IS COS OF ANGLE OF POINT I,J
(SAME FOR ALL GRID NESTS)

```

C      AC(I+11,2,J+11) IS SIN OF ANGLE OF POINT I,J
C      (SAME FOR ALL GRID NESTS)
C      AC(I+11,3...7,J+11) IS RADIUS OF POINT I,J IN NEST 1...5
C      RESPECTIVELY (METERS)
C      REAL RADIUS(4),PFAR(4)
EQUIVALENCE (JTRACK,JA),(EYELAT,JA(2)),(LYLONG,JA(3)),
$ (DIREC,JA(4)),(SPEED,JA(5)),(IQUAD,JA(6)),(EYPRES,JA(7)),
$ (RADIUS,JA(8)),(PFAR,JA(12))
DATA LU/6/
DATA DEG / .017453293/
DATA S45 / .70710678/
C      COMPUTE GRID ANGLES AND DISTANCES (FUNCTION OF OX ONLY)
DO 10 IG = 1,21
10     AD(IG,1) = DX*FLOAT(IG-11)
DO 12 IC = 1,21
DO 12 ID = 1,21
AE = AD(IC,1)**2+AD(ID,1)**2
IF (AE.LE.0) GO TO 12
AC(IC,3,ID) = SQRT(AE)
AC(IC,1,ID) = AD(IC,1)/AC(IC,3,ID)
AC(IC,2,ID) = -AD(ID,1)/AC(IC,3,ID)
DO 11 IE = 4,7
11     AC(IC,IE,ID) = AC(IC,IE-1,ID)+AC(IC,IE-1,JD)
12     CONTINUE
HA(4) = DIREC*DEG
IF (JA(1).NE.0) BA(4) = BA(4)*11.25
BA(5) = SPEED*(1852./3600.)
IF (JA(6).EQ.0) GO TO 280
DO 21 IC = 1,4
    BA(IC+7) = RADIUS(IC)*1.852
    BA(IC+11) = PFAR(IC)-EYPRES
21     CONTINUE
24     DO 25 IC=1,2
25     AP(1,IC) = .25*(BC(1,IC)+BC(2,IC)+BC(3,IC)+BC(4,IC))
IF (JA(6).EQ.2) GO TO 27

```

```

26 DO 26 IC = 1,2
   AP(2,IC) = .5*S45*(BC(1,IC)+BC(2,IC)-BC(3,IC)-BC(4,IC))
   AP(3,IC) = .5*S45*(BC(1,IC)-BC(2,IC)-BC(3,IC)+BC(4,IC))
   GO TO 29

27 DO 28 IC = 1,2
   AP(2,IC) = .5*(EC(2,IC)-BC(4,IC))
   AP(3,IC) = .5*(BC(1,IC)-BC(3,IC))
   CONTINUE

28 GO TO 29
   CONTINUE

280 CONTINUE

29 AP(1,1) = RADIUS(1)*1.852
   AP(1,2) = PFAR(1)-EYFRES
   CONTINUE
   AT(1) = COS(BA(4))
   AT(2) = -SIN(BA(4))
   CR = CR*CT
   CD = CD*CT
   UC = -AT(2)*BA(5)
   VC = AT(1)*BA(5)

31 DO 40 IE = 1,5
   DO 36 ID = 1,21
   DO 35 IC = 1,21
   IF (JA(6).EQ. 0) GO TO 340
   DO 32 IH = 1,2
   BP(1,IH) = AP(1,IH)+AP(2,IH)*AC(IC,1,ID)+AP(3,IH)*AC(IC,2,ID)
   BP(2,IH) = -AP(2,IH)*AC(IC,2,ID)+AP(3,IH)*AC(IC,1,ID)
   IF (AC(IC,3,ID).GT. 0) GO TO 33
   AD(IC,1) = 0.
   AD(IC,2) = 0.
   GO TO 34

33 AE = EXP(-BP(1,1)/AC(IC,IE+2,ID))
   AF = AE*BP(1,2)
   C COMPUTE RADIAL PRESSURE GRADIENT
   AD(IC,1) = AF*BP(1,1)/AC(IC,IE+2,ID)**2
   AD(IC,2) = (AE*BP(2,2)-AF/AC(IC,IE+2,ID)*BP(2,1))/AC(IC,IE+2,ID)
   C TANGENTIAL PRESSURE GRADIENT

```

```

34  AD(IC,3) = AD(IC,1)*AC(IC,1,ID)-AD(IC,2)*AC(IC,2,ID)
    AD(IC,4) = AD(IC,1)*AC(IC,2,ID)+AD(IC,2)*AC(IC,1,ID)
    GO TO 341
340 AD(IC,2) = 0.
C    CIRCULARLY SYMMETRIC PRESSURE FIELD: ZERO TANGENTIAL GRADIENT
    AD(IC,1) = EXP(-AP(1,1)/AC(IC,IE+2,ID))*AP(1,2)*AP(1,1)/
AAC(IC,IE+2,ID)**2
    AD(IC,3) = AD(IC,1)*AC(IC,1,ID)
    AD(IC,4) = AD(IC,1)*AC(IC,2,ID)
341 CONTINUE
    AB(IC,ID,IE+10) = AD(IC,1)
    AB(IC,ID,IE) = AD(IC,3)
35  AB(IC,ID,IE+5) = AD(IC,4)
    IF (IB .EQ. 0) GO TO 38
C    IF NO PROGRAM CHANGES, NORTH IS PRINTED AT TOP
C    OF PAGE, WEST AT LEFT, ETC.
    WRITE (LU,36) AD
36  FORMAT (4(1X,1P21F6.2/))
38  CONTINUE
    IF (IB .EQ. 0) GO TO 40
    WRITE (LU,39)
39  FORMAT (/////)
40  CONTINUE
    RETURN
    END

```

```

C      **** THIS IS MAIN PROGRAM HIST ****
C
C**   A.C.E. PROGRAM TO FIND WINDS AT STATIONS
C
C**   INPUT CARDS:
C       1. NAMELISTS NAME4,NAME5
C       2. HINDCAST LOCATIONS REQUESTED: LAT-DEG,LAT-MIN,LON-DEG,
C           LON-MIN, TERRAIN CODE, STA HT IN METERS,
C           STATION IDENTIFICATION NUMBER.
C           (5I4,F6.1,I4)
C           WEST LONGITUDE IS POSITIVE.
C           1 CARD PER LOCATION. TERMINATED BY &EOF.
C       3. ONE CARD FOR EACH HOUR OF STORM.
C           LAT-DEG OF EYE,LAT-MIN OF EYE,LON-DEG OF
C           EYE,LON-MIN OF EYE,SNAPSHOT 1 RECORD SEQUENCE
C           NUMBER IN FILE,SNAP 2 REC SEQ NBR,
C           ROTATION ANGLE(DEG.CLOCKWISE
C           TO ROTATE WIND ON NESTED GRID),
C           INDICATOR - IF NONZERO WIND ON WAVE GRID IS PRINTED.
C           (6I4,F8.4,2I4) .
C           WEST LONGITUDE IS POSITIVE . TERMINATED BY &EOF .
C**   INPUT FILES:
C       1. FILE 13(LSNAP): SNAPSHOTS FOR STORM (R.A.F.)
C
C**   OUTPUT FILES:
C       1. FILE 20(LTROUT): WIND DATA ON ICOSAHEDRAL GRID(R.A.F.)
C
C**   TEMPORARY FILES
C       1. FILE 10(LTEMP) ALL SNAPSHOTS PLUS ALL INTERPOLATED WIND FIELDS
C
C**   STANDARD UNITS: 5(LR) IS CARD READER, 6(LP) IS PRINTER.
C
C       TERRAIN CODE (LLAKE) 1-6,          LAKE 0-5.
C
C       REAL LAG,LA1,LOG,LO1
C****

```



```

C****
PARAMETER MAXI=62,MAXJ=31,IGRDHT=100
COMMON /C57/ PTH,OTH,HH,ZCOEFF(3,5),LAKE,VV(100),UX(3),UV(3),
1 DUV(3),K35,K2,G,GA,DEN,VV2,HL,K123,Z0,ZLOG,AM,BM,CM,UXV(100,6),
2 TURN(100,6),COST(100),SINT(100)
REAL K2,K35
INTEGER LLAKE(100)
COMMON /D1/LA0,L00,ROT,LA1,L01,DX,STHT,LANSEA,W1,TH1,D,AL,UST
COMMON /D2/ XX(21,21,10)
COMMON/D3/MSNAP1(100),NSNAP2(100),PCT(100),
1 IPI(100),NHT,INTVN,INTVI
DIMENSION NAD(100),NAM(100),NOD(100),NOM(100),IROT(100)
DIMENSION MAD(100),MAM(100),MMOD(100),MOM(100),YLA(100),YLO(100)
DIMENSION JSEQ(100),KDATE(100),KTIME(100)
DIMENSION WIND(2,MAXI,MAXJ)

C****
DIMENSION ZLA(MAXJ), ZLO(MAXI), ZANG(MAXI,MAXJ)
DIMENSION LSTAB(MAXI,MAXJ)

C****
DIMENSION XY(21,21,10)
DIMENSION STAHT(100),DTHI(2),KSTA(100)
DIMENSION JA(15)
EQUIVALENCE (ITRACK,JA),(FYELAT,JA(2)),(LYLONG,JA(3)),
1 (DIREC,JA(4)),(SPEED,JA(5)),(IQUAD,JA(6)),(EYPRES,JA(7)),
2 (RADIUS,JA(8)),(PFAR,JA(12))
EQUIVALENCE (XY,WIND)

C
DATA CON /57.29578/
DATA LR,LP,LSNAP/5,6,13/
DATA LTEMP/10/
DATA LTROUT/20/
DATA KSNAP1,KSNAP2/2*0/

C
NAMELIST/NAME4/NBASE,I,START,IZONE,ICNVRT,NPRT
NAMELIST/NAME5/LAKE,ZCOEFF

```

```

NAMELIST/NAMEP/DTH,HH,LAKE,G,ZCOEFF,GARR,PTH,K35
GRIDHT=FLOAT(IGRDHT)/10.
IMAX=MAXI
JMAX=MAXJ
4 DO 5 J=1,MAXJ
DO 5 I=1,MAXI
LSTAB(I,J)=0
5 ZANG(I,J)=0.
DTH=-2.
HH=650.
LAKE=0
G=9.806
GARR=.035
PTH=300.
K35=.35
DO 10 J=1,5
DO 10 I=1,3
10 ZCOEFF(I,J)=0.
REWIND LSNAP
REWIND LTEMP
READ (LR,NAME4)
WRITE (LP,NAME4)
PRINT 1E9, NBASE, ISTART, IZONE
READ (LSNAP) XX,NAME,DX,JA,SGW,AN1,ST12,DTHI,HH,GARR,PTH,K35
READ (LH,NAME5)
IF(ICNVRT.NE.0) CALL RDGRID(ZLA,ZLO,LSTAB,MAXI,MAXJ)
DTH=DTHI(2)
WRITE (LP,NAME P)
K2=K35**2
GA=GARR/G
DT=10.0*DX
CALL UXXV
CALL UPDOWN
IF (NBASE.NE.NAME) STOP 515
NBR=0

```

```

C      READ HINDCAST LOCATIONS INPUT CARDS
C
C      IF (NBR.EQ.100) STOP 516
C      READ (LR,165,ERR=145,END=20) MAD(NBR+1),MAM(NBR+1),MMOD(NBR+1),MOM(
15      1(NBR+1),LLAKE(NBR+1),STAHT(NBR+1),KSTA(NBR+1)
      NBR=NBR+1
      WRITE(LP,170) MAD(NBR),MAM(NBR),MMOD(NBR),MOM(NBR),
1      LLAKE(NBR),STAHT(NBR),KSTA(NBR)
      XL=IABS(MAD(NBR))
      YLA(NBR)=(XL+FLOAT(MAM(NBR)))/60.0)/CON
      IF (MAD(NBR).LT.0)YLA(NBR)=-YLA(NBR)
      XL=IABS(MMOD(NBR))
      YLO(NBR)=(XL+FLOAT(MOM(NBR)))/60.0)/CON
      IF (MMOD(NBR).LT.0)YLO(NBR)=-YLO(NBR)
      GO TO 15
      CONTINUE
      IF (NBR.NE.0) WRITE (LP,175)
C
C      READ HOURLY INPUT CARDS .
C
      NHT=0
      READ (LR,180,ERR=145,END=30) MAD(NHT+1),NAM(NHT+1),NOD(NHT+1),NOM(
25      1NHT+1),NSNAP1(NHT+1),NSNAP2(NHT+1),PCT(NHT+1),IROT(NHT+1),
      2 IPI(NHT+1)
      NHT=NHT+1
      IF (NHT.LT.100) GO TO 25
      STOP 517
      CONTINUE
      WRITE (LP,185)
      KY=ISTART/10**6+1900
      KH=MOD((ISTART/10**4),100)
      KD=MOD((ISTART/100),100)
      KTIME(I)=MOD(ISTART,100)
      KJD=JULIAN(KM,KD,KY)
      30

```



```

55 READ (LSNAP) XY,NAMEI
60 CONTINUE
CONTINUE
IF (PCT(KHR).EQ.0.) GO TO 70
KSNAP1=0
IF (PCT(KHR).LT.0..OR.PCT(KHR).GT.1.) STOP 444
DO 65 K=1,10
DO 65 J=1,21
DO 65 I=1,21
XX(I,J,K)=(1.-PCT(KHR))*XX(I,J,K)+PCT(KHR)*XY(I,J,K)
CONTINUE
CONTINUE
70 CONTINUE
C
C
IF (KHR.EQ.1) GO TO 75
IF (JSEQ(KHR).EQ.JSEQ(KHR-1)) GO TO 80
WRITE (LTEMP) XX,JSEQ(KHR)
CONTINUE
80 IF (NBR.EQ.0) GO TO 106
C
C
C COMPUTE WIND FOR EACH HINDCAST LOCATION AT THIS TIME STEP
DO 105 K=1,NBR
WRITE (LP,185)
LA1=YLA(K)
LO1=YLO(K)
STHT=STAHT(K)
LANSEA=LLAKE(K)
C
REWIND LTEMP
C
DO 100 KHR=1,NHT
IF (KHR.EQ.1) GO TO 85
IF (JSEQ(KHR).EQ.JSEQ(KHR-1)) GO TO 90
READ (LTEMP,ERR=146) XX,KSEQ
85

```

```

90 XL=IABS(NAD(KHR))
   LA0=(XL+FLOAT(NAM(KHR)))/60.0)/CON
   IF(NAD(KHR).LT.0)LA0=-LA0
   XL=IABS(NOD(KHR))
   L00=(XL+FLOAT(NOM(KHR)))/60.0)/CON
   IF(NOD(KHR).LT.0)L00=-L00
   ROT=IRUT(KHR)
   CALL BREEZE
   UST=UST*100.
   UST IN CM/SEC
   WRITE (LP,195) NAME,KDATE(KHR),KTIME(KHR),W1,TH1,D,AL,UST,KSTA(K),
1MA0(K),MAM(K),MMOD(K),MOM(K),NAD(KHR),NAM(KHR),NOD(KHR),NOM(KHR),L
2LAKE(K),STAHT(K),KHR,KSEQ
   CONTINUE
   WRITE (LP,200)
   CONTINUE
100
   C
105
   C
   C
   C
   C
   CONVERT WIND TO WAVE GRID FOR THIS TIME STEP
   IF(ICVRT.EQ.0) GO TO 135
   C
   REWIND LTEMP
   REWIND LTROUT
   STHT=GRIDHT
   C
106
   DO 113 KHR=1,NHT
   XL=IABS(NAD(KHR))
   LA0=(XL+FLOAT(NAM(KHR)))/60.0)/CON
   IF(NAD(KHR).LT.0)LA0=-LA0
   XL=IABS(NOD(KHR))
   L00=(XL+FLOAT(NOM(KHR)))/60.0)/CON
   IF(NOD(KHR).LT.0)L00=-L00
   ROT=IRUT(KHR)
   IF (KHR.EQ.1) GO TO 1065
   IF (JSEQ(KHR).EQ.JSEQ(KHR-1)) GO TO 107

```

```

1065 READ (LTEMP,ERR=146) XX,KSEQ
107 CONTINUE
DO 111 J=1,MAXJ
C****
LAI=ZLA(J)
C****
DO 110 I=1,MAXI
C****
LOI=ZLO(I)
C****
LANSEA=LSTAB(I,J)
CALL BREEZE
WIND(1,I,J)=W1
WIND(2,I,J)=TH1+ZANG(I,J)
CONTINUE
CONTINUE
110 WRITE (LTHOUT) NBASE,KHR,ISTART,IZONE,IMAX,JMAX,GRIDHT,NAD(KHR),
111 1 NAM(KHR),NCD(KHR),NOM(KHR),WIND
IF (IPI(KHR).NE.0) GO TO 112
IF (NPRT.EQ.0) GO TO 113
IF (MOD((KHR-1),NPRT).NE.0) GO TO 113
CALL PRLAKE (NBASE,KHR,ISTART,IZONE,WIND,LSTAB,MAXI,MAXJ)
CONTINUE
END FILE LTROUT
C
135 WRITE (LP,2J5)
STOP 999
145 STOP 5
146 STOP 146
C
160 FORMAT (4X,A4,4X,IB,A3)
165 FORMAT (5I4,F6.1,1X,13)
170 FORMAT(1X,2(I4,1X,J2),I3,F6.1,I3)
175 FORMAT (//)
180 FORMAT(6I4,F8.4,2I4)
185 FORMAT (1H1)

```

```

190  FORMAT (1H1,/,/,T20,'STORM HISTORY 1ST HOUR IS ',I8,I4,A3,/,/,C1
195  1X,I4,6I4,F8.4,3I4,I8,J2)
      FORMAT (1X,A6,J6,J2,' W1=',F6.2,' TH1=',F5.1,' D=',F6.1,' AL=',F5
1  1,' UST=',F6.2,' STA',I3,'=',I3,1X,J2,I4,1X,J2,
2  ' EYE=',I3,1X,J2,I4,1X,J2,' TERR=',I1,
3  ' HT=',F5.1,I4,I2)
200  FORMAT (/,)
205  FORMAT (1H1,' END OF HIST/MAIN')
      END

```



```

COMPILER (XM=1), (EQUIV=CMN)
SUBROUTINE INVJD (J,M,D,Y)
C REVERSE OF FUNCTION 'JULIAN'.
C COMPUTES INVERSE JULIAN DATE J FROM
C MONTH(M), DAY(D), AND YEAR(Y) INPUT.
INTEGER J,M,D,Y,TJ,TM,TD,TY,MTD
TJ=J-1721119
TY=(4*TJ-1)/146097
TJ=4*TJ-1-146097*TY
TD=TJ/4
MTD=4*TD+3
TJ=MTD/1461
TD=MTD-1461*TJ
TD=(TD+4)/4
MTD=5*TD-3
TM=MTD/153
TD=MTD-153*TM
D=(TD+5)/5
Y=100*TY+TJ
IF (TM.GE.10) GO TO 2
1 M=TM+3
RETURN
2 M=TM-9
Y=Y+1
RETURN
END

```

```

C
C
  COMPILER (XM=1), (EQUIV=CMN)
  FUNCTION JULIAN(MO,DA,YR)
  REVERSE OF SUBROUTINE 'IIVJD'.
  COMPUTES JULIAN DATE.
  INTEGER D,Y,M,C,YA,MU,DA,YR
  M=MO
  D=DA
  Y=YR
  IF (M.LE.2) GO TO 2
1  M=M-3
   GO TO 3
2  M=M+9
   Y=Y-1
   C=Y/100
   YA = Y-100+C
  JULIAN=(146097*C)/4+(1461*YA)/4+(153*M+2)/5+D+1721119
  END
3

```

```

SUBROUTINE OUTBY1(NEST)
C  OUTER BOUNDARY ( NOT AT THE SAME TIME LEVEL )
COMMON /C3/ U(21,21,5),V(21,21,5),UN(21,21,5),VN(21,21,5)
1  ,PX(21,21,5),PY(21,21,5),VTN(21,21,5),ANG(21,21,5)
2  ,LW(21,21,5)
UN(1,1,NEST)=0.5*(UN(6,6,NEST+1)+U(6,6,NEST+1))
VN(1,1,NEST)=0.5*(VN(6,6,NEST+1)+V(6,6,NEST+1))
DO 780 J=1,10
UN(1,2*J+1,NEST)=0.5*(UN(6,J+6,NEST+1) +U(6,J+6,NEST+1))
VN(1,2*J+1,NEST)=0.5*(VN(6,J+6,NEST+1) +V(6,J+6,NEST+1))
UN(21,2*J+1,NEST)=0.5*(UN(16,J+6,NEST+1)+U(16,J+6,NEST+1))
VN(21,2*J+1,NEST)=0.5*(VN(16,J+6,NEST+1)+V(16,J+6,NEST+1))
UN(1,2*J,NEST)=0.250*(UN(6,J+5,NEST+1)+UN(6,J+6,NEST+1)
+ U(6,J+5,NEST+1)+U(6,J+6,NEST+1))
1  VN(1,2*J,NEST)=0.250*(VN(6,J+5,NEST+1)+VN(6,J+6,NEST+1)
+ V(6,J+5,NEST+1)+V(6,J+6,NEST+1))
1  UN(21,2*J,NEST)=0.250*(UN(16,J+5,NEST+1)+UN(16,J+6,NEST+1)
+ U(16,J+5,NEST+1)+U(16,J+6,NEST+1))
1  VN(21,2*J,NEST)=0.250*(VN(16,J+5,NEST+1)+VN(16,J+6,NEST+1)
+ V(16,J+5,NEST+1)+V(16,J+6,NEST+1))
780  CONTINUE
DO 790 I=1,10
UN(2*I+1,1,NEST)=0.5*(UN(I+6,6,NEST+1)+U(I+6,6,NEST+1))
VN(2*I+1,1,NEST)=0.5*(VN(I+6,6,NEST+1)+V(I+6,6,NEST+1))
UN(2*I+1,21,NEST)=0.5*(UN(I+6,16,NEST+1)+U(I+6,16,NEST+1))
VN(2*I+1,21,NEST)=0.5*(VN(I+6,16,NEST+1)+V(I+6,16,NEST+1))
UN(2*I,1,NEST)=0.250*(UN(I+5,6,NEST+1)+UN(I+6,6,NEST+1)
+ U(I+5,6,NEST+1)+U(I+6,6,NEST+1))
1  VN(2*I,1,NEST)=0.250*(VN(I+5,6,NEST+1)+VN(I+6,6,NEST+1)
+ V(I+5,6,NEST+1)+V(I+6,6,NEST+1))
1  UN(2*I,21,NEST)=0.250*(UN(I+5,16,NEST+1)+UN(I+6,16,NEST+1)
+ U(I+5,16,NEST+1)+U(I+6,16,NEST+1))
1  VN(2*I,21,NEST)=0.250*(VN(I+5,16,NEST+1)+VN(I+6,16,NEST+1)
+ V(I+5,16,NEST+1)+V(I+6,16,NEST+1))
790  CONTINUE
      RETURN
      END

```

```

C
SUBROUTINE OUTBY2(NEST)
OUTER BOUNDARY (AT SAME TIME LEVEL)
COMMON /C3/ U(21,21,5),V(21,21,5),UN(21,21,5),VN(21,21,5)
1 ,PX(21,21,5),PY(21,21,5),VTN(21,21,5),ANG(21,21,5)
2 ,LW(21,21,5)
UN(1,1,NEST)=UN(6,6,NEST+1)
VN(1,1,NEST)=VN(6,6,NEST+1)
DO 820 J=1,10
UN(1,2*J+1,NEST)=UN(6,J+6,NEST+1)
VN(1,2*J+1,NEST)=VN(6,J+6,NEST+1)
UN(21,2*J+1,NEST)=VN(16,J+6,NEST+1)
VN(21,2*J+1,NEST)=UN(16,J+6,NEST+1)
UN(1,2*J,NEST)=0.5*(UN(6,J+5,NEST+1)+UN(6,J+6,NEST+1))
VN(1,2*J,NEST)=0.5*(VN(6,J+5,NEST+1)+VN(6,J+6,NEST+1))
UN(21,2*J,NEST)=0.5*(VN(16,J+5,NEST+1)+VN(16,J+6,NEST+1))
VN(21,2*J,NEST)=0.5*(UN(16,J+5,NEST+1)+UN(16,J+6,NEST+1))
P 20 CONTINUE
DO 830 I=1,10
UN(2*I+1,1,NEST)=UN(I+6,6,NEST+1)
VN(2*I+1,1,NEST)=VN(I+6,6,NEST+1)
UN(2*I+1,21,NEST)=VN(I+6,16,NEST+1)
VN(2*I+1,21,NEST)=UN(I+6,16,NEST+1)
UN(2*I,1,NEST)=0.5*(UN(I+5,6,NEST+1)+UN(I+6,6,NEST+1))
VN(2*I,1,NEST)=0.5*(VN(I+5,6,NEST+1)+VN(I+6,6,NEST+1))
UN(2*I,21,NEST)=0.5*(VN(I+5,16,NEST+1)+VN(I+6,16,NEST+1))
VN(2*I,21,NEST)=0.5*(UN(I+5,16,NEST+1)+UN(I+6,16,NEST+1))
P 30 CONTINUE
RETURN
END

```

```
SUBROUTINE OUTFLO
COMMON /C3/ U(21,21,5),V(21,21,5),UN(21,21,5),VN(21,21,5)
1 ,PX(21,21,5),PY(21,21,5),VTN(21,21,5),ANG(21,21,5)
2 ,LW(21,21,5)
DATA C08,S18/.99026807,.1391731/
DO 10 IA = 1,2205
  XX = UN(IA,1,1)*C08+VN(IA,1,1)*S18
  VN(IA,1,1) = VN(IA,1,1)*C08-UN(IA,1,1)*S18
  UN(IA,1,1) = XX
10 CONTINUE
RETURN
END
```

```

SUBROUTINE JUTOUT(I20,NAME,IDENT,NSEQ)
COMMON /C3/ U(21,21,5),V(21,21,5),UN(21,21,5),VN(21,21,5)
1  ,PX(21,21,5),FY(21,21,5),VTN(21,21,5),ANG(21,21,5)
2  ,LW(21,21,5)
DATA LP/6./
WRITE (6,10)
FORMAT (1H1)
IF(IDENT.EQ.4HINIT) GO TO 190
DO 80 NEST = 1,4
DO 80 I=1,10
DO 80 J=1,10
UN(I+6,J+6,NEST+1)=UN(2*I+1,2*J+1,NEST)
VN(I+6,J+6,NEST+1)=VN(2*I+1,2*J+1,NEST)
CONTINUE
80 CALL AANGEL (I20)
190 CALL TVEL(VTN,ANG,NAME,IDENT,NSEG,4,I20)
CALL TVEL(VTN,ANG,NAME,IDENT,NSEQ,3,I20)
CALL TVEL(VTN,ANG,NAME,IDENT,NSEQ,1,I20)
RETURN
END

```



```

SUBROUTINE PXYM
C PXYM CALLS SUBROUTINE GRAD TO GET PRESSURE GRADIENT,
C THEN REARRANGES THE PRESSURE GRADIENT, THEN PRODUCES
C INITIAL GRADIENT WIND FELD.
COMMON /C1/ Z1(2),DX,DT,F,SGW,AN1,Z2(2),UG,VG,Z3(3),ST12
COMMON /C2/ JA(15),BA(21,21,15),BC(21,7,21)
COMMON /C3/ U(21,21,5),V(21,21,5),UN(21,21,5),VN(21,21,5)
1  ,PX(21,21,5),PY(21,21,5),VTN(21,21,5),ANG(21,21,5)
2  ,LW(21,21,5)
DO 50 VEST = 1,5
GO TO (10,30,30,30,30),NEST
CALL GRAD
10 AN2 = AN1*3.14159265/180.
IF (ST12 .LE. 0) GO TO 30
DX2 = .5*DX/ST12
CD2 = COS(AN2)*DX2
SI2 = SIN(AN2)*DX2
DO 31 I = 1,21
DO 31 J = 1,21
MJ=22-J
PX(I,J,NEST) = BA(I,MJ,NEST)*(1E-4/1.15E-3)
PY(I,J,NEST) = BA(I,MJ,NEST+5)*(1E-4/1.15E-3)
AG = BA(I,MJ,NEST+10)*(1E-4/1.15E-3)
AH=BC(I,NEST+2,MJ)*F*500.
AI=AG*BC(I,NEST+2,MJ)*1000.
IF(AI.NE.0.) AI = AI/(AI+SQRT(AH*AH+AI))
U(I,J,NEST) = -AI*BC(I,2,MJ)
V(I,J,NEST) = AI*BC(I,1,MJ)
UN(I,J,NEST) = U(I,J,NEST)
VN(I,J,NEST) = V(I,J,NEST)
SGW NON-ZERO FOR STEERING FLOW.
IF (SGW.EQ.0.) GO TO 50
AG = F*UG
AH = F*VG
31
C
32

```



```
IF (ST12 .GT. 0) GO TO 34
DO 33 I = 1,21
DO 33 J = 1,21
33 PX(I,J,NEST) = PY(I,J,NEST)+AH
PY(I,J,NEST) = PY(I,J,NEST)-AG
GO TO 50
34 C02 = C02+C02
SI2 = SI2+SI2
DO 36 I = 1,21
AI = (I-11)*SI2
DO 35 J = 1,21
AJ = (J-11)*C02
FADE = -.69314718*(AJ-AI)**2
FADE = EXP(FADE)
IF (FADE .LE. 0.) GO TO 35
PX(I,J,NEST) = PX(I,J,NEST)+AH*FADE
PY(I,J,NEST) = PY(I,J,NEST)-AG*FADE
35 CONTINUE
36 CONTINUE
50 CONTINUE
99 RETURN
END
```

```

SUBROUTINE RUGRID (ZLA,ZLO,LSTAB,MAXI,MAXJ)
COMMON /LGRID/ ILAT(31),ILONG(62)
DIMENSION LSTAB(MAXI,MAXJ)
DIMENSION ZLA(MAXJ),ZLO(MAXI)
DO 25 J=1,4
I1=(J-1)*15+1
I2=I1+14
READ 15,(ILONG(I),I=I1,I2),KSEQ
FORMAT (16I5)
IF(KSEQ.EQ.0) GO TO 25
PRINT 20,KSEQ,J,(ILONG(I),I=I1,I2)
FORMAT(/,' GRID INPUT ERROR',16I5)
STOP 21
CONTINUE
READ 30,ILONG(61),ILONG(62),KSEQ
FORMAT(2I5,65X,I5)
IF(KSEQ.EQ.5) GO TO 35
PRINT 20,KSEQ,ILONG(61),ILONG(62)
STOP 21
READ 15,(ILAT(I),I=1,15),KSEQ
IF(KSEQ.NE.1) GO TO 40
READ 15,(ILAT(I),I=16,30),KSEQ
IF(KSEQ.NE.2) GO TO 40
READ 37,ILAT(31),KSEQ
FORMAT(I5,70X,I5)
IF(KSEQ.EQ.3) GO TO 45
PRINT 20,ILAT,KSEQ
STOP 23
CONTINUE
DO 55 J=1,MAXJ
L=IABS(ILAT(J))/100
M=IABS(MOD(ILAT(J),100))
ZLA(J)=(FLOAT(L)+FLOAT(M)/60.)*.0174532
IF(ILAT(J).LT.0) ZLA(J)=-ZLA(J)
READ 50,(LSTAB(I,J),I=1,62),KSEQ
FORMAT(10X,62I1,6X,I2)

```

```
51 IF(KSEQ.EU.J) GO TO 55
   PRINT 51,J,KSEQ,(LSTAB(I,J),I=1,62)
   FORMAT( ' LS INPUT ERROR',2I4,2X,62I1)
55 STOP 51
   CONTINUE
   DO 60 I=1,MAXI
   L=IABS(I LONG(I))/100
   M=IABS(MOD(I LONG(I),100))
   ZLO(I)=(FLOAT(L)+FLOAT(M)/60.)*.0174532
   IF(I LONG(I).LT.0) ZLO(I)=-ZLO(I)
60 CONTINUE
   END
```

```
SUBROUTINE SHORE
COMMON /C3/ U(21,21,5),V(21,21,5),UH(21,21,5),VN(21,21,5)
1 ,PX(21,21,5),PY(21,21,5),VTN(21,21,5),ANG(21,21,5)
2 ,LW(21,21,5)
DO 20 I=1,2205
LW(I)=2
RETURN
END
```

20

```

C      **** THIS IS MAIN PROGRAM SNAP ****
C
C      MAIN PROGRAM FOR SNAPSHOT WINDS ON NESTED GRID.
C      INPUT IB IS SWITCH VARIABLE IB = 0 TO SUPPRESS PRINTING
C                                     OF PRESSURE FIELD
C                                     AND INITIAL WIND FIELD
C      NZ IS NUMBER OF WIND SNAPSHOTS TO PRODUCE.
C      FOR THE QUANTITIES EQUIVALENCED TO JA, SEE COMMENTS TO
C      SUBROUTINE GRAD.
C      NM IS NUMBER OF TIMES TO CYCLE WIND COMPUTATION IN
C                                     INNERMOST GRID NEST.
C      SGW IS MAGNITUDE OF SURFACE GEOSTROPHIC WIND (MTRS/SEC)
C      AN1 IS DIRECTION OF SGW, COUNTERCLOCKWISE FROM EAST (DEG)
C      ST12 IS DIST (KM) FROM AXIS TO 1/2 MAGNITUDE OF SGW#) FROM AXIS TO 1
C      DX IS GRID DISTANCE OF INNERMOST NEST (KILOMETERS).
C      NAME IS SNAPSHOT NAME FORMAT YYL (YY=YEAR,L=1ST LETTER
C                                     OF HURRICANE NAME).
C      FOR ALL ARRAYS IN COMMON C3 :
C      1ST DIMENSION INCREASES FROM WEST TO EAST
C      2ND DIMENSION INCREASES FROM SOUTH TO NORTH
C      3RD DIMENSION (NEST NUMBER) INCREASES FROM
C                                     INNERMOST TO OUTERMOST
C      COMMON/C1/NAME,NSNAP,DX,DT,F,SGW,AN1,UC,VC,UG,VG,CS,NM,IB,ST12
C      COMMON/C2/JA(15),AB(21,21,15),AC(21,7,21)
C      COMMON /C3/ U(21,21,5),V(21,21,5),UN(21,21,5),VN(21,21,5)
C      1 ,PX(21,21,5),PY(21,21,5),VTN(21,21,5),ANG(21,21,5)
C      2 ,LW(21,21,5)
C      COMMON
C      $/C4/ CDR(100,2,2),UXV(100,2),TURN(100,2)
C      $/C5/ FLAT,PTH,DTH(2),HH,ZOLAND,LS,VV(100),UX(3),UV(3),
C      $   DUV(3),K35,K2,G,GA,DEN,VV2,HL,K123,Z0,ZLOG,AM,BM,CM,FF
C      REAL RADIUS(4),PFAR(4)
C      EQUIVALENCE (ITRACK,JA),(EYELAT,JA(2)),(EYLONG,JA(3)),
C      $   (DIREC,JA(4)),(SPEED,JA(5)),(IQUAD,JA(6)),(EYPRES,JA(7)),
C      $   (RADIUS,JA(8)),(PFAR,JA(12))

```

REAL K35,K2

C

DATA LR,LP,LSNAP,LSHORE/5,6,13,14/

DATA PTH/300./

DATA HH/650./

DATA ZOLAND/.08/

DATA K35/.35/

DATA G/9.805/

DATA GARR/.0144/

DATA DTH/0.,-2./

C

NAMELIST/NAME1/IB,NZ

NAMELIST/NAME2/DTH,HH,ZOLAND,GARR,PTH,K35

NAMELIST/NAME3/SGW,AN1,NAME,

\$ EYELAT,EYLONG,DIREC,SPEED,EYPRES,RADIUS,PFAR,

\$ NM,DX,ST12,ITRACK,IQUAD

C

REWIND LSNAP

READ (LR,NAME1)

WRITE (LP,NAME1)

1

FORMAT (2I5)

READ (LR,NAME2)

WRITE (LP,NAME2)

K2=K35**2

GA = GARR/G

C

DO 20 NSNAP= 1,NZ

WRITE (LP,15)

NM = 800

DX = 5.

ST12 = 0.

ITRACK = 0

IQUAD = 0

READ(LR,NAME3)

WRITE(LP,NAME3)

DT = 10.0*DX

```

C      PHI = EYELAT/57.29578
      PHI IS LATITUDE IN RADIANS
      F=2.*7.29 E-5*SIN(PHI)
      F IS CORIOLIS FORCE
      FLAT=F
      CALL CCROSS
      WRITE (LP,15)
      FORMAT(1H1)
      CALL BLOWUG
      WRITE (LSNAP) UN,VN,NAME,DX,JA,SGW,AN1,ST12
1      ,DTH,HH,GARR,PTH,K35
      CONTINUE
      C
      WRITE (LP,25)
      FORMAT('1 END OF SNAP/MAIN')
      END FILE LSNAP
      STOP 999
      END

```

```

SUBROUTINE TVEL(VTN,ANG,NBASE,IDENT,KSEQ,LV,I20)
IF IN ARRAYS VTN,ANG 1ST DIMENSION INCREASES EASTWARD AND
2ND DIMENSION INCREASES NORTHWARD, SUBROUTINE TVEL PRINTS
WEST AT TOP OF PAGE,NORTH AT RIGHT OF PAGE, ETC.
NEST LV IS PRINTED AS INNER NEST, LV+1 AS OUTER NEST.
DIMENSION VTN(21,21,5),ANG(21,21,5)
DIMENSION KREDUC(2)/AHNOT ,1H /
DATA LU/6/
WRITE (LU,100)
FORMAT(1111)
LVP=LV+1
I20P=I20+1
WRITE (LU,200) NBASE,IDENT,KSEQ,LVP,KREDUC(I20P)
FORMAT(1H0,20X,A4,5X,A4,1X,I4, , LEVEL',13,5X,A4,'REDUCED')
1190 WRITE (LU,1200) (J, J=1,12)
1200 FORMAT(1H0,11X,12(12,UX))
DO 1210 I=1,5
1210 WRITE (LU,1220) (I,(VTN(I,J,LVP),J=1,12),(ANG(I,J,LVP),J=1,12))
1220 FORMAT(1H0,6X,I2,12(1PF5.0,5X)/9X,12(0PF5.0,5X),/1H0,/ )
1240 DO 1248 I=1,11
IL=I+5
IO=2*I-1
IE=2*I
IF (I-11) 1242,1246,1246
1242 WRITE (LU,1244) IL,(VTN(IL,J,LVP),J=1,5),(VTN(IO,N,LV),N=1,13)
1 , (ANG(IL,J,LVP),J=1,5),(ANG(IO,N,LV),N=1,13)
2 , (VTN(IE,N,LV),N=1,13),(ANG(IE,N,LV),N=1,13)
1244 FORMAT(1H0,6X,I2,5(1PF5.0,5X),13(1PF5.0)/9X,5(0PF5.0,5X),
1 13(0PF5.0)/1H0,58X,13(1PF5.0)/59X,13(0PF5.0))
GO TO 1248
1246 WRITE (LU,1247) IL,(VTN(IL,J,LVP),J=1,5),(VTN(IO,N,LV),N=1,13)
1 ,(ANG(IL,J,LVP),J=1,5),(ANG(IO,N,LV),N=1,13)
1247 FORMAT(1H0,6X,I2,5(1PF5.0,5X),13(1PF5.0)/9X,5(0PF5.0,5X),
1 13(0PF5.0)/1H0,/)
1248 CONTINUE

```



```

1300 DO 1300 I=17,21
1300 WRITE (LU,1220) (I,(VTN(I,J,LVP),J=1,12),(ANG(I,J,LVP),J=1,12))
1330 WRITE (LU,1330)
1330 FORMAT (1H1,/1H0,15X)
1340 WRITE (LU,1340) (J,J=13,21)
1340 FORMAT(1H0,16X,9(12,8X))
1345 DO 1345 I=1,5
1345 WRITE (LU,1350) ((VTN(I,J,LVP),J=13,21),I,(ANG(I,J,LVP),J=13,21))
1350 FORMAT(1H0,13X,9(1PF5.0,5X),12/14X,9(0PF5.0,5X),/1H0,/)
1370 DO 1378 I=1,11
1370 IL=I+5
1370 IO=2*I-1
1370 IE=2*I
1370 IF(I-11) 1372,1376,1376
1372 WRITE (LU,1374) (VTN(IO,N,LV),N=14,21),(VTN(IL,J,LVP),J=17,21),IL,
1  (ANG(IO,N,LV),N=14,21),(ANG(IL,J,LVP),J=17,21),
1374 2 (VTN(IE,N,LV),N=14,21),(ANG(IE,N,LV),N=14,21)
1374 FORMAT(1H0,8X,8(1PF5.0),5X,5(1PF5.0,5X),12/9X,8(0PF5.0),5X,
1 5(0PF5.0,5X)/1H0,8X, 8(1PF5.0)/9X, 8(0PF5.0))
1376 GO TO 1378
1376 WRITE (LU,1377) (VTN(IO,N,LV),N=14,21),(VTN(IL,J,LVP),J=17,21),IL,
1  (ANG(IO,N,LV),N=14,21),(ANG(IL,J,LVP),J=17,21)
1377 FORMAT(1H0,6X,6(1PF5.0),5X,5(1PF5.0,5X),12/9X,8(0PF5.0),5X,
1378 1 5(0PF5.0,5X)/1H0,/)
1378 CONTINUE
1400 DO 1400 I=17,21
1400 WRITE (LU,1350) ((VTN(I,J,LVP),J=13,21),I,(ANG(I,J,LVP),J=13,21))
1400 RETURN
1400 END

```

```

SUBROUTINE UPDOWN
COMMON /C57/ PTH,DTH,HH,ZCOEFF(3,5),LAKE,VV(100),UX(3),UV(3),
$ DUV(3),K35,K2,G,GA,DEN,VV2,HL,K123,ZU,ZLOG,AM,BM,CM,UXV(100,6),
$ TURN(100,6),COST(100),SINT(100)
REAL K2,K35
REAL VW2(100),TOL(100),TARN(100)
IF (LAKE .EQ. 0) RETURN
BM = 1.95+K35
BM2 = BM**2
HLOG = 1.39-ALOG(HH)
DO 61 IA = 1,100
  UM = VV(IA)*COST(IA)
  VM = VV(IA)*SINT(IA)
  VPLUS = -VV(IA)*UXV(IA,1)
  VTOP = VM+VPLUS
  VW2(IA) = UM**2+VTOP**2
  TOL(IA) = 1E-4*VW2(IA)
  TARN(IA) = UM*VPLUS/(UM**2+VM*VTOP)
CONTINUE
DO 70 INCH = 1,LAKE
  AZ = ZCOEFF(1,INCH)
  BZ = ZCOEFF(2,INCH)
  CZ = ZCOEFF(3,INCH)
  UX(1) = 1.
  IF (AZ*BZ .NE. 0.) UX(1) = CBRT(.5*AZ/BZ)
  ZLOG = HLOG+ALOG(AZ/UX(1)+BZ*UX(1)**2+CZ)
  DO 69 IA = 1,100
    UX(1) = K35*SQRT(VW2(IA)/(ZLOG**2+BM2))
    ZLOG = HLOG+ALOG(AZ/UX(1)+BZ*UX(1)**2+CZ)
    UV(1) = UX(1)**2/K2*(ZLOG**2+BM2)
    DUV(1) = UV(1)-VW2(IA)
    UX(2) = K35*SQRT(VW2(IA)/(ZLOG**2+BM2))
    UV(2) = UX(2)**2/K2*(ZLOG**2+BM2)
    DUV(2) = UV(2)-VW2(IA)
  KSTOP = 0

```

61

```

62      IF (DUV(1).EQ. DUV(2)) GO TO 63
        UX(3) = (UX(1)*DUV(2)-UX(2)*DUV(1))/(DUV(2)-DUV(1))
        ZLOG = HLOG+ALOG(AZ/UX(3)+BZ*UX(3)**2+CZ)
        UV(3) = UX(3)**2/K2*(ZLOG**2+BM2)
        DUV(3) = UV(3)-VV2(IA)
        IF (KSTOP .NE. 0) GO TO 63
        IF (ABS(DUV(3)).LT. TOL) KSTOP = 1
        UX(1) = UX(2)
        UX(2) = UX(3)
        DUV(1) = DUV(2)
        DUV(2) = DUV(3)
        GO TO 62
63      UXV(IA,INCH+1) = K35*SQRT(VV2(IA)/(ZLOG**2+BM2))/VV(IA)
        TURN(IA,INCH+1) = (BM-ZLOG*TARN(IA))/(ZLOG+BM*TARN(IA))
69      CONTINUE
70      CONTINUE
        RETURN
        END

```

```

SUBROUTINE UXXV
COMMON /C57/ PTH,DTH,HH,ZCOEFF(3,5),LAKE,VV(100),UX(3),UV(3),
$ DUV(3),K35,K2,G,GA,DEN,VV2,HL,K123,Z0,ZLOG,AM,BM,CM,UXV(100,6),
$ TURN(100,6),COST(100),SINT(100)
REAL K2,K35
DATA A125/1.25/
DO 10 IA = 1,100
  VV(IA) = FLOAT(IA)/A125
10 CONTINUE
  DEN = G*K2*DTH
  DO 40 IA = 1,100
    IB = 101-IA
    VV2 = VV(IB)**2
    TOL = 1E-4*VV2
    IF (IA .NE. 1) GO TO 20
    CM = 2.55
    K123 = 1
    UX(1) = 2.74
    CALL ABCCC
    K123 = 2
    UX(2) = UX(1)*80./SQRT(UV(1))
    GO TO 30
20 UX(1) = UX(3)
   UV(1) = UV(3)
   DUV(1) = UV(1)-VV2
   K123 = 2
   UX(2) = UX(1)+VV(IB)/VV(IB+1)
30 CALL ABCCC
   KSTOP = 0
   K123 = 3
31 IF (DUV(1).EQ. DUV(2)) GO TO 32
   UX(3) = AMAX1(.5*AMINI(UX(1),UX(2)),
$     AMINI(2.*AMAX1(UX(1),UX(2)),
$     (UX(1)*DUV(2)-UX(2)*DUV(1))/(DUV(2)-DUV(1))))

```

```

CALL ABCCC
IF (KSTOP .NE. 0) GO TO 32
IF (ABS(DUV(3)).LT. TOL) KSTOP = 1
UX(1) = UX(2)
UX(2) = UX(3)
DUV(1) = DUV(2)
DUV(2) = DUV(3)
GO TO 31
32  AB = SQRT((ZLOG+AM)**2+BM**2)
    UXV(IB,1) = K35/AB
    TURN(IB,1) = ATAN(BM/(ZLOG+AM))
    COST(IB) = -(ZLOG+AM)/AB
    SINT(IB) = BM/AB
40  CONTINUE
    RETURN
    END

```

APPENDIX C: PROGRAM HIST LISTING
OF TEST STORM (BETSY) INPUT
AND SAMPLE ANNOTATED OUTPUT


```

*LLT*DLI COEFGM.BEISYDIA7
LL1077 ML1070 10/22-11:29:46-(00)
000001 000 20 59 50 15 3 36.4 1MLV ORLEANS MOISANT -80 1
000002 500 29 51 90 01 3 21.3 2MLV ORLEANS NAS -79
000003 000 31 12 90 02 4 36.6 3MLV ORLEANS LAKEFRONT LAND -78
000004 111 19 54 90 01 6 25.9 4MLV ORLEANS CITY OFFICE -74
000005 100 31 02 90 02 3 10.1 5LAKE FONT. WATCH (OPEN) -72
000006 000 30 02 90 02 2 10.1 6LAKE FONT. LAKE -70
000007 000 25 54 15 10 1 -80 -66
000008 000 21 54 05 26 1 -79 -64
000009 000 21 07 02 42 1 -78 -63
000010 000 26 07 02 54 1 -74 -58
000011 000 26 12 06 14 1 -72 -56
000012 000 26 17 06 30 1 -70 -53
000013 000 26 21 01 45 1 -68 -47
000014 000 26 30 06 58 1 -66 -43
000015 000 26 31 07 31 1 -64 -39
000016 000 26 46 07 24 1 -63 -35
000017 000 26 54 07 37 1 -58 -35
000018 000 27 02 07 50 1 -35 -35
000019 000 27 10 08 13 1 -35 -35
000020 000 27 21 08 14 1 -35 -35
000021 000 27 32 08 25 1 -35 -35
000022 000 27 43 08 36 1 -35 -35
000023 000 27 55 08 46 1 -35 -35
000024 000 28 07 08 56 1 -35 -35
000025 000 28 21 09 06 1 -35 -35
000026 000 28 31 09 22 1 -35 -35
000027 000 28 42 09 38 1 -35 -35
000028 000 28 55 09 54 1 -35 -35
000029 000 29 19 09 04 1 -35 -35
000030 000 29 23 09 21 1 -35 -35
000031 000 29 37 09 34 1 2 -167 -35
000032 000 29 47 09 45 1 2 -334 -35
000033 000 29 56 09 55 1 2 -560 -35
000034 000 30 01 10 05 1 2 -677 -35
000035 000 30 14 10 15 1 2 -834 -35
000036 000 30 23 10 25 1 2 -834 -35
000037 000 30 23 10 25 1 2 -834 -35
000038 000 RECF

```

END ELT.

```

*PACK*COEFGM
FURPUR 27R34 E33 SL73R1 10/22/79 11:29:49
END PACK. TC71=12,UC=1,SYM=26,KCL=19

```

*PREP*COEFGM.
END PREP.

CPRT	COEPM-BELSYDIA
1	5420 9404 9352 9346 9327 9316 9304 9252 9241 9239 9218 9209 9201 9155 9150
2	9146 9143 9140 9137 9134 9131 9127 9121 9114 9106 9056 9144 9031 9021 9013
3	9006 8955 8923 8947 8943 8939 8935 8931 8927 8923 8920 8916 8912 8909 8905
4	8901 8856 8862 8847 8842 8837 8832 8826 8821 8815 8810 8805 8801 8757 8752
5	8746 8729
6	2750 2604 2410 2127 2031 2447 2451 2003 3003 3011 2008 2010 2013 3016 3021 3026 3033 3039
7	2940 2942 2945 2950 2954 2958 2962 2966 2970 2974 2978 2982 2986 2990 2994 2998 3002 3006 3010
8	3045
9	47 50 53 56 59 62 65 68 71 74 77 80 83 86 89 92 95 98 101 104 107 110 113 116 119 122 125 128 131 134 137 140 143 146 149 152 155 158 161 164 167 170 173 176 179 182 185 188 191 194 197 200 203 206 209 212 215 218 221 224 227 230 233 236 239 242 245 248 251 254 257 260 263 266 269 272 275 278 281 284 287 290 293 296 299 302 305 308 311 314 317 320 323 326 329 332 335 338 341 344 347 350 353 356 359 362 365 368 371 374 377 380 383 386 389 392 395 398 401 404 407 410 413 416 419 422 425 428 431 434 437 440 443 446 449 452 455 458 461 464 467 470 473 476 479 482 485 488 491 494 497 500 503 506 509 512 515 518 521 524 527 530 533 536 539 542 545 548 551 554 557 560 563 566 569 572 575 578 581 584 587 590 593 596 599 602 605 608 611 614 617 620 623 626 629 632 635 638 641 644 647 650 653 656 659 662 665 668 671 674 677 680 683 686 689 692 695 698 701 704 707 710 713 716 719 722 725 728 731 734 737 740 743 746 749 752 755 758 761 764 767 770 773 776 779 782 785 788 791 794 797 800 803 806 809 812 815 818 821 824 827 830 833 836 839 842 845 848 851 854 857 860 863 866 869 872 875 878 881 884 887 890 893 896 899 902 905 908 911 914 917 920 923 926 929 932 935 938 941 944 947 950 953 956 959 962 965 968 971 974 977 980 983 986 989 992 995 998 1001 1004 1007 1010 1013 1016 1019 1022 1025 1028 1031 1034 1037 1040 1043 1046 1049 1052 1055 1058 1061 1064 1067 1070 1073 1076 1079 1082 1085 1088 1091 1094 1097 1100 1103 1106 1109 1112 1115 1118 1121 1124 1127 1130 1133 1136 1139 1142 1145 1148 1151 1154 1157 1160 1163 1166 1169 1172 1175 1178 1181 1184 1187 1190 1193 1196 1199 1202 1205 1208 1211 1214 1217 1220 1223 1226 1229 1232 1235 1238 1241 1244 1247 1250 1253 1256 1259 1262 1265 1268 1271 1274 1277 1280 1283 1286 1289 1292 1295 1298 1301 1304 1307 1310 1313 1316 1319 1322 1325 1328 1331 1334 1337 1340 1343 1346 1349 1352 1355 1358 1361 1364 1367 1370 1373 1376 1379 1382 1385 1388 1391 1394 1397 1400 1403 1406 1409 1412 1415 1418 1421 1424 1427 1430 1433 1436 1439 1442 1445 1448 1451 1454 1457 1460 1463 1466 1469 1472 1475 1478 1481 1484 1487 1490 1493 1496 1499 1502 1505 1508 1511 1514 1517 1520 1523 1526 1529 1532 1535 1538 1541 1544 1547 1550 1553 1556 1559 1562 1565 1568 1571 1574 1577 1580 1583 1586 1589 1592 1595 1598 1601 1604 1607 1610 1613 1616 1619 1622 1625 1628 1631 1634 1637 1640 1643 1646 1649 1652 1655 1658 1661 1664 1667 1670 1673 1676 1679 1682 1685 1688 1691 1694 1697 1700 1703 1706 1709 1712 1715 1718 1721 1724 1727 1730 1733 1736 1739 1742 1745 1748 1751 1754 1757 1760 1763 1766 1769 1772 1775 1778 1781 1784 1787 1790 1793 1796 1799 1802 1805 1808 1811 1814 1817 1820 1823 1826 1829 1832 1835 1838 1841 1844 1847 1850 1853 1856 1859 1862 1865 1868 1871 1874 1877 1880 1883 1886 1889 1892 1895 1898 1901 1904 1907 1910 1913 1916 1919 1922 1925 1928 1931 1934 1937 1940 1943 1946 1949 1952 1955 1958 1961 1964 1967 1970 1973 1976 1979 1982 1985 1988 1991 1994 1997 2000 2003 2006 2009 2012 2015 2018 2021 2024 2027 2030 2033 2036 2039 2042 2045 2048 2051 2054 2057 2060 2063 2066 2069 2072 2075 2078 2081 2084 2087 2090 2093 2096 2099 2102 2105 2108 2111 2114 2117 2120 2123 2126 2129 2132 2135 2138 2141 2144 2147 2150 2153 2156 2159 2162 2165 2168 2171 2174 2177 2180 2183 2186 2189 2192 2195 2198 2201 2204 2207 2210 2213 2216 2219 2222 2225 2228 2231 2234 2237 2240 2243 2246 2249 2252 2255 2258 2261 2264 2267 2270 2273 2276 2279 2282 2285 2288 2291 2294 2297 2300 2303 2306 2309 2312 2315 2318 2321 2324 2327 2330 2333 2336 2339 2342 2345 2348 2351 2354 2357 2360 2363 2366 2369 2372 2375 2378 2381 2384 2387 2390 2393 2396 2399 2402 2405 2408 2411 2414 2417 2420 2423 2426 2429 2432 2435 2438 2441 2444 2447 2450 2453 2456 2459 2462 2465 2468 2471 2474 2477 2480 2483 2486 2489 2492 2495 2498 2501 2504 2507 2510 2513 2516 2519 2522 2525 2528 2531 2534 2537 2540 2543 2546 2549 2552 2555 2558 2561 2564 2567 2570 2573 2576 2579 2582 2585 2588 2591 2594 2597 2600 2603 2606 2609 2612 2615 2618 2621 2624 2627 2630 2633 2636 2639 2642 2645 2648 2651 2654 2657 2660 2663 2666 2669 2672 2675 2678 2681 2684 2687 2690 2693 2696 2699 2702 2705 2708 2711 2714 2717 2720 2723 2726 2729 2732 2735 2738 2741 2744 2747 2750 2753 2756 2759 2762 2765 2768 2771 2774 2777 2780 2783 2786 2789 2792 2795 2798 2801 2804 2807 2810 2813 2816 2819 2822 2825 2828 2831 2834 2837 2840 2843 2846 2849 2852 2855 2858 2861 2864 2867 2870 2873 2876 2879 2882 2885 2888 2891 2894 2897 2900 2903 2906 2909 2912 2915 2918 2921 2924 2927 2930 2933 2936 2939 2942 2945 2948 2951 2954 2957 2960 2963 2966 2969 2972 2975 2978 2981 2984 2987 2990 2993 2996 2999 3002 3005 3008 3011 3014 3017 3020 3023 3026 3029 3032 3035 3038 3041 3044 3047 3050 3053 3056 3059 3062 3065 3068 3071 3074 3077 3080 3083 3086 3089 3092 3095 3098 3101 3104 3107 3110 3113 3116 3119 3122 3125 3128 3131 3134 3137 3140 3143 3146 3149 3152 3155 3158 3161 3164 3167 3170 3173 3176 3179 3182 3185 3188 3191 3194 3197 3200 3203 3206 3209 3212 3215 3218 3221 3224 3227 3230 3233 3236 3239 3242 3245 3248 3251 3254 3257 3260 3263 3266 3269 3272 3275 3278 3281 3284 3287 3290 3293 3296 3299 3302 3305 3308 3311 3314 3317 3320 3323 3326 3329 3332 3335 3338 3341 3344 3347 3350 3353 3356 3359 3362 3365 3368 3371 3374 3377 3380 3383 3386 3389 3392 3395 3398 3401 3404 3407 3410 3413 3416 3419 3422 3425 3428 3431 3434 3437 3440 3443 3446 3449 3452 3455 3458 3461 3464 3467 3470 3473 3476 3479 3482 3485 3488 3491 3494 3497 3500 3503 3506 3509 3512 3515 3518 3521 3524 3527 3530 3533 3536 3539 3542 3545 3548 3551 3554 3557 3560 3563 3566 3569 3572 3575 3578 3581 3584 3587 3590 3593 3596 3599 3602 3605 3608 3611 3614 3617 3620 3623 3626 3629 3632 3635 3638 3641 3644 3647 3650 3653 3656 3659 3662 3665 3668 3671 3674 3677 3680 3683 3686 3689 3692 3695 3698 3701 3704 3707 3710 3713 3716 3719 3722 3725 3728 3731 3734 3737 3740 3743 3746 3749 3752 3755 3758 3761 3764 3767 3770 3773 3776 3779 3782 3785 3788 3791 3794 3797 3800 3803 3806 3809 3812 3815 3818 3821 3824 3827 3830 3833 3836 3839 3842 3845 3848 3851 3854 3857 3860 3863 3866 3869 3872 3875 3878 3881 3884 3887 3890 3893 3896 3899 3902 3905 3908 3911 3914 3917 3920 3923 3926 3929 3932 3935 3938 3941 3944 3947 3950 3953 3956 3959 3962 3965 3968 3971 3974 3977 3980 3983 3986 3989 3992 3995 3998 4001 4004 4007 4010 4013 4016 4019 4022 4025 4028 4031 4034 4037 4040 4043 4046 4049 4052 4055 4058 4061 4064 4067 4070 4073 4076 4079 4082 4085 4088 4091 4094 4097 4100 4103 4106 4109 4112 4115 4118 4121 4124 4127 4130 4133 4136 4139 4142 4145 4148 4151 4154 4157 4160 4163 4166 4169 4172 4175 4178 4181 4184 4187 4190 4193 4196 4199 4202 4205 4208 4211 4214 4217 4220 4223 4226 4229 4232 4235 4238 4241 4244 4247 4250 4253 4256 4259 4262 4265 4268 4271 4274 4277 4280 4283 4286 4289 4292 4295 4298 4301 4304 4307 4310 4313 4316 4319 4322 4325 4328 4331 4334 4337 4340 4343 4346 4349 4352 4355 4358 4361 4364 4367 4370 4373 4376 4379 4382 4385 4388 4391 4394 4397 4400 4403 4406 4409 4412 4415 4418 4421 4424 4427 4430 4433 4436 4439 4442 4445 4448 4451 4454 4457 4460 4463 4466 4469 4472 4475 4478 4481 4484 4487 4490 4493 4496 4499 4502 4505 4508 4511 4514 4517 4520 4523 4526 4529 4532 4535 4538 4541 4544 4547 4550 4553 4556 4559 4562 4565 4568 4571 4574 4577 4580 4583 4586 4589 4592 4595 4598 4601 4604 4607 4610 4613 4616 4619 4622 4625 4628 4631 4634 4637 4640 4643 4646 4649 4652 4655 4658 4661 4664 4667 4670 4673 4676 4679 4682 4685 4688 4691 4694 4697 4700 4703 4706 4709 4712 4715 4718 4721 4724 4727 4730 4733 4736 4739 4742 4745 4748 4751 4754 4757 4760 4763 4766 4769 4772 4775 4778 4781 4784 4787 4790 4793 4796 4799 4802 4805 4808 4811 4814 4817 4820 4823 4826 4829 4832 4835 4838 4841 4844 4847 4850 4853 4856 4859 4862 4865 4868 4871 4874 4877 4880 4883 4886 4889 4892 4895 4898 4901 4904 4907 4910 4913 4916 4919 4922 4925 4928 4931 4934 4937 4940 4943 4946 4949 4952 4955 4958 4961 4964 4967 4970 4973 4976 4979 4982 4985 4988 4991 4994 4997 5000 5003 5006 5009 5012 5015 5018 5021 5024 5027 5030 5033 5036 5039 5042 5045 5048 5051 5054 5057 5060 5063 5066 5069 5072 5075 5078 5081 5084 5087 5090 5093 5096 5099 5102 5105 5108 5111 5114 5117 5120 5123 5126 5129 5132 5135 5138 5141 5144 5147 5150 5153 5156 5159 5162 5165 5168 5171 5174 5177 5180 5183 5186 5189 5192 5195 5198 5201 5204 5207 5210 5213 5216 5219 5222 5225 5228 5231 5234 5237 5240 5243 5246 5249 5252 5255 5258 5261 5264 5267 5270 5273 5276 5279 5282 5285 5288 5291 5294 5297 5300 5303 5306 5309 5312 5315 5318 5321 5324 5327 5330 5333 5336 5339 5342 5345 5348 5351 5354 5357 5360 5363 5366 5369 5372 5375 5378 5381 5384 5387 5390 5393 5396 5399 5402 5405 5408 5411 5414 5417 5420 5423 5426 5429 5432 5435 5438 5441 5444 5447 5450 5453 5456 5459 5462 5465 5468 5471 5474 5477 5480 5483 5486 5489 5492 5495 5498 5501 5504 5507 5510 5513 5516 5519 5522 5525 5528 5531 5534 5537 5540 5543 5546 5549 5552 5555 5558 5561 5564 5567 5570 5573 5576 5579 5582 5585 5588 5591 5594 5597 5600 5603 5606 5609 5612 5615 5618 5621 5624 5627 5630 5633 5636 5639 5642 5645 5648 5651 5654 5657 5660 5663 5666 5669 5672 5675 5678 5681 5684 5687 5690 5693 5696 5699 5702 5705 5708 5711 5714 5717 5720 5723 5726 5729 5732 5735 5738 5741 5744 5747 5750 5753 5756 5759 5762 5765 5768 5771 5774 5777 5780 5783 5786 5789 5792 5795 5798 5801 5804 5807 5810 5813 5816 5819 5822 5825 5828 5831 5834 5837 5840 5843 5846 5849 5852 5855 5858 5861 5864 5867 5870 5873 5876 5879 5882 5885 5888 5891 5894 5897 5900 5903 5906 5909 5912 5915 5918 5921 5924 5927 5930 5933 5936 5939 5942 5945 5948 5951 5954 5957 5960 5963 5966 5969 5972 5975 5978 5981 5984 5987 5990 5993 5996 5999 6002 6005 6008 6011 6014 6017 6020 6023 6026 6029 6032 6035 6038 6041 6044 6047 6050 6053 6056 6059 6062 6065 6068 6071 6074 6077 6080 6083 6086 6089 6092 6095 6098 6101 6104 6107 6110 6113 6116 6119 6122 6125 6128 6131 6134 6137 6140 6143 6146 6149 6152 6155 6158 6161 6164 6167 6170 6173 6176 6179 6182 6185 6188 6191 6194 6197 6200 6203 6206 6209 6212 6215 6218 6221 6224 6227 6230 6233 6236 6239 6242 6245 6248 6251 6254 6257 6260 6263 6266 6269 6272 6275 6278 6281 6284 6287 6290 6293 6296 6299 6302 6305 6308 6311 6314 6317 6320 6323 6326 6329 6332 6335 6338 6341 6344 6347 6350 6353 6356 6359 6362 6365 6368 6371 6374 6377 6380 6383 6386 6389 6392 6395 6398 6401 6404 6407 6410 6413 6416 6419 6422 6425 6428 6431 6434 6437 6440 6443 6446 6449 6452 6455 6458 6461 6464 6467 6470 6473 6476 6479 6482 6485 6488 6491 6494 6497 6500 6503 6506 6509 6512 6515 6518 6521 6524 6527 6530 6533 6536 6539 6542 6545 6548 6551 6554 6557 6560 6563 6566 6569 6572 6575 6578 6581 6584 6587 6590 6593 6596 6599 6602 6605 6608 6611 6614 6617 6620 6623 6626 6629 6632 6635 6638 6641 6644 6647 6650 6653 6656 6659 6662 6665 6668 6671 6674 6677 6680 6683 6686 6689 6692 6695 6698 6701 6704 6707 6710 6713 6716 6719 6722 6725 6728 6731 6734 6737 6740 6743 6746 6749 6752 6755 6758 6761 6764 6767 6770 6773 6776 6779 6782 6785 6788 6791 6794 6797 6800 6803 6806 6809 6812 6815 6818 6821 6824 6827 6830 6833 6836 6839 6842 6845 6848 6851 6854 6857 6860 6863 6866 6869 6872 6875 6878 6881 6884 6887 6890 6893 6896 6899 6902 6905 6908 6911 6914 6917 6920 6923 6926 6929 6932 6935 6938 6941 6944 6947 6950 6953 6956 6959 6962 6965 6968 6971 6974 6977 6980 6983 6986 6989 6992 6995 6998 7001 7004 7007 7010 7013 7016 7019 7022 7025 7028 7031 7034 7037 7040 7043 7046 7049 7052 7055 7058 7061 7064 7067 7070 7073 7076 7079 7082 7085 7088 7091 7094 7097 7100 7103 7106 7109 7112 7115 7118 7121 7124 7127 7130 7133 7136 7139 7142 7145 7148 7151 7154 7157 7160 7163 7166 7169 7172 7175 7178 7181 7184 7187 7190 7193 7196 7199 7202 7205 7208 7211 7214 7217 7220 72

OCM=CUFF-OR(1).BETSYDATA

1	29	59	26	31	3	16.2	1	NEW ORLEANS MODICANT	-80	1
2	29	56	50	61	3	21.3	1	2NEW ORLEANS NAS	-79	
3	30	02	90	02	4	16.2	1	3NEW ORLEANS LAKEFRONT LAND	-78	
4	29	56	90	08	4	25.9	1	4NEW ORLEANS CITY OFFICE	-76	
5	30	02	90	02	1	11.1	1	5LAKE FRONT WATER (UPIN)	-74	
6	30	02	90	02	2	10.1	1	6LAKE FRONT LAKE	-72	
7	EOF								-70	
8	25	54	85	10	1		1		-68	
9	25	58	85	26	1		1		-64	
10	26	03	85	42	1		1		-61	
11	26	07	85	52	1		1		-58	1
12	21	12	86	14	1		1		-55	
13	26	17	85	30	1		1		-51	
14	26	22	86	45	1		1		-47	
15	26	30	86	58	1		1		-43	
16	16	36	87	11	1		1		-39	
17	26	46	87	24	1		1		-35	
18	26	54	87	37	1		1		-35	
19	27	02	87	50	1		1		-35	
20	27	10	84	03	1		1		-35	
21	27	21	84	14	1		1		-35	
22	27	32	84	25	1		1		-35	
23	27	43	88	36	1		1		-35	
24	27	55	84	46	1		1		-35	
25	26	07	84	56	1		1		-35	
26	28	20	89	06	1		1		-35	
27	28	31	89	22	1		1		-35	
28	26	42	89	38	1		1		-35	
29	28	55	89	54	1		1		-35	
30	29	09	90	04	1		1		-35	
31	29	23	90	21	1		1		-35	
32	29	37	90	34	1		2	.167	-35	
33	29	47	90	45	1		2	.234	-35	
34	29	56	90	55	1		2	.500	-35	
35	30	05	91	05	1		2	.667	-35	
36	30	14	91	15	1		2	.824	-35	
37	30	23	91	25	2		2		-35	
38	EOF									

TYGT

ADD.P COLPGM.NAME/IBETSY

SNAME =

KBASE = 98818754

ISTART = 65090901

IZONE = 874752341

ICVRT = 1

NPRT = 0

SEND

65R1 65090901CDT

ADD.P COLPGM.LAKLPONTGR11

```

*NAMEP =
DTM = -.260000001+01
PH = .650000001+03
LAKE = *S
L = *980600001+01
ZCOEFF = .000000001+00
      .000000001+00
      .100000001+00
      .000000001+00
      .350000001+03
      .300000001+03
      .350000001+00

```

```

.357000001+02
.400000001+01
.000000001+00
.000000001+00
.120000001+01
.150000001+01
.000000001+00
.000000001+00
.320000001+00
.000000001+00

```

1E6D

ADD.P COEFGH.BEISYDATA

```

29 59 90 15 3 16.2 1
29 50 90 01 5 21.3 2
30 02 90 02 4 16.2 3
29 56 90 08 6 25.9 4
30 02 90 02 1 16.1 5
30 02 90 02 2 10.1 6

```

STORM HISTORY 1ST HOUR 15 65090901 CDT

1	25	54	65	1	0	-0000	-60	1	1	65090901
2	25	54	65	1	0	-0000	-75	0	1	65090902
3	25	54	65	1	0	-0000	-75	0	1	65090903
4	26	7	85	54	1	-0000	-74	0	1	65090904
5	26	12	86	14	1	-0000	-74	0	1	65090905
6	26	17	86	31	1	-0000	-72	0	1	65090906
7	26	22	86	41	1	-0000	-70	0	1	65090907
8	26	30	86	56	1	-0000	-68	0	1	65090908
9	26	36	87	11	1	-0000	-66	0	1	65090909
10	26	46	87	24	1	-0000	-64	0	1	65090910
11	26	54	87	37	1	-0000	-61	0	1	65090911
12	27	10	88	50	1	-0000	-58	1	1	65090912
13	27	10	88	3	1	-0000	-55	0	1	65090913
14	27	21	88	14	1	-0000	-51	0	1	65090914
15	27	32	88	25	1	-0000	-47	0	1	65090915
16	27	43	88	36	1	-0000	-43	0	1	65090916
17	27	55	88	46	1	-0000	-39	0	1	65090917
18	28	7	88	56	1	-0000	-35	0	1	65090918
19	28	20	89	1	1	-0000	-35	0	1	65090919
20	28	31	89	22	1	-0000	-35	0	1	65090920
21	28	42	89	36	1	-0000	-35	0	1	65090921
22	28	55	89	54	1	-0000	-35	0	1	65090922
23	29	5	90	2	1	-0000	-35	0	1	65090923
24	29	23	90	21	1	-0000	-35	1	1	65091000
25	29	37	90	34	1	-1670	-35	0	2	65091001
26	29	47	90	45	1	-3340	-35	0	3	65091002
27	29	58	90	55	1	-5000	-35	1	4	65091003
28	30	5	91	1	1	-6670	-35	0	5	65091004
29	30	14	91	15	1	-8340	-35	0	6	65091005
30	30	23	91	25	1	-0000	-35	1	7	65091006

Sample listings of time history of
surface wind field at individual stations

65B1 Storm identification
65091001 Year, month, day, hour
W1 Wind speed in knots
TH1 Wind direction (meteorological) in degrees
D Distance of station from eye of hurricane (km)
AL Bearing of station from eye (degrees)
UST Friction velocity (cm/sec)
STA Station number, latitude (deg, min) longitude (deg, min)
EYE Eye latitude and longitude (deg, min)
TERR Terrain roughness category
H Anemometer height at station

6561	65090901	WJ= 21.81 THJ= 40.4 D= 678.5 AL=313.4 UST= 75.27 STA	1= 29 59 90 15	EYE= 25 54	15 10	TEAR=3 HT= 16.2	1 1
6561	65090902	WJ= 22.30 THJ= 46.1 DF 650.0 AL=314.5 UST= 66.89 STA	1= 29 59 90 15	EYE= 25 58	15 26	TEAR=3 HT= 16.2	1 1
6561	65090903	WJ= 22.87 THJ= 39.4 D= 674.1 AL=315.4 UST= 66.57 STA	1= 29 59 90 15	EYE= 26 03	15 42	TEAR=3 HT= 16.2	2 1
6561	65090904	WJ= 23.37 THJ= 40.1 D= 680.1 AL=316.4 UST= 66.57 STA	1= 29 59 90 15	EYE= 26 07	15 52	TEAR=3 HT= 16.2	2 1
6561	65090905	WJ= 23.76 THJ= 40.2 D= 675.7 AL=317.4 UST= 70.51 STA	1= 29 59 90 15	EYE= 26 12	16 14	TEAR=3 HT= 16.2	4 1
6561	65090906	WJ= 24.42 THJ= 40.3 D= 681.3 AL=318.4 UST= 73.24 STA	1= 29 59 90 15	EYE= 26 17	16 20	TEAR=3 HT= 16.2	5 1
6561	65090907	WJ= 25.06 THJ= 40.5 D= 676.5 AL=320.2 UST= 75.11 STA	1= 29 59 90 15	EYE= 26 22	16 45	TEAR=3 HT= 16.2	6 1
6561	65090908	WJ= 25.76 THJ= 40.2 D= 683.1 AL=321.1 UST= 77.33 STA	1= 29 59 90 15	EYE= 26 30	16 58	TEAR=3 HT= 16.2	7 1
6561	65090909	WJ= 26.45 THJ= 39.8 D= 676.0 AL=321.8 UST= 79.32 STA	1= 29 59 90 15	EYE= 26 38	17 11	TEAR=3 HT= 16.2	8 1
6561	65090910	WJ= 27.17 THJ= 39.3 D= 653.2 AL=322.7 UST= 81.49 STA	1= 29 59 90 15	EYE= 26 46	17 24	TEAR=3 HT= 16.2	9 1
6561	65090911	WJ= 28.04 THJ= 39.4 D= 628.6 AL=324.2 UST= 86.10 STA	1= 29 59 90 15	EYE= 26 54	17 37	TEAR=3 HT= 16.2	10 1
6561	65090912	WJ= 29.05 THJ= 39.5 D= 603.5 AL=324.8 UST= 87.11 STA	1= 29 59 90 15	EYE= 27 02	17 50	TEAR=3 HT= 16.2	11 1
6561	65090913	WJ= 30.08 THJ= 39.5 D= 579.5 AL=326.1 UST= 90.20 STA	1= 29 59 90 15	EYE= 27 10	18 03	TEAR=3 HT= 16.2	12 1
6561	65090914	WJ= 31.27 THJ= 39.0 D= 552.5 AL=326.6 UST= 92.79 STA	1= 29 59 90 15	EYE= 27 21	18 14	TEAR=3 HT= 16.2	13 1
6561	65090915	WJ= 32.71 THJ= 38.5 D= 525.6 AL=327.2 UST= 98.09 STA	1= 29 59 90 15	EYE= 27 32	18 25	TEAR=3 HT= 16.2	14 1
6561	65090916	WJ= 34.21 THJ= 37.8 D= 296.7 AL=327.9 UST=102.61 STA	1= 29 59 90 15	EYE= 27 43	18 36	TEAR=3 HT= 16.2	15 1
6561	65090917	WJ= 36.07 THJ= 36.6 D= 271.2 AL=328.2 UST=102.61 STA	1= 29 59 90 15	EYE= 27 55	18 46	TEAR=3 HT= 16.2	16 1
6561	65090918	WJ= 38.15 THJ= 35.7 D= 245.7 AL=328.7 UST=104.16 STA	1= 29 59 90 15	EYE= 28 07	18 56	TEAR=3 HT= 16.2	17 1
6561	65090919	WJ= 41.28 THJ= 35.5 D= 214.6 AL=329.0 UST=123.80 STA	1= 29 59 90 15	EYE= 28 20	19 06	TEAR=3 HT= 16.2	18 1
6561	65090920	WJ= 45.92 THJ= 34.2 D= 184.1 AL=332.5 UST=137.72 STA	1= 29 59 90 15	EYE= 28 31	19 16	TEAR=3 HT= 16.2	19 1
6561	65090921	WJ= 51.60 THJ= 36.7 D= 154.6 AL=337.4 UST=154.75 STA	1= 29 59 90 15	EYE= 28 42	19 26	TEAR=3 HT= 16.2	20 1
6561	65090922	WJ= 58.91 THJ= 41.2 D= 123.3 AL=344.1 UST=176.66 STA	1= 29 59 90 15	EYE= 28 55	19 36	TEAR=3 HT= 16.2	21 1
6561	65090923	WJ= 77.75 THJ= 49.1 D= 53.2 AL=353.1 UST=203.17 STA	1= 29 59 90 15	EYE= 29 09	19 46	TEAR=3 HT= 16.2	22 1
6561	65091001	WJ= 75.56 THJ= 46.6 D= 67.4 AL= 8.2 UST=226.66 STA	1= 29 59 90 15	EYE= 29 23	19 56	TEAR=3 HT= 16.2	23 1
6561	65091002	WJ= 72.44 THJ=101.6 D= 50.9 AL= 36.8 UST=217.37 STA	1= 29 59 90 15	EYE= 29 37	20 06	TEAR=3 HT= 16.2	24 1
6561	65091003	WJ= 67.66 THJ=127.4 D= 53.1 AL= 65.1 UST=202.97 STA	1= 29 59 90 15	EYE= 29 47	20 16	TEAR=3 HT= 16.2	25 1
6561	65091004	WJ= 62.80 THJ=143.2 D= 64.4 AL= 84.9 UST=188.32 STA	1= 29 59 90 15	EYE= 29 50	20 26	TEAR=3 HT= 16.2	26 1
6561	65091005	WJ= 57.86 THJ=152.4 D= 40.9 AL= 97.7 UST=173.53 STA	1= 29 59 90 15	EYE= 30 05	20 36	TEAR=3 HT= 16.2	27 1
6561	65091006	WJ= 52.66 THJ=157.2 D= 100.1 AL=105.5 UST=157.91 STA	1= 29 59 90 15	EYE= 30 16	20 46	TEAR=3 HT= 16.2	28 1
6561	65091007	WJ= 47.42 THJ=159.8 D= 120.1 AL=111.3 UST=142.22 STA	1= 29 59 90 15	EYE= 30 23	20 56	TEAR=3 HT= 16.2	29 1

6501	65090901	W1= 23.42	TH1= 39.0	D= 646.4	AL=313.6	UST= 67.17	STA	2= 29 50	90 01	EYE= 25 54	45 10	TERR=3	HT= 21.3	1 1
6501	65090902	W1= 23.59	TH1= 36.8	D= 622.1	AL=314.7	UST= 66.81	STA	2= 29 50	90 01	EYE= 25 58	65 26	TERR=3	HT= 21.3	2 1
6501	65090903	W1= 24.62	TH1= 38.4	D= 596.4	AL=315.9	UST= 70.62	STA	2= 29 50	90 01	EYE= 26 03	65 42	TERR=3	HT= 21.3	3 1
6501	65090904	W1= 25.15	TH1= 36.7	D= 573.1	AL=317.0	UST= 72.13	STA	2= 29 50	90 01	EYE= 26 07	85 58	TERR=3	HT= 21.3	4 1
6501	65090905	W1= 25.77	TH1= 36.2	D= 548.3	AL=318.5	UST= 73.52	STA	2= 29 50	90 01	EYE= 26 12	16 14	TERR=3	HT= 21.3	5 1
6501	65090906	W1= 26.47	TH1= 38.9	D= 523.5	AL=319.7	UST= 75.93	STA	2= 29 50	90 01	EYE= 26 17	66 30	TERR=3	HT= 21.3	6 1
6501	65090907	W1= 27.15	TH1= 39.1	D= 500.5	AL=321.0	UST= 76.00	STA	2= 29 50	90 01	EYE= 26 22	66 45	TERR=3	HT= 21.3	7 1
6501	65090908	W1= 27.59	TH1= 36.8	D= 475.6	AL=321.6	UST= 80.27	STA	2= 29 50	90 01	EYE= 26 30	86 58	TERR=3	HT= 21.3	8 1
6501	65090909	W1= 28.75	TH1= 38.4	D= 450.9	AL=322.7	UST= 82.45	STA	2= 29 50	90 01	EYE= 26 38	87 11	TERR=3	HT= 21.3	9 1
6501	65090910	W1= 29.81	TH1= 38.2	D= 426.2	AL=323.7	UST= 85.45	STA	2= 29 50	90 01	EYE= 26 46	87 24	TERR=3	HT= 21.3	10 1
6501	65090911	W1= 20.75	TH1= 38.2	D= 401.2	AL=324.4	UST= 81.32	STA	2= 29 50	90 01	EYE= 26 54	67 27	TERR=3	HT= 21.3	11 1
6501	65090912	W1= 31.56	TH1= 38.4	D= 377.2	AL=326.1	UST= 91.64	STA	2= 29 50	90 01	EYE= 27 02	87 50	TERR=3	HT= 21.3	12 1
6501	65090913	W1= 33.26	TH1= 38.6	D= 353.1	AL=327.5	UST= 95.23	STA	2= 29 50	90 01	EYE= 27 10	88 63	TERR=3	HT= 21.3	13 1
6501	65090914	W1= 34.66	TH1= 36.2	D= 328.2	AL=328.2	UST= 99.41	STA	2= 29 50	90 01	EYE= 27 21	88 14	TERR=3	HT= 21.3	14 1
6501	65090915	W1= 36.41	TH1= 37.7	D= 299.4	AL=329.0	UST=104.44	STA	2= 29 50	90 01	EYE= 27 32	88 25	TERR=3	HT= 21.3	15 1
6501	65090916	W1= 38.25	TH1= 37.2	D= 272.7	AL=329.9	UST=109.71	STA	2= 29 50	90 01	EYE= 27 43	88 36	TERR=3	HT= 21.3	16 1
6501	65090917	W1= 40.57	TH1= 36.4	D= 245.3	AL=330.6	UST=116.35	STA	2= 29 50	90 01	EYE= 27 55	88 46	TERR=3	HT= 21.3	17 1
6501	65090918	W1= 43.11	TH1= 35.7	D= 217.5	AL=331.4	UST=123.64	STA	2= 29 50	90 01	EYE= 28 07	88 56	TERR=3	HT= 21.3	18 1
6501	65090919	W1= 47.16	TH1= 34.2	D= 169.0	AL=332.1	UST=125.32	STA	2= 29 50	90 01	EYE= 28 20	89 06	TERR=3	HT= 21.3	19 1
6501	65090920	W1= 52.56	TH1= 36.4	D= 159.3	AL=333.4	UST=131.50	STA	2= 29 50	90 01	EYE= 28 31	89 22	TERR=3	HT= 21.3	20 1
6501	65090921	W1= 59.65	TH1= 40.9	D= 131.3	AL=333.7	UST=138.10	STA	2= 29 50	90 01	EYE= 28 42	89 38	TERR=3	HT= 21.3	21 1
6501	65090922	W1= 68.24	TH1= 49.4	D= 102.5	AL=353.7	UST=155.73	STA	2= 29 50	90 01	EYE= 28 55	89 54	TERR=3	HT= 21.3	22 1
6501	65090923	W1= 76.66	TH1= 64.4	D= 76.6	AL= 8.4	UST=215.52	STA	2= 29 50	90 01	EYE= 29 09	90 02	TERR=3	HT= 21.3	23 1
6501	65091000	W1= 75.72	TH1= 52.7	D= 59.2	AL= 32.7	UST=228.66	STA	2= 29 50	90 01	EYE= 29 23	90 21	TERR=3	HT= 21.3	24 1
6501	65091001	W1= 73.38	TH1=125.6	D= 56.3	AL= 65.5	UST=210.47	STA	2= 29 50	90 01	EYE= 25 37	90 34	TERR=3	HT= 21.3	25 2
6501	65091002	W1= 67.46	TH1=141.9	D= 70.9	AL= 85.3	UST=193.32	STA	2= 29 50	90 01	EYE= 29 47	90 45	TERR=3	HT= 21.3	26 3
6501	65091003	W1= 61.67	TH1=150.7	D= 87.4	AL= 97.1	UST=176.88	STA	2= 29 50	90 01	EYE= 29 56	90 55	TERR=3	HT= 21.3	27 4
6501	65091004	W1= 56.68	TH1=155.4	D= 106.4	AL=104.9	UST=160.85	STA	2= 29 50	90 01	EYE= 30 05	91 05	TERR=3	HT= 21.3	28 5
6501	65091005	W1= 50.52	TH1=158.2	D= 126.7	AL=110.2	UST=144.91	STA	2= 29 50	90 01	EYE= 30 14	91 15	TERR=3	HT= 21.3	29 6
6501	65091006	W1= 45.77	TH1=160.6	D= 147.8	AL=114.1	UST=131.25	STA	2= 29 50	90 01	EYE= 30 23	91 25	TERR=3	HT= 21.3	30 7

65090001	VI= 20.37	THI= 37.4	DE= 62.1	AL=315.0	UST= 74.4	STA= 3= 30 02	90 02	EYE= 25.54	AS 10	TERR=4	HT= 16.2	1 1
65090002	VI= 20.62	THI= 37.2	DE= 63.2	AL=116.1	UST= 70.45	STA= 3= 30 02	90 02	EYE= 25.58	AS 26	TERR=4	HT= 16.2	2 1
65090003	VI= 21.14	THI= 36.4	DE= 61.3	AL=217.2	UST= 82.43	STA= 3= 30 02	90 02	EYE= 26.03	AS 42	TERR=4	HT= 16.2	3 1
65090004	VI= 21.59	THI= 37.2	DE= 59.0	AL=318.4	UST= 74.20	STA= 3= 30 02	90 02	EYE= 26.07	AS 58	TERR=4	HT= 16.2	4 1
65090005	VI= 22.12	THI= 37.5	DE= 60.7	AL=219.7	UST= 76.27	STA= 3= 30 02	90 02	EYE= 26.17	AS 14	TERR=4	HT= 16.2	5 1
65090006	VI= 22.17	THI= 37.7	DE= 59.1	AL=321.1	UST= 78.34	STA= 3= 30 02	90 02	EYE= 26.17	AS 30	TERR=4	HT= 16.2	6 1
65090007	VI= 23.13	THI= 36.6	DE= 61.9	AL=325.5	UST= 70.56	STA= 3= 30 02	90 02	EYE= 26.22	AS 45	TERR=4	HT= 16.2	7 1
65090008	VI= 23.17	THI= 37.7	DE= 65.1	AL=323.3	UST= 93.07	STA= 3= 30 02	90 02	EYE= 26.30	AS 58	TERR=4	HT= 16.2	8 1
65090009	VI= 24.56	THI= 37.5	DE= 65.1	AL=324.2	UST= 95.74	STA= 3= 30 02	90 02	EYE= 26.38	AS 11	TERR=4	HT= 16.2	9 1
65090010	VI= 25.30	THI= 37.3	DE= 64.5	AL=325.2	UST= 96.66	STA= 3= 30 02	90 02	EYE= 26.46	AS 24	TERR=4	HT= 16.2	10 1
65090011	VI= 26.12	THI= 37.2	DE= 62.1	AL=326.4	UST= 101.94	STA= 3= 30 02	90 02	EYE= 26.54	AS 37	TERR=4	HT= 16.2	11 1
65090012	VI= 27.06	THI= 37.4	DE= 59.1	AL=327.7	UST= 105.24	STA= 3= 30 02	90 02	EYE= 27.02	AS 50	TERR=4	HT= 16.2	12 1
65090013	VI= 28.13	THI= 38.1	DE= 37.2	AL=329.2	UST= 109.25	STA= 3= 30 02	90 02	EYE= 27.10	AS 63	TERR=4	HT= 16.2	13 1
65090014	VI= 28.44	THI= 37.5	DE= 61.3	AL=330.0	UST= 114.69	STA= 3= 30 02	90 02	EYE= 27.21	AS 14	TERR=4	HT= 16.2	14 1
65090015	VI= 31.91	THI= 37.2	DE= 29.1	AL=331.9	UST= 124.64	STA= 3= 30 02	90 02	EYE= 27.32	AS 25	TERR=4	HT= 16.2	15 1
65090016	VI= 25.71	THI= 37.6	DE= 26.5	AL=332.7	UST= 131.45	STA= 3= 30 02	90 02	EYE= 27.43	AS 36	TERR=4	HT= 16.2	16 1
65090017	VI= 25.76	THI= 36.0	DE= 28.1	AL=333.6	UST= 139.52	STA= 3= 30 02	90 02	EYE= 27.55	AS 46	TERR=4	HT= 16.2	17 1
65090018	VI= 34.14	THI= 36.5	DE= 20.1	AL=334.6	UST= 151.44	STA= 3= 30 02	90 02	EYE= 27.67	AS 56	TERR=4	HT= 16.2	18 1
65090019	VI= 43.13	THI= 39.5	DE= 180.1	AL=339.2	UST= 168.15	STA= 3= 30 02	90 02	EYE= 28.31	AS 66	TERR=4	HT= 16.2	19 1
65090020	VI= 48.12	THI= 39.9	DE= 153.1	AL=345.4	UST= 187.42	STA= 3= 30 02	90 02	EYE= 28.42	AS 78	TERR=4	HT= 16.2	20 1
65090021	VI= 54.25	THI= 46.1	DE= 124.8	AL=354.1	UST= 211.54	STA= 3= 30 02	90 02	EYE= 28.55	AS 84	TERR=4	HT= 16.2	21 1
65090022	VI= 61.12	THI= 52.0	DE= 58.2	AL=356.6	UST= 236.44	STA= 3= 30 02	90 02	EYE= 29.09	AS 94	TERR=4	HT= 16.2	22 1
65090023	VI= 65.50	THI= 73.6	DE= 78.4	AL=357.9	UST= 260.07	STA= 3= 30 02	90 02	EYE= 29.29	AS 101	TERR=4	HT= 16.2	23 1
65090024	VI= 65.30	THI= 101.7	DE= 69.2	AL=358.2	UST= 285.64	STA= 3= 30 02	90 02	EYE= 29.37	AS 104	TERR=4	HT= 16.2	24 1
65090025	VI= 60.87	THI= 121.0	DE= 74.4	AL=359.6	UST= 311.64	STA= 3= 30 02	90 02	EYE= 29.47	AS 105	TERR=4	HT= 16.2	25 1
65090026	VI= 56.31	THI= 135.3	DE= 85.7	AL=361.2	UST= 339.56	STA= 3= 30 02	90 02	EYE= 29.56	AS 105	TERR=4	HT= 16.2	26 1
65090027	VI= 51.32	THI= 141.2	DE= 101.1	AL=362.9	UST= 370.12	STA= 3= 30 02	90 02	EYE= 30.05	AS 105	TERR=4	HT= 16.2	27 1
65090028	VI= 46.25	THI= 146.5	DE= 119.1	AL=365.5	UST= 406.51	STA= 3= 30 02	90 02	EYE= 30.14	AS 105	TERR=4	HT= 16.2	28 1
65090029	VI= 41.64	THI= 149.9	DE= 138.4	AL=368.0	UST= 445.53	STA= 3= 30 02	90 02	EYE= 30.23	AS 105	TERR=4	HT= 16.2	29 1
65090030	VI= 36.62	THI= 152.7	DE= 158.4	AL=370.5	UST= 487.06	STA= 3= 30 02	90 02	EYE= 30.32	AS 105	TERR=4	HT= 16.2	30 1

65E1	65090901	W1= 17.78	TH1= 26.8	D= 662.2	AL=213.7	UST=104.43	STA	4= 29 56	90 00	EYL= 25 54	85 10	TEAR=6	HT= 25.9	1 1
65B1	65090902	W1= 18.20	TH1= 26.5	D= 637.9	AL=314.8	UST=104.97	STA	4= 29 56	90 00	EYL= 25 50	85 26	TEAR=6	HT= 25.9	2 1
65B1	65090903	W1= 18.27	TH1= 26.2	D= 612.4	AL=315.8	UST=111.74	STA	4= 29 56	90 00	EYL= 26 03	85 42	TEAR=6	HT= 25.9	3 1
65B1	65090904	W1= 19.09	TH1= 28.5	D= 588.9	AL=317.0	UST=114.28	STA	4= 29 56	90 00	EYL= 26 07	85 58	TEAR=6	HT= 25.9	4 1
65B1	65090905	W1= 19.45	TH1= 28.6	D= 564.1	AL=318.2	UST=116.45	STA	4= 29 56	90 00	EYL= 26 12	86 14	TEAR=6	HT= 25.9	5 1
65B1	65090906	W1= 20.00	TH1= 26.7	D= 539.7	AL=319.6	UST=119.73	STA	4= 29 56	90 00	EYL= 26 17	86 30	TEAR=6	HT= 25.9	6 1
65B1	65090907	W1= 20.52	TH1= 26.9	D= 516.4	AL=320.9	UST=122.88	STA	4= 29 56	90 00	EYL= 26 22	86 45	TEAR=6	HT= 25.9	7 1
65B1	65090908	W1= 21.13	TH1= 28.7	D= 491.4	AL=321.4	UST=124.50	STA	4= 29 56	90 00	EYL= 26 30	86 58	TEAR=6	HT= 25.9	8 1
65B1	65090909	W1= 21.67	TH1= 28.2	D= 466.4	AL=322.5	UST=125.73	STA	4= 29 56	90 00	EYL= 26 38	87 11	TEAR=6	HT= 25.9	9 1
65B1	65090910	W1= 22.34	TH1= 27.9	D= 441.9	AL=323.4	UST=133.75	STA	4= 29 56	90 00	EYL= 26 46	87 24	TEAR=6	HT= 25.9	10 1
65B1	65090911	W1= 23.69	TH1= 28.0	D= 417.2	AL=324.5	UST=138.24	STA	4= 29 56	90 00	EYL= 26 54	87 37	TEAR=6	HT= 25.9	11 1
65B1	65090912	W1= 23.91	TH1= 28.1	D= 392.8	AL=325.7	UST=143.14	STA	4= 29 56	90 00	EYL= 27 02	87 50	TEAR=6	HT= 25.9	12 1
65B1	65090913	W1= 24.47	TH1= 28.3	D= 368.1	AL=327.0	UST=148.58	STA	4= 29 56	90 00	EYL= 27 10	88 02	TEAR=6	HT= 25.9	13 1
65B1	65090914	W1= 25.21	TH1= 27.8	D= 341.7	AL=327.6	UST=154.55	STA	4= 29 56	90 00	EYL= 27 21	88 14	TEAR=6	HT= 25.9	14 1
65B1	65090915	W1= 27.04	TH1= 27.3	D= 314.8	AL=328.3	UST=162.10	STA	4= 29 56	90 00	EYL= 27 32	88 25	TEAR=6	HT= 25.9	15 1
65B1	65090916	W1= 28.32	TH1= 26.8	D= 288.0	AL=329.1	UST=169.55	STA	4= 29 56	90 00	EYL= 27 43	88 36	TEAR=6	HT= 25.9	16 1
65B1	65090917	W1= 29.04	TH1= 25.9	D= 260.5	AL=329.7	UST=179.24	STA	4= 29 56	90 00	EYL= 27 55	88 46	TEAR=6	HT= 25.9	17 1
65B1	65090918	W1= 31.71	TH1= 25.0	D= 233.1	AL=330.3	UST=189.87	STA	4= 29 56	90 00	EYL= 28 07	88 56	TEAR=6	HT= 25.9	18 1
65B1	65090919	W1= 34.46	TH1= 23.0	D= 204.1	AL=330.8	UST=205.94	STA	4= 29 56	90 00	EYL= 28 20	89 06	TEAR=6	HT= 25.9	19 1
65B1	65090920	W1= 38.26	TH1= 24.5	D= 174.1	AL=334.9	UST=230.86	STA	4= 29 56	90 00	EYL= 28 31	89 22	TEAR=6	HT= 25.9	20 1
65B1	65090921	W1= 43.34	TH1= 27.8	D= 145.4	AL=340.7	UST=259.59	STA	4= 29 56	90 00	EYL= 28 42	89 38	TEAR=6	HT= 25.9	21 1
65B1	65090922	W1= 49.26	TH1= 33.7	D= 115.2	AL=348.8	UST=294.92	STA	4= 29 56	90 00	EYL= 28 55	89 54	TEAR=6	HT= 25.9	22 1
65B1	65090923	W1= 56.52	TH1= 44.4	D= 87.1	AL=	UST=336.39	STA	4= 29 56	90 00	EYL= 29 09	90 08	TEAR=6	HT= 25.9	23 1
65B1	65091000	W1= 61.45	TH1= 66.3	D= 64.4	AL= 16.4	UST=347.91	STA	4= 29 56	90 00	EYL= 29 23	90 21	TEAR=6	HT= 25.9	24 1
65B1	65091001	W1= 67.19	TH1=101.0	D= 54.6	AL= 49.8	UST=345.41	STA	4= 29 56	90 00	EYL= 29 37	90 34	TEAR=6	HT= 25.9	25 2
65B1	65091002	W1= 53.86	TH1=122.3	D= 61.7	AL= 74.2	UST=322.46	STA	4= 29 56	90 00	EYL= 29 47	90 45	TEAR=6	HT= 25.9	26 3
65B1	65091003	W1= 49.57	TH1=134.6	D= 75.4	AL= 89.8	UST=296.49	STA	4= 29 56	90 00	EYL= 29 56	90 55	TEAR=6	HT= 25.9	27 4
65B1	65091004	W1= 45.22	TH1=141.7	D= 92.5	AL=100.1	UST=270.76	STA	4= 29 56	90 00	EYL= 30 05	91 05	TEAR=6	HT= 25.9	28 5
65B1	65091005	W1= 40.94	TH1=145.5	D= 112.4	AL=107.0	UST=244.35	STA	4= 29 56	90 00	EYL= 30 14	91 15	TEAR=6	HT= 25.9	29 6
65B1	65091006	W1= 36.87	TH1=147.8	D= 133.1	AL=111.8	UST=221.02	STA	4= 29 56	90 00	EYL= 30 23	91 25	TEAR=6	HT= 25.9	30 7

6581	65090901	41	26.44	THI	48.1	DE	642.1	AL=315.0	US1=	51.27	STA	5= 30 07	90 02	EYE= 25 54	62 11	TEAR=1	HT= 10.1	1 1
6581	65090902	41	26.91	THI	48.2	DE	638.2	AL=316.1	US1=	52.44	STA	5= 30 02	90 02	EYE= 25 58	85 26	TEAR=1	HT= 10.1	2 1
6581	65090903	41	27.43	THI	47.7	DE	633.3	AL=317.2	US1=	53.74	STA	5= 30 02	90 02	EYE= 26 03	85 42	TEAR=1	HT= 10.1	3 1
6581	65090904	41	27.89	THI	48.0	DE	630.1	AL=318.4	US1=	54.05	STA	5= 30 02	90 02	EYE= 26 07	85 58	TEAR=1	HT= 10.1	4 1
6581	65090905	41	28.42	THI	48.1	DE	625.7	AL=319.7	US1=	54.27	STA	5= 31 02	90 02	EYE= 26 12	86 14	TEAR=1	HT= 10.1	5 1
6581	65090906	41	28.95	THI	48.1	DE	621.0	AL=321.1	US1=	54.64	STA	5= 30 02	90 02	EYE= 26 17	86 26	TEAR=1	HT= 10.1	6 1
6581	65090907	41	29.57	THI	48.1	DE	619.1	AL=322.5	US1=	55.17	STA	5= 30 02	90 02	EYE= 26 22	86 45	TEAR=1	HT= 10.1	7 1
6581	65090908	41	30.23	THI	47.7	DE	614.1	AL=323.3	US1=	60.42	STA	5= 30 02	90 02	EYE= 26 30	86 54	TEAR=1	HT= 10.1	8 1
6581	65090909	41	30.55	THI	47.3	DE	609.5	AL=324.2	US1=	62.77	STA	5= 30 02	90 02	EYE= 26 34	87 11	TEAR=1	HT= 10.1	9 1
6581	65090910	41	31.72	THI	46.9	DE	605.0	AL=325.3	US1=	64.74	STA	5= 30 02	90 02	EYE= 26 46	87 24	TEAR=1	HT= 10.1	10 1
6581	65090911	41	32.57	THI	46.4	DE	620.6	AL=326.4	US1=	67.05	STA	5= 30 02	90 02	EYE= 26 54	87 37	TEAR=1	HT= 10.1	11 1
6581	65090912	41	33.49	THI	47.0	DE	396.1	AL=327.7	US1=	69.52	STA	5= 30 02	90 02	EYE= 27 02	87 50	TEAR=1	HT= 10.1	12 1
6581	65090913	41	34.57	THI	47.1	DE	372.7	AL=329.2	US1=	72.43	STA	5= 30 02	90 02	EYE= 27 10	88 03	TEAR=1	HT= 10.1	13 1
6581	65090914	41	35.73	THI	46.6	DE	345.9	AL=330.0	US1=	75.67	STA	5= 30 02	90 02	EYE= 27 21	88 14	TEAR=1	HT= 10.1	14 1
6581	65090915	41	38.69	THI	45.5	DE	292.4	AL=331.9	US1=	83.95	STA	5= 30 02	90 02	EYE= 27 32	88 25	TEAR=1	HT= 10.1	15 1
6581	65090916	41	42.51	THI	44.6	DE	265.5	AL=333.7	US1=	89.17	STA	5= 30 02	90 02	EYE= 27 43	88 36	TEAR=1	HT= 10.1	16 1
6581	65090917	41	42.65	THI	43.4	DE	238.1	AL=333.6	US1=	95.50	STA	5= 30 02	90 02	EYE= 28 07	88 46	TEAR=1	HT= 10.1	17 1
6581	65090918	41	45.41	THI	43.9	DE	209.5	AL=334.6	US1=	102.05	STA	5= 30 02	90 02	EYE= 28 20	89 00	TEAR=1	HT= 10.1	18 1
6581	65090919	41	50.20	THI	43.2	DE	180.5	AL=335.4	US1=	118.91	STA	5= 30 02	90 02	EYE= 28 31	89 11	TEAR=1	HT= 10.1	19 1
6581	65090920	41	55.14	THI	46.4	DE	153.1	AL=335.4	US1=	135.35	STA	5= 30 02	90 02	EYE= 28 42	89 24	TEAR=1	HT= 10.1	20 1
6581	65090921	41	61.26	THI	52.1	DE	124.4	AL=336.1	US1=	161.72	STA	5= 30 02	90 02	EYE= 28 55	89 34	TEAR=1	HT= 10.1	21 1
6581	65090922	41	68.11	THI	61.5	DE	98.6	AL=	5.0	US1=181.50	STA	5= 30 02	90 02	EYE= 29 09	89 48	TEAR=1	HT= 10.1	22 1
6581	65090923	41	73.61	THI	74.6	DE	76.4	AL=	22.9	US1=202.90	STA	5= 30 02	90 02	EYE= 29 23	90 01	TEAR=1	HT= 10.1	23 1
6581	65090924	41	72.04	THI	107.0	DE	69.2	AL=	47.9	US1=196.69	STA	5= 30 02	90 02	EYE= 29 37	90 31	TEAR=1	HT= 10.1	24 1
6581	65091001	41	67.92	THI	126.6	DE	74.4	AL=	67.9	US1=180.49	STA	5= 30 02	90 02	EYE= 29 47	90 45	TEAR=1	HT= 10.1	25 1
6581	65091002	41	63.34	THI	139.2	DE	85.7	AL=	82.3	US1=164.01	STA	5= 30 02	90 02	EYE= 29 56	90 55	TEAR=1	HT= 10.1	26 1
6581	65091003	41	58.45	THI	147.5	DE	101.1	AL=	92.9	US1=146.50	STA	5= 30 02	90 02	EYE= 30 05	91 05	TEAR=1	HT= 10.1	27 1
6581	65091004	41	53.41	THI	153.1	DE	119.0	AL=	100.5	US1=125.38	STA	5= 30 02	90 02	EYE= 30 14	91 15	TEAR=1	HT= 10.1	28 1
6581	65091005	41	48.72	THI	157.0	DE	139.4	AL=	106.0	US1=116.18	STA	5= 30 02	90 02	EYE= 30 23	91 25	TEAR=1	HT= 10.1	29 1
6581	65091006	41	48.72	THI	157.0	DE	139.4	AL=	106.0	US1=116.18	STA	5= 30 02	90 02	EYE= 30 23	91 25	TEAR=1	HT= 10.1	30 1

65B1	65090901	W1=	21.56	TH1=	42.0	D=	662.5	AL=	315.0	UST=	60.45	STA	6=	30	02	90	02	EYE=	25	54	PS	10	TERR=2	HT=	10.1	1	1
65B1	65090902	W1=	22.07	TH1=	41.8	D=	638.5	AL=	316.1	UST=	61.86	STA	6=	30	02	90	02	EYE=	25	56	PS	26	TERR=2	HT=	10.1	2	1
65B1	65090903	W1=	22.61	TH1=	41.5	D=	613.5	AL=	317.2	UST=	63.41	STA	6=	30	02	90	02	EYE=	26	03	PS	42	TERR=2	HT=	10.1	3	1
65B1	65090904	W1=	23.05	TH1=	41.4	D=	590.1	AL=	318.4	UST=	64.80	STA	6=	30	02	90	02	EYE=	26	07	PS	58	TERR=2	HT=	10.1	4	1
65B1	65090905	W1=	23.65	TH1=	42.1	D=	565.7	AL=	319.7	UST=	66.42	STA	6=	30	02	90	02	EYE=	26	12	PS	14	TERR=2	HT=	10.1	5	1
65B1	65090906	W1=	24.23	TH1=	42.3	D=	541.1	AL=	321.1	UST=	68.08	STA	6=	30	02	90	02	EYE=	26	17	PS	30	TERR=2	HT=	10.1	6	1
65B1	65090907	W1=	24.82	TH1=	42.0	D=	519.0	AL=	322.5	UST=	69.80	STA	6=	30	02	90	02	EYE=	26	22	PS	45	TERR=2	HT=	10.1	7	1
65B1	65090908	W1=	25.50	TH1=	42.3	D=	494.1	AL=	323.3	UST=	71.78	STA	6=	30	02	90	02	EYE=	26	30	PS	58	TERR=2	HT=	10.1	8	1
65B1	65090909	W1=	26.23	TH1=	42.1	D=	469.5	AL=	324.2	UST=	73.92	STA	6=	30	02	90	02	EYE=	26	38	PS	11	TERR=2	HT=	10.1	9	1
65B1	65090910	W1=	27.01	TH1=	41.9	D=	445.0	AL=	325.3	UST=	76.19	STA	6=	30	02	90	02	EYE=	26	46	PS	24	TERR=2	HT=	10.1	10	1
65B1	65090911	W1=	27.67	TH1=	42.1	D=	420.1	AL=	326.4	UST=	78.72	STA	6=	30	02	90	02	EYE=	26	54	PS	37	TERR=2	HT=	10.1	11	1
65B1	65090912	W1=	28.10	TH1=	42.3	D=	396.5	AL=	327.7	UST=	81.46	STA	6=	30	02	90	02	EYE=	27	02	PS	50	TERR=2	HT=	10.1	12	1
65B1	65090913	W1=	29.48	TH1=	42.6	D=	372.7	AL=	329.2	UST=	84.65	STA	6=	30	02	90	02	EYE=	27	10	PS	03	TERR=2	HT=	10.1	13	1
65B1	65090914	W1=	31.04	TH1=	42.3	D=	348.9	AL=	330.0	UST=	88.11	STA	6=	30	02	90	02	EYE=	27	21	PS	14	TERR=2	HT=	10.1	14	1
65B1	65090915	W1=	32.46	TH1=	42.0	D=	319.7	AL=	330.8	UST=	92.19	STA	6=	30	02	90	02	EYE=	27	32	PS	25	TERR=2	HT=	10.1	15	1
65B1	65090916	W1=	34.00	TH1=	41.7	D=	292.1	AL=	331.9	UST=	97.02	STA	6=	30	02	90	02	EYE=	27	43	PS	36	TERR=2	HT=	10.1	16	1
65B1	65090917	W1=	35.81	TH1=	41.6	D=	265.5	AL=	332.7	UST=	102.51	STA	6=	30	02	90	02	EYE=	27	55	PS	46	TERR=2	HT=	10.1	17	1
65B1	65090918	W1=	37.55	TH1=	40.4	D=	238.3	AL=	333.6	UST=	109.10	STA	6=	30	02	90	02	EYE=	28	07	PS	56	TERR=2	HT=	10.1	18	1
65B1	65090919	W1=	41.10	TH1=	38.6	D=	205.5	AL=	334.6	UST=	118.94	STA	6=	30	02	90	02	EYE=	28	20	PS	06	TERR=2	HT=	10.1	19	1
65B1	65090920	W1=	45.46	TH1=	40.5	D=	180.5	AL=	339.2	UST=	132.91	STA	6=	30	02	90	02	EYE=	28	31	PS	22	TERR=2	HT=	10.1	20	1
65B1	65090921	W1=	50.42	TH1=	44.0	D=	153.1	AL=	345.4	UST=	149.28	STA	6=	30	02	90	02	EYE=	28	42	PS	38	TERR=2	HT=	10.1	21	1
65B1	65090922	W1=	56.62	TH1=	50.0	D=	124.0	AL=	354.1	UST=	170.27	STA	6=	30	02	90	02	EYE=	28	55	PS	54	TERR=2	HT=	10.1	22	1
65B1	65090923	W1=	63.37	TH1=	59.7	D=	98.2	AL=	362.5	UST=	193.34	STA	6=	30	02	90	02	EYE=	29	09	PS	00	TERR=2	HT=	10.1	23	1
65B1	65091000	W1=	68.65	TH1=	77.2	D=	78.4	AL=	372.9	UST=	214.97	STA	6=	30	02	90	02	EYE=	29	23	PS	21	TERR=2	HT=	10.1	24	1
65B1	65091001	W1=	67.37	TH1=	105.3	D=	69.2	AL=	377.9	UST=	229.15	STA	6=	30	02	90	02	EYE=	29	37	PS	34	TERR=2	HT=	10.1	25	2
65B1	65091002	W1=	63.10	TH1=	124.1	D=	74.4	AL=	377.5	UST=	193.36	STA	6=	30	02	90	02	EYE=	29	47	PS	45	TERR=2	HT=	10.1	26	3
65B1	65091003	W1=	54.65	TH1=	137.2	D=	85.7	AL=	382.3	UST=	177.38	STA	6=	30	02	90	02	EYE=	29	56	PS	55	TERR=2	HT=	10.1	27	4
65B1	65091004	W1=	53.72	TH1=	145.2	D=	101.1	AL=	382.9	UST=	160.27	STA	6=	30	02	90	02	EYE=	30	05	PS	05	TERR=2	HT=	10.1	28	5
65B1	65091005	W1=	46.62	TH1=	150.6	D=	119.0	AL=	380.5	UST=	143.32	STA	6=	30	02	90	02	EYE=	30	14	PS	15	TERR=2	HT=	10.1	29	6
65B1	65091006	W1=	44.01	TH1=	154.2	D=	138.4	AL=	380.0	UST=	128.16	STA	6=	30	02	90	02	EYE=	30	23	PS	25	TERR=2	HT=	10.1	30	7

Sample listing of surface wind speed direction on Wes grid:

. Six pages of output are required to list the wind field at one time level. Grid points are identified on each page by latitude (deg, min), left side margin, and longitude (deg, min), top margin. At each grid point location are printed the wind speed at 10 meter height in knots (top), the wind direction in degrees (middle) and the terrain classification code of the grid points (bottom). The sample listing shown is for the 24th hour of the test Betsy simulation, for the rectangular grid system provided by WES.

STORM 65E3 LAKE FRONT WINDS AT HOUR :4 1ST HOUR IS 65-790901CD1

	9420	9406	9352	9340	9327	9316	9304	9252	9241	9229	9218	9209	9201	9155	9150	9146	9143	9140	9137	9134	9131	9127	9121	9114	
3045	15.9	16.9	17.0	18.7	19.7	20.6	21.7	22.9	24.0	25.3	26.6	27.7	28.8	29.9	30.1	30.6	30.9	31.4	31.9	32.3	32.8	33.4	34.2	35.3	3045
3046	15.9	17.0	18.0	19.0	20.0	21.0	22.0	23.0	24.0	25.0	26.0	27.0	28.0	29.0	30.0	31.0	32.0	33.0	34.0	35.0	36.0	37.0	38.0	39.0	3046
3039	15.9	16.8	17.8	18.7	19.7	20.7	21.7	22.7	23.7	24.7	25.7	26.7	27.7	28.7	29.7	30.7	31.7	32.7	33.7	34.7	35.7	36.7	37.7	38.7	3039
3035	15.9	16.8	17.8	18.7	19.7	20.7	21.7	22.7	23.7	24.7	25.7	26.7	27.7	28.7	29.7	30.7	31.7	32.7	33.7	34.7	35.7	36.7	37.7	38.7	3035
3033	15.9	16.8	17.8	18.7	19.7	20.7	21.7	22.7	23.7	24.7	25.7	26.7	27.7	28.7	29.7	30.7	31.7	32.7	33.7	34.7	35.7	36.7	37.7	38.7	3033
3026	15.9	16.8	17.8	18.7	19.7	20.7	21.7	22.7	23.7	24.7	25.7	26.7	27.7	28.7	29.7	30.7	31.7	32.7	33.7	34.7	35.7	36.7	37.7	38.7	3026
3021	15.9	16.8	17.8	18.7	19.7	20.7	21.7	22.7	23.7	24.7	25.7	26.7	27.7	28.7	29.7	30.7	31.7	32.7	33.7	34.7	35.7	36.7	37.7	38.7	3021
3021	15.9	16.8	17.8	18.7	19.7	20.7	21.7	22.7	23.7	24.7	25.7	26.7	27.7	28.7	29.7	30.7	31.7	32.7	33.7	34.7	35.7	36.7	37.7	38.7	3021
3016	15.9	16.8	17.8	18.7	19.7	20.7	21.7	22.7	23.7	24.7	25.7	26.7	27.7	28.7	29.7	30.7	31.7	32.7	33.7	34.7	35.7	36.7	37.7	38.7	3016
3013	15.9	16.8	17.8	18.7	19.7	20.7	21.7	22.7	23.7	24.7	25.7	26.7	27.7	28.7	29.7	30.7	31.7	32.7	33.7	34.7	35.7	36.7	37.7	38.7	3013
3013	15.9	16.8	17.8	18.7	19.7	20.7	21.7	22.7	23.7	24.7	25.7	26.7	27.7	28.7	29.7	30.7	31.7	32.7	33.7	34.7	35.7	36.7	37.7	38.7	3013
3010	15.9	16.8	17.8	18.7	19.7	20.7	21.7	22.7	23.7	24.7	25.7	26.7	27.7	28.7	29.7	30.7	31.7	32.7	33.7	34.7	35.7	36.7	37.7	38.7	3010
3110	15.9	16.8	17.8	18.7	19.7	20.7	21.7	22.7	23.7	24.7	25.7	26.7	27.7	28.7	29.7	30.7	31.7	32.7	33.7	34.7	35.7	36.7	37.7	38.7	3110
3108	15.9	16.8	17.8	18.7	19.7	20.7	21.7	22.7	23.7	24.7	25.7	26.7	27.7	28.7	29.7	30.7	31.7	32.7	33.7	34.7	35.7	36.7	37.7	38.7	3108
3106	15.9	16.8	17.8	18.7	19.7	20.7	21.7	22.7	23.7	24.7	25.7	26.7	27.7	28.7	29.7	30.7	31.7	32.7	33.7	34.7	35.7	36.7	37.7	38.7	3106
3006	15.9	16.8	17.8	18.7	19.7	20.7	21.7	22.7	23.7	24.7	25.7	26.7	27.7	28.7	29.7	30.7	31.7	32.7	33.7	34.7	35.7	36.7	37.7	38.7	3006
3006	15.9	16.8	17.8	18.7	19.7	20.7	21.7	22.7	23.7	24.7	25.7	26.7	27.7	28.7	29.7	30.7	31.7	32.7	33.7	34.7	35.7	36.7	37.7	38.7	3006
3003	15.9	16.8	17.8	18.7	19.7	20.7	21.7	22.7	23.7	24.7	25.7	26.7	27.7	28.7	29.7	30.7	31.7	32.7	33.7	34.7	35.7	36.7	37.7	38.7	3003
2959	15.9	16.8	17.8	18.7	19.7	20.7	21.7	22.7	23.7	24.7	25.7	26.7	27.7	28.7	29.7	30.7	31.7	32.7	33.7	34.7	35.7	36.7	37.7	38.7	2959
2959	15.9	16.8	17.8	18.7	19.7	20.7	21.7	22.7	23.7	24.7	25.7	26.7	27.7	28.7	29.7	30.7	31.7	32.7	33.7	34.7	35.7	36.7	37.7	38.7	2959
2954	15.9	16.8	17.8	18.7	19.7	20.7	21.7	22.7	23.7	24.7	25.7	26.7	27.7	28.7	29.7	30.7	31.7	32.7	33.7	34.7	35.7	36.7	37.7	38.7	2954
2954	15.9	16.8	17.8	18.7	19.7	20.7	21.7	22.7	23.7	24.7	25.7	26.7	27.7	28.7	29.7	30.7	31.7	32.7	33.7	34.7	35.7	36.7	37.7	38.7	2954
2950	15.9	16.8	17.8	18.7	19.7	20.7	21.7	22.7	23.7	24.7	25.7	26.7	27.7	28.7	29.7	30.7	31.7	32.7	33.7	34.7	35.7	36.7	37.7	38.7	2950
2945	15.9	16.8	17.8	18.7	19.7	20.7	21.7	22.7	23.7	24.7	25.7	26.7	27.7	28.7	29.7	30.7	31.7	32.7	33.7	34.7	35.7	36.7	37.7	38.7	2945
2945	15.9	16.8	17.8	18.7	19.7	20.7	21.7	22.7	23.7	24.7	25.7	26.7	27.7	28.7	29.7	30.7	31.7	32.7	33.7	34.7	35.7	36.7	37.7	38.7	2945
2940	15.9	16.8	17.8	18.7	19.7	20.7	21.7	22.7	23.7	24.7	25.7	26.7	27.7	28.7	29.7	30.7	31.7	32.7	33.7	34.7	35.7	36.7	37.7	38.7	2940
2940	15.9	16.8	17.8	18.7	19.7	20.7	21.7	22.7	23.7	24.7	25.7	26.7	27.7	28.7	29.7	30.7	31.7	32.7	33.7	34.7	35.7	36.7	37.7	38.7	2940
2936	15.9	16.8	17.8	18.7	19.7	20.7	21.7	22.7	23.7	24.7	25.7	26.7	27.7	28.7	29.7	30.7	31.7	32.7	33.7	34.7	35.7	36.7	37.7	38.7	2936
2936	15.9	16.8	17.8	18.7	19.7	20.7	21.7	22.7	23.7	24.7	25.7	26.7	27.7	28.7	29.7	30.7	31.7	32.7	33.7	34.7	35.7	36.7	37.7	38.7	2936

STORM (51) LAKE POIT VIRUS AT HOUR 24 1ST HOUR IS 65090:DJCDT

	9134	9131	9127	9121	9114	9106	9056	9044	9021	9013	9006	8959	8953	8947	8943	8939	8935	8931	8927	8923	8920	8916	8912	
3045	31.3	32.8	33.4	34.1	35.3	36.4	37.7	39.1	40.1	40.7	40.9	41.0	40.9	40.7	40.5	40.4	40.2	35.9	39.6	39.3	39.1	38.8	38.5	3045
3046	21.0	22.0	23.0	24.0	25.0	26.0	27.0	28.0	29.0	30.0	31.0	32.0	33.0	34.0	35.0	36.0	37.0	38.0	39.0	40.0	41.0	42.0	43.0	3046
3039	33.1	33.5	34.2	35.2	37.1	38.9	40.4	41.7	42.3	42.6	42.8	42.8	42.8	42.8	42.8	42.8	42.8	42.8	42.8	42.8	42.8	42.8	42.8	3039
3035	19.0	20.0	21.0	22.0	23.0	24.0	25.0	26.0	27.0	28.0	29.0	30.0	31.0	32.0	33.0	34.0	35.0	36.0	37.0	38.0	39.0	40.0	41.0	3035
3033	41.5	42.5	43.3	44.4	46.1	47.1	48.2	49.4	49.9	49.2	49.3	49.2	49.0	48.7	48.5	48.2	47.9	47.6	47.2	46.6	45.8	45.0	44.0	3033
3033	27.0	28.0	29.0	30.0	31.0	32.0	33.0	34.0	35.0	36.0	37.0	38.0	39.0	40.0	41.0	42.0	43.0	44.0	45.0	46.0	47.0	48.0	49.0	3033
3024	42.5	43.6	44.6	45.7	47.6	49.4	51.9	53.1	53.3	53.3	53.3	53.3	53.3	53.3	53.3	53.3	53.3	53.3	53.3	53.3	53.3	53.3	53.3	3024
3026	15.0	16.0	17.0	18.0	19.0	20.0	21.0	22.0	23.0	24.0	25.0	26.0	27.0	28.0	29.0	30.0	31.0	32.0	33.0	34.0	35.0	36.0	37.0	3026
3021	43.6	44.3	45.4	46.9	48.6	50.7	53.0	55.1	57.6	60.0	62.3	64.5	66.6	68.7	70.8	72.9	75.0	77.1	79.2	81.3	83.4	85.5	87.6	3021
3016	44.4	45.1	46.1	47.4	49.1	51.9	54.1	56.5	59.3	62.3	65.2	68.1	71.0	73.9	76.8	79.7	82.6	85.5	88.4	91.3	94.2	97.1	100.0	3016
3013	44.8	45.6	46.6	48.3	50.3	52.6	55.4	58.6	62.3	66.6	71.4	76.6	82.2	88.2	94.5	101.1	108.0	115.2	122.7	130.5	138.7	147.2	156.0	3013
3010	45.2	46.0	47.1	48.4	50.1	52.3	55.0	58.1	61.6	65.5	69.8	74.5	79.6	85.1	90.9	97.1	103.7	110.7	118.1	125.8	133.8	142.1	150.6	3010
3006	45.4	46.3	47.5	49.1	51.4	53.7	56.5	59.7	63.4	67.6	72.2	77.2	82.5	88.2	94.2	100.5	107.1	114.0	121.2	128.7	136.5	144.6	152.9	3006
3006	6.0	7.0	8.0	9.0	10.0	11.0	12.0	13.0	14.0	15.0	16.0	17.0	18.0	19.0	20.0	21.0	22.0	23.0	24.0	25.0	26.0	27.0	28.0	3006
3003	46.0	46.9	47.8	49.0	50.7	52.9	55.9	59.4	63.4	67.9	72.7	77.8	83.2	88.9	94.9	101.1	107.5	114.1	120.9	127.9	135.1	142.4	149.8	3003
2959	48.2	49.1	50.3	51.7	53.6	56.1	59.1	62.5	66.3	70.5	75.0	79.8	84.9	90.2	95.7	101.3	107.1	113.1	119.2	125.4	131.7	138.1	144.6	2959
2959	5.0	6.0	7.0	8.0	9.0	10.0	11.0	12.0	13.0	14.0	15.0	16.0	17.0	18.0	19.0	20.0	21.0	22.0	23.0	24.0	25.0	26.0	27.0	2959
2954	46.9	47.8	48.8	50.1	51.8	54.0	56.6	59.6	63.0	66.8	70.9	75.3	79.9	84.7	89.7	94.7	99.9	105.1	110.4	115.8	121.3	126.9	132.6	2954
2950	47.1	47.1	47.1	47.1	47.1	47.1	47.1	47.1	47.1	47.1	47.1	47.1	47.1	47.1	47.1	47.1	47.1	47.1	47.1	47.1	47.1	47.1	47.1	2950
2945	47.3	48.3	49.8	52.1	55.1	58.5	62.4	66.7	71.4	76.3	81.4	86.7	92.2	97.9	103.7	109.6	115.6	121.7	127.9	134.2	140.6	147.1	153.6	2945
2945	355.0	356.0	357.0	358.0	359.0	360.0	361.0	362.0	363.0	364.0	365.0	366.0	367.0	368.0	369.0	370.0	371.0	372.0	373.0	374.0	375.0	376.0	377.0	2945
2940	47.5	48.6	50.1	52.5	55.4	58.8	62.6	66.8	71.4	76.3	81.4	86.7	92.2	97.9	103.7	109.6	115.6	121.7	127.9	134.2	140.6	147.1	153.6	2940
2936	48.0	49.0	50.1	51.5	53.5	56.0	58.9	62.2	65.9	69.9	74.2	78.8	83.6	88.5	93.5	98.6	103.7	108.9	114.1	119.4	124.8	130.3	135.8	2936
2936	352.0	353.0	354.0	355.0	356.0	357.0	358.0	359.0	360.0	361.0	362.0	363.0	364.0	365.0	366.0	367.0	368.0	369.0	370.0	371.0	372.0	373.0	374.0	2936

STOMP (51) LAKE POINT WINGS AT HOUR 24 1ST HOUR 15 6:50/6:10

3045	3046	3047	3048	3049	3050	3051	3052	3053	3054	3055	3056	3057	3058	3059	3060	3061	3062	3063	3064	3065	3066	3067	3068	3069	3070	3071	3072	3073	3074	3075	3076	3077	3078	3079	3080	3081	3082	3083	3084	3085	3086	3087	3088	3089	3090	3091	3092	3093	3094	3095	3096	3097	3098	3099	3100	3101	3102	3103	3104	3105	3106	3107	3108	3109	3110	3111	3112	3113	3114	3115	3116	3117	3118	3119	3120	3121	3122	3123	3124	3125	3126	3127	3128	3129	3130	3131	3132	3133	3134	3135	3136	3137	3138	3139	3140	3141	3142	3143	3144	3145	3146	3147	3148	3149	3150	3151	3152	3153	3154	3155	3156	3157	3158	3159	3160	3161	3162	3163	3164	3165	3166	3167	3168	3169	3170	3171	3172	3173	3174	3175	3176	3177	3178	3179	3180	3181	3182	3183	3184	3185	3186	3187	3188	3189	3190	3191	3192	3193	3194	3195	3196	3197	3198	3199	3200
3045	3046	3047	3048	3049	3050	3051	3052	3053	3054	3055	3056	3057	3058	3059	3060	3061	3062	3063	3064	3065	3066	3067	3068	3069	3070	3071	3072	3073	3074	3075	3076	3077	3078	3079	3080	3081	3082	3083	3084	3085	3086	3087	3088	3089	3090	3091	3092	3093	3094	3095	3096	3097	3098	3099	3100	3101	3102	3103	3104	3105	3106	3107	3108	3109	3110	3111	3112	3113	3114	3115	3116	3117	3118	3119	3120	3121	3122	3123	3124	3125	3126	3127	3128	3129	3130	3131	3132	3133	3134	3135	3136	3137	3138	3139	3140	3141	3142	3143	3144	3145	3146	3147	3148	3149	3150	3151	3152	3153	3154	3155	3156	3157	3158	3159	3160	3161	3162	3163	3164	3165	3166	3167	3168	3169	3170	3171	3172	3173	3174	3175	3176	3177	3178	3179	3180	3181	3182	3183	3184	3185	3186	3187	3188	3189	3190	3191	3192	3193	3194	3195	3196	3197	3198	3199	3200

9420	9406	9352	9340	9327	9316	9304	9252	9241	9229	9218	9209	9201	9155	9150	9146	9143	9140	9137	9134	9131	9127	9121	9114	
2945	18.7	20.0	21.3	20.4	30.1	31.5	33.2	29.0	30.9	30.7	25.4	39.1	41.1	42.8	42.4	35.5	35.3	35.1	35.4	45.4	46.3	47.3	92.1	2945
2946	17.6	19.8	27.2	24.4	30.0	31.4	33.1	30.0	33.0	33.0	35.0	37.4	41.1	42.7	44.1	45.3	45.3	45.1	45.2	47.5	48.1	47.5	92.1	2946
2936	16.0	25.7	27.0	24.0	29.1	31.2	32.9	32.9	32.6	36.9	35.6	35.4	34.6	34.7	34.7	35.1	35.1	35.1	35.1	35.1	35.1	35.1	35.1	2936
2536	5.0	10.0	7.0	4.0	2.0	3.0	3.0	3.0	3.0	3.0	3.0	3.0	3.0	3.0	3.0	3.0	3.0	3.0	3.0	3.0	3.0	3.0	2536	
2532	24.3	21.5	24.5	24.2	29.7	31.1	32.1	32.1	32.1	32.1	32.1	32.1	32.1	32.1	32.1	32.1	32.1	32.1	32.1	32.1	32.1	32.1	2532	
2932	12.0	9.0	6.0	3.0	0.0	3.0	3.0	3.0	3.0	3.0	3.0	3.0	3.0	3.0	3.0	3.0	3.0	3.0	3.0	3.0	3.0	3.0	2932	
2927	24.1	25.4	26.7	28.0	29.4	30.9	32.6	34.1	36.3	34.1	36.3	34.1	36.3	34.1	36.3	34.1	36.3	34.1	36.3	34.1	36.3	34.1	2927	
2922	23.9	25.2	26.5	27.8	29.2	30.7	32.3	34.1	36.3	34.1	36.3	34.1	36.3	34.1	36.3	34.1	36.3	34.1	36.3	34.1	36.3	34.1	2922	
2918	23.7	25.0	26.3	27.6	29.1	30.5	32.1	33.5	35.0	36.0	38.4	40.8	44.0	46.4	47.7	46.9	45.9	45.8	45.8	45.8	45.8	45.8	2918	
2914	23.4	24.5	26.1	27.4	28.9	30.2	31.9	33.7	35.7	38.1	40.5	42.9	46.5	46.0	47.3	48.5	49.4	49.4	49.4	49.4	49.4	49.4	2914	
2909	23.4	24.6	25.9	27.2	28.6	29.9	31.6	33.5	35.2	37.7	40.1	42.2	44.0	45.5	46.9	48.0	48.7	49.5	50.4	51.3	52.3	53.6	2909	
2903	23.1	24.3	25.6	26.9	28.3	29.6	31.3	33.3	35.3	37.3	39.4	41.5	43.4	45.4	46.0	47.1	47.5	48.7	49.6	50.4	51.2	52.3	2903	
2856	22.7	23.9	25.3	26.4	27.8	29.2	30.7	32.4	34.2	36.2	38.4	40.7	42.5	43.9	45.1	46.1	46.8	47.5	48.3	49.0	49.8	50.9	2856	
2847	22.2	23.5	24.7	25.9	27.2	28.6	30.0	31.7	33.5	35.3	37.4	39.4	41.2	42.5	43.5	44.5	45.2	46.0	46.6	47.2	47.9	48.7	2847	
2837	21.6	22.8	24.1	25.3	26.6	27.7	29.3	30.7	32.3	34.0	35.7	37.8	39.5	40.8	41.8	42.6	43.2	43.9	44.5	45.1	45.7	46.4	2837	
2827	20.8	22.1	23.4	24.5	25.9	27.1	28.4	29.9	31.3	33.1	34.7	36.6	38.2	39.6	40.6	41.5	42.3	42.9	43.5	44.1	44.7	45.3	2827	
2816	19.0	20.3	21.6	22.7	23.9	25.1	26.5	27.8	29.4	30.8	32.6	34.2	36.0	37.6	38.6	39.2	39.9	40.6	41.1	41.7	42.3	42.9	2816	
2804	18.0	20.0	20.3	21.6	22.7	23.9	25.1	26.5	27.8	29.4	30.8	32.6	34.2	36.0	37.6	38.6	39.2	39.9	40.6	41.1	41.7	42.3	2804	
2750	18.1	19.2	20.4	21.5	22.4	23.7	24.9	26.2	27.5	28.5	29.8	30.9	32.0	32.9	33.8	34.6	35.4	36.1	36.8	37.4	37.9	38.5	2750	
2751	34.7	34.2	33.7	33.3	32.8	32.5	32.0	31.6	31.2	30.7	30.3	29.9	29.6	29.2	28.9	28.8	28.7	28.7	28.5	28.4	28.4	28.0	2750	

STORM 6581 LAKE POUL WINDS AT MOUK 24 1ST HOUR IS 65090501C01

2945	62.6	62.0	61.8	60.7	59.7	59.0	58.1	57.2	55.9	54.5	52.5	53.9	52.9	51.6	50.9	49.9	49.3	48.6	47.8	47.0	46.0	2945
2945	116.	116.	117.	117.	116.	116.	116.	115.	115.	115.	122.	123.	124.	125.	125.	126.	126.	126.	127.	127.	129.	2945
2940	64.1	62.9	61.9	60.8	59.9	59.3	58.2	57.1	56.0	54.8	52.5	54.1	53.1	51.9	50.9	50.0	49.3	48.7	47.9	47.1	46.1	2940
2940	121.	121.	121.	122.	122.	122.	122.	122.	122.	122.	122.	122.	122.	122.	122.	122.	122.	122.	122.	122.	122.	2940
2936	64.2	63.1	62.1	61.1	59.9	59.1	58.1	57.3	56.8	55.9	54.2	53.1	52.0	51.0	50.0	49.3	48.7	48.0	47.1	46.1	45.1	2936
2936	121.	121.	121.	121.	121.	121.	121.	121.	121.	121.	121.	121.	121.	121.	121.	121.	121.	121.	121.	121.	121.	2936
2932	63.9	62.9	62.2	60.9	59.7	59.0	58.0	57.0	56.6	55.4	54.2	53.2	52.0	51.1	50.1	49.4	48.7	48.0	47.1	46.0	45.0	2932
2932	132.	131.	131.	130.	129.	130.	132.	131.	131.	131.	131.	131.	131.	131.	131.	131.	131.	131.	131.	131.	131.	2932
2927	63.0	62.3	61.6	60.7	59.4	58.6	57.4	56.3	55.3	54.1	53.1	51.9	51.0	50.1	49.4	48.7	48.0	47.1	46.0	45.0	44.0	2927
2927	136.	137.	136.	136.	136.	136.	136.	136.	135.	134.	134.	134.	134.	134.	134.	134.	134.	134.	134.	134.	134.	2927
2922	60.4	59.7	58.5	57.4	56.4	55.4	54.2	53.1	52.0	50.9	49.9	49.3	48.6	47.8	47.0	46.0	45.0	44.0	43.0	42.0	41.0	2922
2922	144.	143.	144.	143.	142.	141.	140.	139.	138.	137.	137.	137.	136.	135.	134.	133.	132.	131.	130.	129.	128.	2922
2910	59.1	58.7	58.2	57.1	56.1	55.1	54.0	52.9	51.8	50.9	49.9	49.3	48.6	47.8	47.0	46.0	45.0	44.0	43.0	42.0	41.0	2910
2910	145.	145.	145.	145.	145.	145.	145.	145.	145.	145.	145.	145.	145.	145.	145.	145.	145.	145.	145.	145.	145.	2910
2914	58.0	57.5	57.2	56.5	55.8	55.3	54.2	53.1	52.0	51.0	50.1	49.4	48.6	47.8	47.0	46.0	45.0	44.0	43.0	42.0	41.0	2914
2914	154.	151.	145.	146.	146.	147.	145.	145.	144.	143.	142.	142.	141.	140.	140.	139.	139.	139.	139.	139.	139.	2914
2909	62.8	61.1	59.7	58.5	57.1	56.6	55.7	54.8	54.0	53.2	52.1	51.3	50.3	49.5	48.8	48.2	47.6	46.9	46.0	45.0	44.0	2909
2909	163.	156.	157.	157.	157.	157.	157.	157.	157.	157.	157.	157.	157.	157.	157.	157.	157.	157.	157.	157.	157.	2909
2903	61.1	60.7	60.5	59.1	58.1	57.1	56.6	55.7	54.8	54.0	53.2	52.1	51.3	50.3	49.5	48.8	48.2	47.6	46.9	46.0	45.0	2903
2903	163.	163.	163.	161.	157.	156.	155.	152.	150.	149.	148.	147.	147.	146.	145.	144.	144.	144.	143.	143.	143.	2903
2856	58.6	58.4	58.4	56.2	55.7	55.6	55.3	54.7	54.2	53.8	53.0	52.3	51.7	50.9	50.0	49.3	48.6	47.8	47.0	46.0	45.0	2856
2856	171.	171.	169.	167.	165.	163.	161.	159.	158.	156.	155.	152.	151.	150.	149.	148.	147.	147.	147.	147.	147.	2856
2847	56.1	56.1	56.1	54.9	54.7	54.6	54.4	54.2	54.0	53.8	53.6	53.4	53.2	53.0	52.8	52.6	52.4	52.2	52.0	51.8	51.6	2847
2847	184.	181.	179.	176.	174.	172.	170.	168.	165.	164.	162.	160.	158.	156.	155.	153.	152.	151.	151.	150.	149.	2847
2837	53.9	53.0	53.7	53.4	53.3	53.0	52.8	52.2	51.7	51.2	50.6	49.9	49.3	48.5	47.8	47.2	46.5	45.8	45.3	44.6	43.7	2837
2837	191.	186.	183.	180.	179.	178.	176.	174.	171.	169.	167.	165.	164.	162.	161.	159.	158.	155.	155.	153.	152.	2837
2827	51.5	51.6	51.2	51.1	50.9	50.5	50.1	49.9	49.3	48.7	48.2	47.6	46.9	46.3	45.6	45.2	44.7	44.2	43.8	43.2	42.6	2827
2827	193.	191.	188.	186.	184.	181.	179.	176.	174.	172.	170.	168.	167.	165.	164.	162.	161.	160.	159.	158.	157.	2827
2816	49.2	49.0	48.9	48.6	48.3	48.1	47.8	47.5	47.0	46.5	46.1	45.8	45.3	44.8	44.1	43.7	43.3	42.6	42.0	41.5	40.9	2816
2816	201.	197.	192.	190.	188.	186.	184.	181.	179.	177.	175.	173.	171.	169.	168.	167.	165.	164.	163.	162.	161.	2816
2804	46.3	46.3	46.2	46.1	45.8	45.7	45.6	45.3	45.1	44.9	44.4	44.1	43.7	43.4	43.1	42.6	42.1	41.4	40.8	40.3	39.6	2804
2804	201.	199.	197.	194.	192.	190.	188.	185.	183.	181.	180.	178.	176.	174.	172.	171.	170.	168.	167.	165.	164.	2804
2750	43.0	42.9	42.8	42.8	42.9	42.9	42.8	42.6	42.4	42.3	42.2	42.1	41.9	41.5	41.2	40.9	40.6	40.4	40.0	39.7	39.0	2750
2750	201.	202.	199.	198.	196.	194.	192.	190.	186.	184.	182.	181.	179.	177.	175.	174.	173.	172.	171.	170.	168.	2750